The Role of Apoptosis Repressor with Caspase Recruitment Domain in Aging Mouse Skeletal Muscle Morphology and Apoptotic Signaling

By

Kira Vorobej

A thesis
presented to the University of Waterloo
in fulfillment of the
thesis requirement for the degree of
Master of Science
in
Kinesiology

Waterloo, Ontario, Canada, 2014.

Author's Declaration

I hereby declare that I am the sole author of this thesis. This is a true copy of the thesis, including any required final revisions, as accepted by my examiners.

I understand that my thesis may be made electronically available to the public.

Abstract

Aging is associated with a loss of skeletal muscle mass, known as sarcopenia, which results in numerous degenerative alterations and decreased strength. One of the major mechanisms influencing muscle wasting in aged skeletal muscle is through augmented apoptotic signaling. Altered apoptotic signaling can result in cell dysfunction, and degradation of muscle contractile proteins and loss of myonuclei; ultimately contributing to muscle atrophy and contractile dysfunction. Apoptosis repressor with caspase recruitment domain (ARC) is an anti-apoptotic protein that is highly expressed in terminally differentiated tissue (heart and skeletal muscle) which can regulate several apoptotic pathways. Interestingly, ARC knockout (KO) mice display morphological and phenotypic differences, as well as altered protein expression of a number of key apoptotic regulatory factors in skeletal muscle compared to wild-type (WT) mice. Currently, the influence of ARC in aging skeletal muscle has not been studied. Therefore, the current work examined the role of ARC protein on age-related muscle wasting, and apoptosis by utilizing an ARC-deficient mouse (along with age-matched WT controls) model at several time-points throughout the lifespan (18-week, 1 year, and 2 years). Slow (oxidative) and fast (glycolytic) muscle was used to compare differences between ages and genotypes. Soleus weight, CSA, type I and IIA CSA, and total fiber number decreased in the 2 year animals, with a fiber shift towards a slower MHC expression. Contractility measurements revealed a higher rate of contraction and relaxation in the 2 year animals. No differences were found in pro-apoptotic proteins, and caspase and calpain activity; however, four anti-apoptotic proteins were increased in the 2 year animals. However, the Bax:Bcl-2 ratio, and ARC expression decreased in the 2 year animals. Subfractionation analysis in the RQ revealed increased cytosolic SMAC in the 2 year animals and increased mitochondrial Bax in the 18 week animals. Furthermore, the 2 year KO

vs. WT mice had an increased release of mitochondrial housed pro-apoptotic proteins and an increased Bax:Bcl-2 ratio. Additionally, ARC KO mice display a decreased total fiber number. Plantaris weight, CSA, type IIA, IIX, and IIB CSA, and total fiber number decreased in the 2 year animals, with a fiber shift towards a faster MHC expression. Contractility measurements revealed lower contraction and relaxation rates in the 2 year animals. Similar to the soleus, three anti-apoptotic proteins increased, and the Bax:Bcl-2 ratio decreased in the 2 year animals, with no differences in caspase and calpain activity. In the WQ cytosolic AIF decreased in the 18 week animals, whereas cytosolic SMAC increased in the aged animals. The effects influenced exclusively by genotype were a decreased plantaris weight, and an increased Bcl-XL expression in the KO group. Overall, these results indicate that aged mice display increased muscle atrophy despite an increase in anti-apoptotic protein expression, as well as altered force characteristics. With aged ARC KO mice displaying several altered protein expressions. This work provides a better understanding of the role of cell death signaling and ARC protein in the skeletal muscle morphological and functional alterations observed during the aging process.

Acknowledgements

I would like to thank my supervisor, Dr. Joe Quadrilatero, and to the members of my committee, Dr. Russ Tupling and Dr. John Mielke for their time and advice. Thank you to my lab mates and members of the Tupling lab. Lastly, thank you to my family and friends for their support.

Table of Contents

List of Figures

List of Appendix Figures

List of Tables

Introduction

Apoptosis

The maintenance of tissues within the body is critical for normal development, growth, and preserving tissue function. One important regulator of cellular homeostasis is apoptosis. Apoptosis is a highly regulated form of programmed cell death that is critical for the removal of damaged and unneeded cells[1]. The importance of apoptosis is seen through its essential role in cell differentiation and tissue remodeling. For example, the removal of the webbing of skin between the digits of the hand is accomplished by selective deletion of interdigital cells through apoptotic signaling[2]. Additionally, during the early stages of myogenic differentiation, there is an increase in the anti-apoptotic protein Bcl-2, which is required for the formation of healthy myotubes[3]. Also, erythrocyte differentiation is prevented when caspase-3 activity is inhibited, limiting DNA fragmentation and nucleus removal[4]. Dysfunction in apoptosis is also a common feature of diseases such as cancer[5], myocardial infarction[6], autoimmune disorders[7], sarcopenia[8], and diabetes[9].

Apoptotic Pathways

Apoptosis occurs through three main signaling pathways; the death receptor, mitochondrial-mediated, and the endoplasmic reticulum (ER) stress pathway. A key event during apoptosis is the activation of a class of proteolytic enzymes known as caspases. Caspases are aspartate-specific cysteine proteases that cleave target proteins resulting in destruction of the cell. These include both initiator caspases, such as caspase-8, which activate and cleave executioner caspases, such as caspase-3[10]. Executor caspases can cleave other proteases, cytoskeletal proteins, and multiple cellular substrates, ultimately leading to dysfunction and/or

death of the cell[11].

Death receptor signaling, results from an extracellular ligand binding to a cell surface receptor. These include Fas ligand (FasL) and tumor necrosis factor (TNF), which bind to a death receptor, such as Fas receptor or TNF-α receptor (TNFR) causing death domains on the receptors to become activated. This recruits and binds the adaptor proteins, Fas-associated protein with a death domain (FADD) and tumor necrosis factor receptor type 1-associated death domain (TRADD), which then forms the death-inducing signaling complex (DISC), activating caspase-8, and ultimately leading to the activation of caspase-3[12,13].

The mitochondrial pathway is predominantly regulated by the B-cell lymphoma 2 (Bcl-2) family. The primary members of this family are the pro-apoptotic Bcl-2 associated X protein (Bax) and the anti-apoptotic protein Bcl-2[11]. In response to cellular stress, pro-apoptotic proteins, such as Bax, migrate from the cytosol and insert into the outer mitochondria membrane. This contributes to mitochondria outer membrane permeabilization (MOMP), which allows entry of cytosolic proteases into the mitochondria to cleave specific substrates, resulting in the release of pro-apoptotic proteins from the inter-mitochondrial membrane space into the cytosol[14]. Additionally, a pre-existing mitochondrial channel called the permeability transition pore (mPTP) contributes to MOMP. In response to sustained cellular stress such as increased Ca^{2+} levels, adenine nucleotide translocator (ANT), voltage-dependent ion channel (VDAC), and Cyclophilin D proteins come together and form the mPTP[15,16]. This causes solutes to leak into the mitochondria from the cytosol, causing mitochondria swelling, and depolarization of the membrane potential, resulting in rupture of the membrane and release of pro-apoptotic proteins into the cytosol[17]. These pro-apoptotic proteins include cytochrome c (Cyto-c), second mitochondrial derived activator of caspase (SMAC), apoptosis inducing factor (AIF), and

endonuclease G (EndoG). Once released, Cyto-c can bind to dATP and apoptotic protease-activating factor (APAF1) forming the apoptosome, which leads to the activation of caspase-9, and ultimately cleavage and activation of caspase-3[18]. In addition to caspase-mediated cell death, apoptosis can be triggered through caspase-independent pathways. Once released into the cytosol, AIF and EndoG translocate to the nucleus causing DNA fragmentation and chromatin condensation independent of caspase activation[17]. Caspases can be indirectly activated through SMAC, as SMAC release from the mitochondria causes inhibition of X-linked inhibitor of apoptosis protein (XIAP), which normally blocks caspase-9 and caspase-3 activity[19].

The endoplasmic reticulum (ER) stress pathway initiates apoptosis through its regulation of calcium. Apoptosis is triggered when the ER releases cytotoxic levels of calcium into the cytosol, activating calcium dependent proteases known as calpains. Calpains can cleave both structural proteins (including skeletal muscle contractile proteins) and caspases, such as caspase-12[20]. Induction of this pathway occurs as a consequence of increased cellular stress and an accumulation of misfolded proteins in the ER, resulting in the initiation of the unfolded protein response (UPR). The activation of this pathway increases the number of protein foldases and attenuates the rate of protein translation in an attempt to lessen the damage of increased misfolded proteins[21]. If this response fails or if the stress is prolonged, the UPR can induce apoptosis[22,23].

Apoptosis in Skeletal Muscle

Skeletal muscle is a long-lived, post mitotic tissue that is highly resistant to apoptotic stimuli[24]. Given its unique and diverse morphology, skeletal muscle requires special consideration with respect to apoptosis. Firstly, skeletal muscle is multinucleated, and under goes

a process known as myonuclear apoptosis whereby individual nuclei are lost rather than the entire cell being destroyed [41]. In this process, the loss of the nuclei also results in loss of its associated cytoplasmic domain[25]. Given the important role of myonuclei in the maintenance of gene and protein synthesis for the muscle, a loss of nuclei through elevated apoptotic signaling can lead to skeletal muscle atrophy, whereas the addition of nuclei results in muscle hypertrophy[26]. In addition, caspase and calpains are known to directly degrade several contractile proteins such as actin, myosin, titin, and nebulin[42].

Secondly, skeletal muscle is unique in that it is a diverse tissue consisting of several fiber types, which differ in their metabolic function, morphology, mitochondrial content, and apoptotic protein expression and apoptotic susceptibility[24,27]. For example, different fiber types express varying protein expression such that the level of key apoptotic proteins such as ARC, Bcl-2, and caspase-3 are higher in type I fibers[24]. In addition, given the role of the mitochondria in apoptosis, changes in the number of mitochondria can influence apoptotic signaling[28]. For example, since mitochondria house many important pro-apoptotic proteins, oxidative fibers with higher mitochondrial content, show differences in apoptotic signaling. As well, mitochondria can produce reactive oxygen species (ROS), which may lead to fiber type differences in apoptotic signaling[24]. These factors contribute to variations in apoptotic resistance between slow (red) and fast (white) muscle. One study demonstrated that in the red gastrocnemius muscle of rats, there was an increase in both pro- and anti-apoptotic proteins, increased ROS generation and increased mitochondrial mediated apoptotic events[24].

Aging

Sarcopenia is defined as a decrease in both skeletal muscle mass and function, which can

ultimately increase an individual's risk for adverse health outcomes[29]. Sarcopenia is a steadily, progressive condition, frequently seen with advancing age[8]. Aging is accompanied by atrophy of skeletal muscle, with a 1% loss of skeletal muscle mass per year after the age of 50[30]. Although this occurrence has been well documented the mechanisms leading to sarcopenia are not fully understood. Muscle atrophy is an outcome of both a reduction is muscle fiber size and number[31]. The development of muscle atrophy with increasing age leads to a sizeable decrease in type II fibers with less of an effect on the more oxidative type I fibers[32]. The etiologies of age-related skeletal muscle atrophy include an increase in nuclear apoptotic signaling[26], increased oxidative stress, and decreased satellite cell content or regenerative ability[30]. Collectively, these changes lead to increased protein degradation[33] and an attenuated rate of protein synthesis in aging skeletal muscle[26].

Increased oxidative stress has been demonstrated with aging. Aged animals display higher basal levels of ROS in skeletal muscle, which can be involved in the mitochondrial dysfunction commonly observed in aging[34]. Given the important role of mitochondria during apoptosis, mitochondrial dysfunction with age may ultimately lead to an increase in apoptotic signaling. Furthermore, since myonuclei are post-mitotic and incapable of undergoing cell division, satellite cells are essential for regeneration and hypertrophy of skeletal muscle. If skeletal muscle becomes damaged, satellite cells can proliferate and help with this repair; however, aging results in a decreased number of satellite cells, slowed activation, and decreased proliferation[35]. Thereby decreasing the regenerative ability of the muscle, resulting in damaged sections being removed through apoptosis[26].

Increased DNA fragmentation, a hallmark of apoptosis, is commonly reported in aging skeletal muscle[36]. Additionally, the expression of apoptotic proteins becomes altered with age.

Basel levels of pro-apoptotic proteins such as Bax, are higher in skeletal muscle of aged vs. young animals. As well, aged animals show an increased Bax:Bcl-2 ratio, and caspase-3 levels[26]. Supporting this, Song et al. reported an age-associated increase in the Bax:Bcl-2 ratio in both the white gastrocnemius and the soleus muscle of aging rats[43]. Additionally, increased cytosolic and nuclear levels of AIF and EndoG have been reported in aged rats[37].

Anti-apoptotic proteins are also up-regulated with aging. For example, FLICE-like inhibitory protein (FLIP) which is highly expressed in skeletal muscle and known to inhibit the death-receptor pathway, is increased with aging[38]. Even with the attempt to increase anti-apoptotic proteins, this is ineffective at attenuating the myonuclear loss in aged muscles[31]. Hindlimb suspension, used to induce skeletal muscle atrophy, increases AIF and EndoG translocation from the mitochondria to the nucleus in aged but not of young rats[37]. Thus, in response to a stress, aged muscle demonstrates increased apoptotic signaling in skeletal muscle vs. young muscle[39].

Certain fiber types also exhibit differences in apoptotic signaling with age. For example, Bax content was found to be elevated in the EDL but not the soleus, yet an increase in TUNEL staining was shown in both muscles of aged animals, indicating DNA fragmentation was still occurring[40]. In another study, TNF-α, FADD, and caspase-8 content were higher in the superficial vastus lateralis, composed mainly of type II fibers, but not the soleus of aged rats[44]. However, others have observed differences in a number of apoptotic factors in both slow and fast muscle. Aged rats demonstrated increases in DNA fragmentation, caspase-3, and caspase-8 in both the soleus and plantaris, but significant correlations between these measures and the muscle weight was found only in the plantaris[38]. Overall, this data suggest that apoptosis is a common feature of aging muscle that may significantly contribute to muscle wasting and contractile

dysfunction with age. However, many of the key proteins that regulate these responses in aging muscle have not been closely studied. Furthermore, the apoptotic signaling pathways responsible for the observed DNA fragmentation and muscle wasting may be different in slow vs. fast muscle.

ARC

A particularly unique anti-apoptotic protein is apoptosis repressor with caspase recruitment domain (ARC). ARC is highly expressed in long-lived terminally differentiated tissue, such as skeletal, and cardiac muscle as well as neurons, but is absent is most other tissues. Accordingly, these tissues display a high resistance to apoptotic signaling. ARC is also unique because it is one of the only proteins that can act as an inhibitor of all three major apoptotic pathways (Figure 1). In the death receptor pathway, ARC can interact with Fas and FADD impairing death receptor activation, DISC assembly and, caspase-8 activation[41]. ARC can also directly bind and inhibit procaspase-8, preventing the mature caspase-8 from interacting with DISC assembly. Although ARC can bind caspases-2 and -8, it does not directly interact with any other caspases[42]. In the mitochondrial apoptotic pathway, ARC can inhibit Bax activation and translocation to the mitochondria. As well, ARC can bind to upstream Bax activators, such as Bcl-2 associated death promoter (Bad) and p53 upregulated modulator of apoptosis (PUMA), thereby preventing mitochondrial Bax pore formation[43]. ARC can also prevent MOMP by inhibiting mitochondrial fission. Dynamin-related protein-1 (Drp-1) is a fission protein that translocates from the cytosol to accumulate on the mitochondria to initiate fission once activated. Drp-1 accumulation requires PUMA, and ARC can inhibit this interaction[44]. Furthermore, ARC can antagonize p53-induced apoptosis by directly inhibiting the tetramerization domain of p53,

disabling p53's transcriptional function and exposing a p53 nuclear export signal that relocates p53 to the cytoplasm[45]. p53 can also inhibit ARC transcription[43] and promote ARC degradation through mouse double mutant 2 (MDM2) [46]. The extrinsic pathway can also activate mitochondrial-mediated apoptosis. This occurs through caspase-8-mediated cleavage of Bcl-2 homology3-interacting death domain agonist (BID) resulting in its activation and contribution to MOMP though its activation of Bax[14]. Additionally, ARC can inhibit ER-stress-induced cell death by buffering harmful signaling ions, such as cytosolic free calcium[47]. ARC's structure permits its many mechanisms of action. ARC is a 30 kDa protein with an n-terminal caspase recruitment domain (CARD), and an acidic-proline/glutamine (P/E) rich c-terminal. The P/E rich domain allows the binding of cytosolic free Ca^{2+}, and the CARD domain enables ARC to bind and inhibit many other apoptotic signaling proteins containing similar domains[42].

ARC expression changes with different metabolic states. Decreased ARC levels have been found in the soleus in states such as hypertension[48], in the heart in ischemia-reperfusion injury[49], and in skeletal muscle in states such as hypoxia and oxidative stress[50]. Conversely, increased ARC expression has been demonstrated in many cancers[5,50]. Interestingly, these conditions are associated with increased and decrease apoptosis, respectively. Furthermore, in healthy cells, ARC normally resides in the cytosol and the mitochondria, but in cancer ARC translocates to the nucleus where it inhibits the tumor suppressor p53-meditated apoptosis[45]. Therefore, not only is the presence/absence or expression of ARC important in regulating apoptosis in cells, but its localization may also be critical.

Moreover, ectopic expression of ARC in numerous cell types results in an increased resistance to apoptosis[51,52]. When no apoptotic stimulus is given, ARC knockdown in H9c2 cells causes spontaneous Bax activation and cell death[41,53], indicating that ARC is required for a basal

level of apoptotic resistance. Interestingly there is decreased ARC levels in heart failure; however, overexpressing ARC in adult rat hearts reduces ischemia-reperfusion-induced apoptosis and infarct size[53]. In contrast, ARC KO mice show a 50% increase in infarct size following ischemia-reperfusion injury and display increased Bax activation[49]. Additionally, the level of ROS can influence ARC expression. Varying levels of H_2O_2 have been shown to affect ARC differently. High and/or prolonged levels of H_2O_2 promote ARC degradation, by p53 prompting the transcription of MDM2, whereas low levels of H_2O_2 result in p53 inhibiting its transcription[43,46].

ARC and Aging

ARC expression has been measured in many studies, yet few have examined this in an aging model. These few studies have shown varying levels of ARC expression in different tissues and in its localization with aging. For example, in mouse ventricles ARC was shown to increase with age[54], whereas in the cytosolic fraction of rats frontal brain cortices, ARC decreases with age. In the same study, lifelong caloric restriction of the aged rats, actually increased the expression of ARC, thereby attenuating the increased mitochondrial apoptosis seen in aging, by decreasing the amount of Cyto-c release[55]. Total ARC expression did not change in rat gastrocnemius muscle, but decreased in the cytosolic fraction and increased in the mitochondrial fraction with age[56]. Given that the expression and localization of ARC changes with age, which may influence-aged associated muscle atrophy, further examination of ARC's role in aging skeletal muscle is necessary.

ARC in Skeletal Muscle

ARC has a vital role in skeletal muscle differentiation, with ARC content being undetectable in mono-nucleated myoblasts but with ARC content dramatically increasing as myoblasts differentiate into multi-nucleated myotubes[57]. Interestingly, this increased ARC expression in myotubes is associated with increase apoptotic resistance[58]. Recent work in our lab has demonstrated ARC's important role in skeletal muscle morphology. ARC has been shown to be fiber type specific, with type I fibers displaying a higher ARC content compared to type II fibers[48]. Red muscle contains a higher percentage of type I fibers compared to white skeletal muscle, therefore also having an increased ARC content. Work from our lab has also found that adult ARC KO mice display a fiber type shift towards a faster phenotype, along with decreased fiber cross sectional area and increased DNA fragmentation in soleus muscle. Additional findings using subfractionation of red quadriceps, demonstrated an increased Bax:Bcl-2 in isolated mitochondrial fractions, as well as an increased cytosolic AIF protein content. Furthermore, mitochondria from adult ARC KO animals are more susceptible to calcium-induced mPTP formation and mitochondrial membrane depolarization, two early events during mitochondria-mediated apoptotic signaling. Another study, found decreased ARC protein levels in the soleus of hypertensive rats, along with increased DNA fragmentation and nuclear AIF[59]. Given the critical role of ARC in apoptotic signaling, and the current evidence showing altered morphology, basal apoptosis, and mitochondrial apoptotic susceptibility in skeletal muscle in ARC-deficient animals, it is of interest to examine the role of ARC in aging-related apoptosis and wasting.

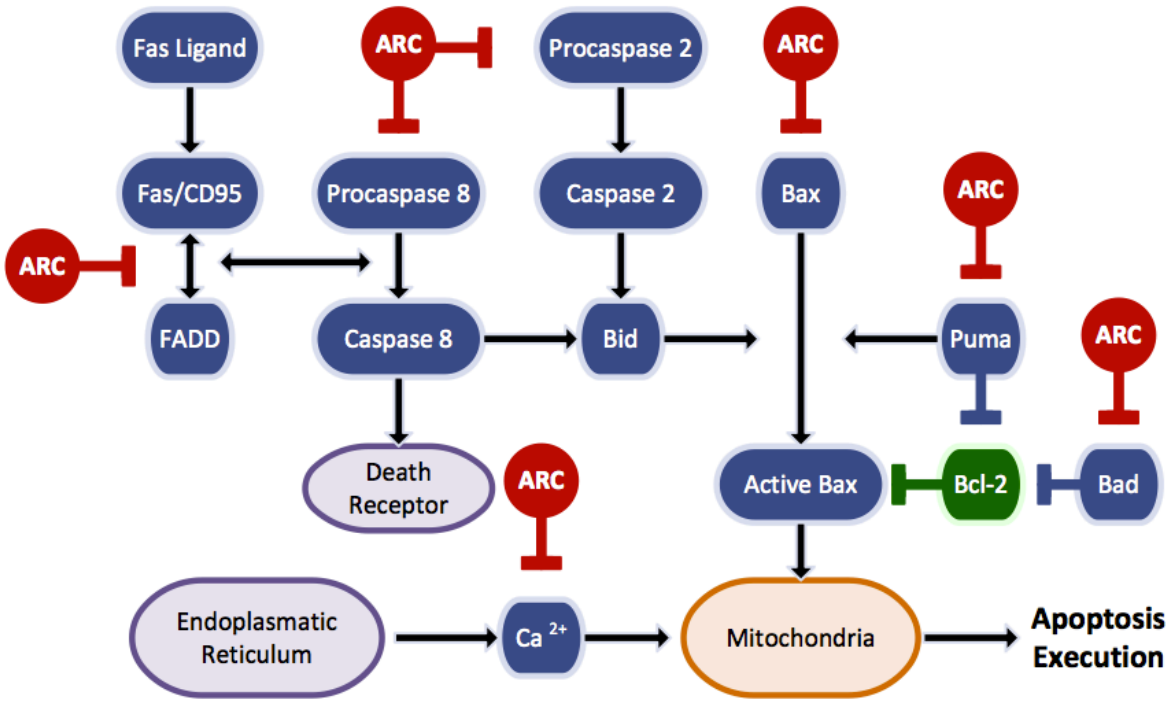

Figure 1. Diagram of ARC's anti-apoptotic influence. Adapted from Ludwig-Galezowska et al., 2011[42].

Purpose

ARC is an anti-apoptotic protein shown to influence a number of apoptotic signaling pathways; however, most research has focused on ARC's role in cardiac muscle and cancer. Previous research has examined the content of ARC in skeletal muscle, with more recent work in our lab having revealed ARC's important role in apoptotic signaling and morphology in skeletal muscle. Aging is associated with muscle wasting, resulting from an increased apoptotic signaling. Currently, there is no research examining the influence of ARC on aging-related skeletal muscle apoptosis and wasting.

Therefore, the purpose of this thesis was to examine the role of ARC in aging skeletal muscle and to specifically study ARC's influence on apoptosis, muscle wasting, contractile function, and muscle fiber distribution. Experiments were performed between wild-type and ARC-deficient mice at three different ages (Figure 2) and outcomes were measured in both oxidative and glycolytic muscles containing different fiber type compositions. Morphological and phenotypic measurements included muscle weights, muscle cross sectional area, fiber type composition, and fiber-specific cross sectional area. Apoptotic signaling examination included the expression of a number of key apoptotic proteins and proteases, both in whole muscle and subcellular fractions. In addition, muscle contractility measurements were conducted in both the soleus and plantaris.

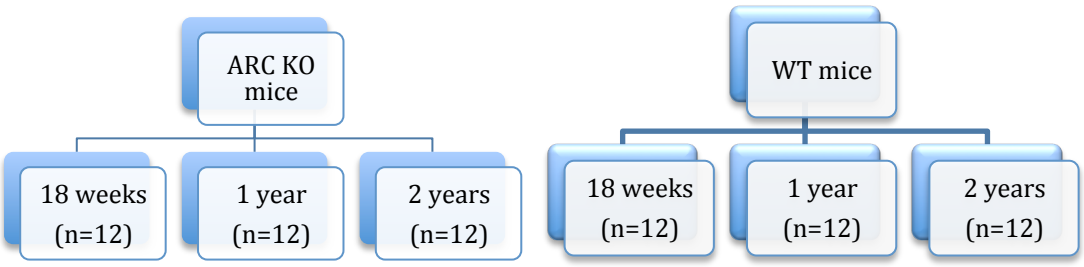

Figure 2. Experimental design.

Hypothesis

The hypotheses for this work were as follows:

- There will be greater skeletal muscle atrophy in animals as they age, with two year old animals displaying the greatest changes
    - Aging WT mice will display a decrease in type I fiber cross sectional area with a greater decrease in type II fibers.
    - Since ARC is an anti-apoptotic protein we hypothesize that as ARC KO mice age they will display a greater decrease in fiber cross sectional area in both type II and type I fibers.
    - Since ARC is highly expressed in type I fibers, the fiber atrophy will be further exacerbated in type I fibers.
    - Aging WT mice will also display a shift toward a slower myosin heavy chain expression. This fiber type shift will be attenuated in aging ARC KO mice.
- Apoptotic signaling will increase in the skeletal muscle as mice age with two year old mice displaying the greatest changes
    - Aging WT mice will display an increase in pro-apoptotic signaling in both slow and fast muscle, but to a greater extent in fast muscle.
    - We hypothesize that as ARC KO mice age they will display the greatest increase in pro-apoptotic signaling in both fast and slow muscle.
    - Since ARC is highly expressed in type I fibers, the pro-apoptotic signaling will be further exacerbated in slow muscle.
- The greater apoptotic signaling seen with increasing age will be mediated by the mitochondrial pathway in animals as they age, with the two year old animals displaying

the greatest changes

    - We hypothesize that aging WT mice will display increased mitochondrial levels of Bax and increased cytosolic levels of AIF, and cytochrome c.
    - We hypothesize that aging ARC KO mice will display higher levels of mitochondrial Bax and higher cytosolic levels of AIF, and cytochrome c.

- The greater apoptotic signaling and skeletal muscle atrophy demonstrated with increasing age, will result in decreased force production and fatigue resistance in mice as they age, with the 2 year old mice displaying the greatest changes
    - Aging WT mice will display decreased force production in both soleus and plantaris, but a greater decrease in the plantaris.
    - Aging ARC KO mice will display the greatest decrease in force production in both the soleus and plantaris.
    - Since ARC is highly expressed in the soleus, the decreased force production will be further exacerbated in the soleus.

Methods

Animals

ARC KO mice were obtained from Dr. Rudiger VonHarsdorf and Dr. Stefan Donath and were derived from C57BL/6 mice (Charles River). ARC KO mice were crossbred with C57BL/6 mice to generate mice heterozygous for wild-type (WT) and disrupted ARC alleles. Breeding pairs were established with heterozygous mice to produce male pups homozygous for the WT or ARC KO allele, which were used for the analyses. Three age groups were examined: a young adult group (WT-18.74±1.27 weeks, KO-18.56±2.28 weeks), a middle age adult group (WT-53.48±3.83, KO-55.72±3.32 weeks), and an old adult group (WT-103.03±1.58, KO-102.51±3.06 weeks). Littermates were used whenever feasible. Mice are housed with littermates on a 12:12hr reverse light-dark cycle in a temperature (20-21°C) and humidity (≈50%) controlled environment. Mice were provided with standard rodent lab chow and tap water ad libitum. All animal procedures were approved and performed in accordance with the guidelines established by the University of Waterloo Animal Care Committee.

Genotyping

Mice were genotyped at four weeks of age using an ear notch, snap frozen in liquid nitrogen. Using Purelink DNA extraction kit (Invitrogen), the DNA was extracted, purified and stored at 4°C for less than 48 hours. A mixture of RedTaq Polymerase (Sigma-Aldrich), H_20, and the forward and reverse primers were added to the DNA. Sequences of the WT ARC allele forward and reverse primers are 5'GATACCAGGAGATCTCTCAAAATT3' and 5'CAGCGCATCCAAGGCTTCGTACTC3', respectively. The disrupted ARC allele forward and reverse primers are 5'GATACCAGGAGATCTCTCAAAATT3' and

5’GATTGGGAAGACAATAGCAGGCATGC3’, respectively. Samples were placed in a thermal cycler (BIO-RAD) and denatured at 93°C for two minutes, followed by 1 minute of annealing at 55°C and five minutes of extension. Subsequently, samples underwent 28 cycles of denaturing for 30 seconds at 93°C, annealing for 30 seconds at 55°C, and extension for three minutes at 72°C. Lastly, samples underwent extension for seven minutes at 72°C. Samples were then separated on a 1% agrose gel containing 0.01% ethidium bromide (BioShop) and imaged using ChemiGenius 2 Bio-Imaging System (Syngene). Verification of genotyping was completed using western blot analysis for ARC protein expression.

Isolation of Skeletal Muscle

At the appropriate age, mice were weighed and anesthetized with pentobarbital sodium and euthanized by removing the heart. The soleus, plantaris, extensor digitorum longus (EDL), heart, gastrocnemius, tibialis anterior (TA), and quadriceps were removed, placed on ice and weighed. Whole quadriceps, TA and gastrocnemius were separated into red and white portions. The mid-belly of the soleus, plantaris, and EDL was mounted in OCT (Tissue-Tek) embedding media, frozen in liquid nitrogen cooled isopentane, and stored at -80°C until sectioned for immunohistochemistry. All remaining muscles were snap frozen in liquid nitrogen and stored at -80°C until analysis.

Muscle Contractility Measurements

For contractile measures, intact soleus and plantaris muscle were isolated from opposing hind limbs of the mice and held in a Tyrode’s dissecting solution (136.5 mM NaCl, 5.0 mM KCl, 11.9 mM $NaHCO_3$, 1.8 mM $CaCl_2$, 0.4 mM NaH_2PO_4, 0.1 mM EDTA, and 0.5 mM $MgCl_2$; pH

7.5) on ice, until experimentation. Muscles were mounted vertically in a 1200A *in vitro* test system (Aurora Scientific Inc.) as previously described[115]. The distal end of soleus muscles clamped at the calcaneus, while the proximal end was tied and super glued to a 10-0 silk suture loop attached to a stainless steel hook. The hook was attached to a dual mode model 300C servomotor (Aurora Scientific Inc.), which was used to measure force. The plantaris was mounted in an inverted position with the calcaneus tied to the hook with a suture loop, while the proximal end of the muscle was left attached to the knee and the bone was clamped to hold the muscle in place. Experiments were performed in an oxygenated (95% O_2, 5% CO_2) Tyrode's solution (121 mM NaCl, 5.0 mM KCl, 24 mM $NaHCO_3$, 1.8 mM $CaCl_2$, 0.4 mM NaH_2PO_4, 5.5 mM glucose, 0.1 mM EDTA, and 0.5 mM $MgCl_2$; pH 7.3) maintained at 25°C via a jacked water bath. A model 701C stimulator (Aurora Scientific Inc.) applied computer controlled stimulation via flanking plate field stimulus electrodes at supramaximal voltage, 0.2 ms pulse width. Muscles were stimulated at 100 Hz for 0.35 s to take up any slack in the system prior to and following determination of optimal length for twitch force production (L_o), where all subsequent experiments were performed. A force-frequency relationship was generated for each muscle using select frequencies between 1 and 100 Hz, applied at 60 s intervals. This was followed by a 5 minute fatiguing protocol consisting of 350 ms volleys of 70 Hz stimulation applied once every 1.5 s, following which tendon-free muscle mass was recorded. Fatigue indices included the number of contractions required for 70 Hz force to be reduced by 50%, and the percent decline in 70 Hz force between the first and final contractions in the 5 minute protocol.

Immunofluorescence Analyses

OCT embedded soleus and plantaris skeletal muscles were cut into 10 μm thick serial

cross sections with a cryostat (Thermo Electronic) maintained at -20°C as previously described[48]. Myosin heavy chain (MHC) expression was analyzed using immunofluorescence staining as previously described[60]. Slides were blocked with 10% goat serum, and then incubated with primary antibodies against MHCI (BA-F8), MHCIIa (SC-71), and MHCIIb (BF-F3) (Developmental Studies Hybridoma Bank). Sections were washed 3 x 5 minutes in PBS and incubated with anti-mouse isotype-specific Alexa Fluor 350, Alexa Fluor 488, and Alexa Fluor 555 secondary antibodies (Molecular Probes). Sections were washed 3 x 5 minutes in PBS, than coverslips mounted using Prolong Gold antifade reagent (Molecular Probes). This resulted in detection of type I fibers (blue), type IIA fibers (green), type IIB fibers (red), and type IIX fibers (unstained). Background staining was previously tested using only fluorescent-conjugated secondary antibody cocktails[60]. Slides were visualized using an Axio Observer Z1 fluorescent microscope equipped with an AxioCam HRm camera and associated AxioVision software (CarlZeiss). Fiber type number and percentage were analyzed by examining whole muscle composites of 20X magnification by counting all fibers within the section. Whole muscle and individual fiber cross sectional area was determined by counting 30 fibers per fiber type per section using Image Pro-Plus imaging software.

Preparation of Whole Muscle Lysates and Subcellular Fractions

Whole muscle lysates of soleus and plantaris were homogenized in ice-cold muscle lysis buffer (20 mM HEPES, 10 mM NaCl, 1.5 mM MgCl, 1 mM DTT, 20% glycerol and 0.1% Triton X100; pH 7.4) and protease inhibitors (Complete Cocktail; Roche Diagnostics) using a glass mortar and pestle. Homogenates were then centrifuged at 1000 x g for 10 minutes at 4°C, and the supernatant was collected.

Subcellular fractions were prepared as previously described[24]. Briefly, red and white quadriceps muscle was gently homogenized on ice using a glass mortar and pestle in a subcellular fractionation buffer (250 mM sucrose, 20 mM HEPES, 10 mM KCl, 1 mM EDTA, 1 mM DTT; pH 7.4) with protease inhibitors (Complete Cocktail; Roche Diagnostics). The resulting homogenates were centrifuged at 800 g at 4°C for 10 min, yielding a pellet (P1) and supernatant (S1). The S1 fraction was then centrifuged at 800 g at 4°C for 10 min again, and the supernatant was transferred to a new tube (S2). The S2 fraction was centrifuged at 20,800 g at 4°C for 20 min, yielding a pellet containing mitochondria (M1) and the cytosolic supernatant (C1). The M1 pellet was washed with subcellular fractionation buffer and centrifuged at 16,000 g at 4°C for 20 min. This pellet resulted in the mitochondrial-enriched fraction. The cytosolic (C1) supernatant was centrifuged at 20,800 g at 4°C for 20 min to ensure that it contained no residual mitochondria. The resulting supernatant was the cytosolic-enriched fraction. The P1 pellet was washed and centrifuged three more times at 800 g at 4°C for 10 min. Lysis buffer (200 μl) and 5 M NaCl (27.7 μl) was added to the resulting pellet and rotated for one hour at 4°C, following which the samples were centrifuged at 20,800 g at 4°C for 15 min. This supernatant resulted in the nuclear-enriched fraction. Whole and subcellular fraction protein content was determined using the BCA protein assay. The purity of each subcellular fraction was verified by immunoblot analysis using antibodies against adenine nucleotide translocase (ANT) (Santa Cruz Biotechology) for the mitochondrial fraction, copper zinc superoxide dismutase (CuZnSOD) (Stressgen Bioreagents) for the cytosolic fraction, and histone H2B (Santa Cruz Biotechnology) for the nuclear fraction (Figure 26).

Immunoblot Analyses

Equal amounts of protein were loaded and separated on 12% or 15% SDS-PAGE gels, with each gel containing two samples from each group. Gels were then transferred onto PVDF membranes (Bio-Rad Laboratories), and blocked in 5% milk-TBST for one hour at room temperature. Membranes were incubated either overnight at 4°C or for one hour at room temperature with primary antibodies against: apoptosis inducing factor (AIF) (1:2000, sc-13116), adenine nucleotide translocase (ANT) (1:1000, sc-11433), apoptosis repressor with caspase recruitment domain (ARC) (1:1000, sc-11435), Bcl-2 associated X protein (Bax) (1:1000, sc-493), B-cell lymphoma 2 (Bcl-2) (1:150, sc-7382), B-cell lymphoma-extra large (Bcl-XL) (1:250, sc-8392), BH3 interacting-domain death agonist (BID) (1:500, sc-11423), cytochrome c (Cyto-c) (1:3000, sc-13156), histone H2B (1:500, sc-8650) (Santa Cruz Biotechnology); catalase (1:2000: mAb 12980), dynamin-related protein 1 (Drp1) (1:300, mAb 8570) (Cell Signaling); second mitochondrial activator of caspase (SMAC) (1:2000, ADI-905-244) (Assays Designs); copper zinc superoxide dismutase (CuZnSOD) (1:3000, ADI-SOD-101), heat shock protein 70 (Hsp70) (1:2000, ADI-SPA-810), manganese superoxide dismutase (MnSOD) (1:7500, ADI-SOD-110), and X-linked inhibitor of apoptosis (XIAP) (1:1000, ADI-AAM-050-E) (Stressgen Bioreagents). Membranes were washed with TBST and incubated with the appropriate horseradish peroxide (HRP)-conjugated secondary antibody (1:5000) (Santa Cruz Biotechnology) for one hour at room temperature. Proteins were visualized using the Amersham Enhanced Chemiluminescence Western Blotting detection reagents (GE Healthcare) and the ChemiGenius 2 Bio-Imaging System (Syngene). After imaging, to ensure equal loading and quality of protein transfer, membranes were stained with Ponceau S (Sigma-Aldrich). To account for any variations between gels, a standard was loaded with each gel and all samples normalized

relative to this standard.

Caspase and Calpain Activity

The enzymatic activity of caspase-2, caspase-3, caspase-8, and caspase-9 were determined in duplicate in muscle homogenates using the substrates, Ac-VDVAD-AMC (Alexis Biochemicals), Ac-DEVD-AMC (Alexis Biochemicals), Ac-IETD-AMC (Sigma-Aldrich), and Ac-LEHD-AMC (Alexis Biochemicals), respectively[24]. Briefly, muscle was homogenized in ice-cold muscle lysis buffer, without protease inhibitors, and centrifuged at 1000 x g for ten minutes at 4°C. The supernatants were then incubated in duplicate with the appropriate substrate at room temperature for two hours. During this time, the florescence was measured every 15 minutes using SPECTRAmax Gemini XS microplate spectrofluorometer (Molecular Devices) with excitation and emission wavelengths of 360 nm and 440 nm, respectively. Control experiments included samples containing purified active enzymes and specific caspase inhibitors (caspase-2, Ac-VDVAD-CHO; caspase-3, Ac-DEVD-CHO; capsase-8, Ac-IETD-CHO; caspase-9, Ac-LEHD-CHO). Caspase activity was normalized to total protein content and expressed as mean fluorescence intensity in AU per mg of protein.

Calpain activity was determined using muscle homogenates (processed as above) and the samples were incubated in duplicates at 37°C with the substrate, Suc-LLVY-AMC (Enzo Life Sciences) with or without the specific calpain inhibitor, Z-LL-CHO (Enzo Life Sciences). Fluorescence was measured using a SPECTRAmax Gemini XS microplate spectrofluorometer (Molecular Devices) with excitation and emission wavelengths of 380 nm and 460 nm, respectively. The fluorescence was subtracted from the sample with the calpain inhibitor, from the sample without the calpain inhibitor to determine calpain activity, as previously described[45].

Statistical Analysis

All data is represented as means ± SEM. All data was analyzed using two-way analyses of variance (ANOVA) with $p<0.05$ considered statistically significant and $p<0.10$ considered a trend. Significant interaction effects were assessed using the Tukey HSD post-hoc test. All statistical analyses were performed using Prism 5 statistical software.

Results

ARC KO Mouse Model

Transgenic mice with a mutated ARC gene were used to examine the role of ARC in skeletal muscle. Firstly, PCR analysis was used to determine that the wild type ARC allele was absent from KO mice (Figure 3A). Western blotting was subsequently performed for ARC protein to verify the lack of ARC expression in both the soleus and plantaris muscles of KO mice (Figure 3B). ARC protein expression was found to be higher in the soleus versus the plantaris muscle when normalized for total protein content in previous studies[24].

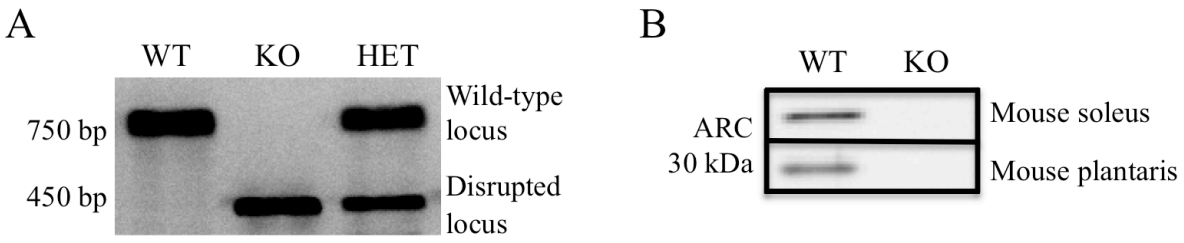

Figure 3. Generation of ARC knockout (KO) animals. A: PCR analysis showing expression of the wild type (WT) (750 bp) and disrupted (450 bp) allele. B: Western blot analysis of ARC protein content in WT and ARC KO animals.

Morphological Characteristics

Body and muscle weights were examined to determine changes in size (Table 1). There was a main effect of age ($p<0.0001$) for body weight, with the 18 week group having significantly lower weights than the 1 and 2 year groups ($p<0.0001$). Heart weight relative to kidney weight was not different between groups. However, there was a trend towards a main effect of genotype ($p=0.084$) for heart weight relative to body weight, with the KO group having a higher ratio. There was also a main effect of age ($p<0.0001$), with the 1 year group having a

significantly lower ratio then the 18 week ($p<0.05$) and 2 year groups ($p<0.0001$). Additionally, a significantly lower ratio was found in the 18 week compared to the 2 year group ($p<0.05$). There was a main effect of genotype ($p<0.05$) for kidney weight relative to body weight, with the KO group having a higher ratio. There was also a main effect of age ($p<0.0001$), with the 1 year group having a significantly lower ratio then the 18 week ($p<0.05$) and 2 year groups ($p<0.0001$). There was a trend ($p=0.06$) towards a main effect of genotype on soleus weight, with decreased weights in the KO group. There was also a main effect of age ($p<0.0001$), with the 2 year group having significantly decreased weights compared to the 18 week ($p<0.01$) and 1 year groups ($p<0.0001$). There was a main effect of age ($p<0.0001$) for soleus weight relative to body weight, with the ratio decreasing with age. The 18 week group had a significantly increased ratio compared to the 1 and 2 year groups ($p<0.0001$), as well as the 1 year group having a significantly increased ratio compared to the 2 year group ($p<0.05$). There was a main effect of genotype ($p<0.05$) for soleus weight relative to kidney weight, with the ratio lower in the KO group. There was also a main effect of age ($p<0.0001$), with the ratio decreasing with age. The 18 week group had a significantly increased ratio compared to the 1 and 2 year groups ($p<0.0001$), as well as the 1 year group having a significantly increased ratio compared to the 2 year group ($p<0.0001$). There was a main effect of genotype ($p<0.05$) for plantaris weight, being decreased in the KO group. There was also a main effect of age ($p<0.0001$), with the 2 year group having a significantly lower weight than the 18 week ($p<0.001$) and 1 year groups ($p<0.0001$). There was a decreased ratio for the 2 year ($p<0.0001$) compared to the 18 week and 1 year groups for plantaris weight relative to body weight. There was also an increased ratio in the 1 year KO compared to the 1 year WT group ($p<0.0005$). There was a main effect of genotype ($p<0.001$) for plantaris weight relative to kidney weight, with the ratio being decreased

in the KO group. There was also a main effect of age ($p<0.0001$), with the ratio significantly decreasing with age. The 18 week group had a significantly increased ratio compared to the 1 and 2 year groups ($p<0.0001$), as well as the 1 year group having a significantly increased ratio compared to the 2 year group ($p<0.0001$).

Total cross-sectional area (CSA) of both soleus and plantaris muscles were measured through histological staining (Figure 5 and 8). There was a main effect of age ($p<0.0001$) on CSA of the soleus, with significantly decreased CSA in the 2 year compared to the 18 week ($p<0.01$) and 1 year groups ($p<0.0001$). Further, there was a trend towards a decreased size with genotype in the KO group ($p=0.092$) (Figure 4A). There was a main effect of age ($p<0.0001$) on CSA of the plantaris, with the 2 year group being significantly smaller compared to the 18 week and 1 year groups ($p<0.0001$) (Figure 4B).

There was a main effect of age ($p<0.0001$) for total fiber number in the soleus, with the 2 year group having significantly fewer number of fibers compared to the 18 week ($p<0.0001$) and 1 year groups ($p<0.001$). There was also a main effect of genotype ($p<0.05$), with KO mice having fewer fibers (Appendix Figure 1A). In the plantaris there was a main effect of age ($p<0.01$), with the 2 year group having significantly fewer fibers compared to the 18 week ($p<0.01$) and 1 year groups ($p<0.05$) (Appendix Figure 1B).

To more closely examine the changes in total CSA and fiber number, fiber type-specific CSA and distribution were examined. In the soleus, there was a main effect of age ($p<0.0001$), with the 2 year group having a significant decrease in type I fiber CSA compared to the 18 week

($p<0.05$) and 1 year groups ($p<0.0001$) (Figure 6A). There was a main effect of age ($p<0.001$), with the 1 year group having a significant increase in type IIA fiber CSA compared to the 18 week ($p<0.001$) and 2 year groups ($p<0.01$) (Figure 6B). There was a trend towards a decrease in type IIX CSA with age ($p=0.055$) (Figure 6C), and no differences in type IIB CSA (Figure 6D). In the plantaris, there were no differences in type I fiber CSA between groups (Figure 9A); however, a main effect of age was found in type IIA CSA ($p<0.01$), with the 2 year group having a significant decrease in CSA compared to the 1 year group ($p<0.01$) (Figure 9B). There was a main effect of age ($p<0.0001$), with the 2 year group having a significant decrease in type IIX fiber CSA compared to the 18 week ($p<0.01$) and 1 year groups ($p<0.0001$) (Figure 9C). There was a main effect of age ($p<0.0001$), with the 2 year group having a significant decrease in type IIB fiber CSA compared to the 18 week and 1 year groups ($p<0.001$) (Figure 9D).

In the soleus, the percentage of type I fibers was significantly higher in 2 year compared to the 18 week ($p<0.0001$) and 1 year groups ($p<0.01$) (Figure 7A). Type IIA fiber percentage was not different between groups (Figure 7B). Type IIX fiber percentage was significantly higher in the 18 week group than the 1 year ($p<0.05$) and 2 year groups ($p<0.0001$) (Figure 7C). Type IIB fiber percentage was significantly higher in the 18 week group compared to the 1 and 2 year groups ($p<0.05$) (Figure 7D). In the plantaris, the 18 week group had a significantly higher percentage of type I fibers than the 2 year group ($p<0.001$) (Figure 10A). Type IIA fiber percentage was significantly lower in the 2 year group than the 18 week ($p<0.01$) and 1 year groups ($p<0.05$) (Figure 10B). Type IIX fiber percentage was not different between groups (Figure 10C). Type IIB fiber percentage was significantly higher in the 2 year compared to the 18 week and 1 year groups ($p<0.01$) (Figure 10D).

Table 1. Biometric characteristics of WT and ARC KO animals. Data are expressed as means ± SEM (n=12-22).

		18 Week		1 Year		2 Years		Significance	
		WT	KO	WT	KO	WT	KO	Age	Genotype
Age (weeks)		18.74 ± 1.27	18.56 ± 2.28	53.48 ± 3.83	55.72 ± 3.32	103.03 ± 1.58	102.51 ± 3.06		
Body Weight (g)		30.98 ± 1.98	29.04 ± 2.72	41.60 ± 6.97	40.51 ± 8.22	37.46 ± 4.14	38.92 ± 5.97	18 ($p<0.0001$) vs 1 and 2	
Heart Weight (mg)		121.78 ± 12.01	125.55 ± 9.44	146.49 ± 22.43	151.05 ± 16.09	163.72 ± 19.76	167.6 ± 27.73	18 vs 1 and 2 ($p<0.0001$), 1 vs 2 ($p<0.001$)	
Kidney Weight (mg)		178.85 ± 16.68	185.55 ± 18	213.24 ± 31.62	229.06 ± 25.07	232.57 ± 30.28	241.9 ± 28.41	18 vs 1 and 2 ($p<0.0001$), 1 vs 2 ($p<0.05$)	
Heart Weight (mg)/ Body Weight (g)		3.92 ± 0.36	4.16 ± 0.07	3.55 ± 0.36	3.83 ± 0.65	4.4 ± 0.56	4.34 ± 0.55	18 vs 1 and 2 ($p<0.05$), 1 vs 2 ($p<0.0001$)	
Heart Weight (mg)/ Kidney Weight (mg)		0.68 ± 0.25	0.68 ± 0.05	0.69 ± 0.07	0.66 ± 0.06	0.71 ± 0.04	0.69 ± 0.07		
Muscle Weight (mg)	**Soleus**	8.69 ± 1.02	8.47 ± 1.36	9.27 ± 1.5	8.52 ± 1.41	7.76 ± 1.25	7.35 ± 0.98	2 vs 18 ($p<0.01$) and 1 ($p<0.0001$)	
	Plantaris	18.06 ± 2.15	17.60 ± 1.37	18.27 ± 2.29	17.64 ± 2.06	16.48 ± 1.73	15.22 ± 2.04	2 vs 18 ($p<0.001$) and 1 ($p<0.0001$)	$p<0.05$ vs WT
Muscle Weight (mg)/ Body Weight (g)	**Soleus**	0.28 ± 0.03	0.29 ± 0.04	0.23 ± 0.04	0.21 ± 0.03	0.21 ± 0.04	0.19 ± 0.03	18 vs 1 and 2 ($p<0.0001$), 1 vs 2 ($p<0.05$)	
	Plantaris	0.58 ± 0.06	0.61 ± 0.06	0.44 ± 0.05	0.79 ± 0.23	0.44 ± 0.05	0.4 ± 0.06	2 ($p<0.0001$) vs 18 and 1	1 KO vs 1 WT ($p<0.001$)
Muscle Weight (mg)/ Kidney Weight (mg)	**Soleus**	0.05 ± 0.004	0.05 ± 0.01	0.04 ± 0.006	0.04 ± 0.005	0.03 ± 0.007	0.03 ± 0.005	18 vs 1 and 2, 1 vs 2 ($p<0.0001$)	$p<0.05$ vs WT
	Plantaris	0.10 ± 0.01	0.1 ± 0.01	0.09 ± 0.008	0.078 ± 0.007	0.07 ± 0.01	0.06 ± 0.009	18 vs 1 and 2, 1 vs 2 ($p<0.0001$)	$p<0.001$ vs WT

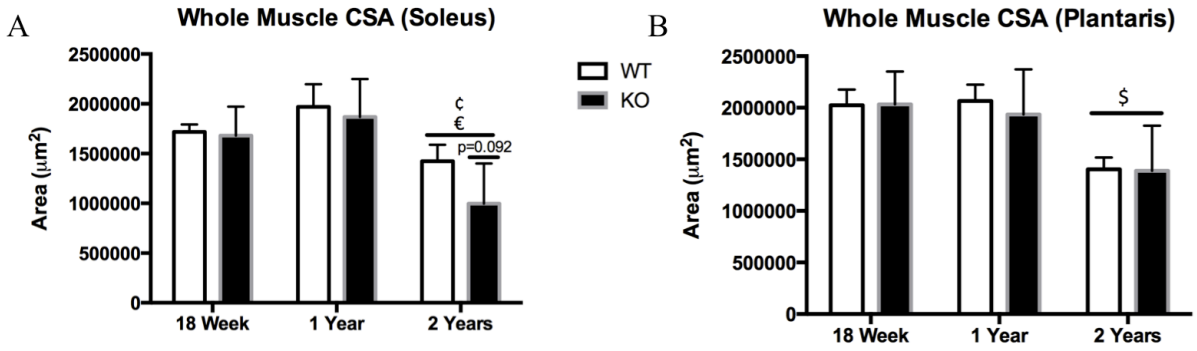

Figure 4. Total skeletal muscle cross-sectional area. A-B: Total muscle cross-sectional area in soleus and plantaris of wild type (WT) and ARC knockout (KO) animals (n=11-12). Data are expressed as means ± SEM (¢ main effect $p<0.01$ vs. 18 week, € main effect $p<0.001$ vs. 1 year, $ main effect $p<0.001$ vs. 18 week and 1 year).

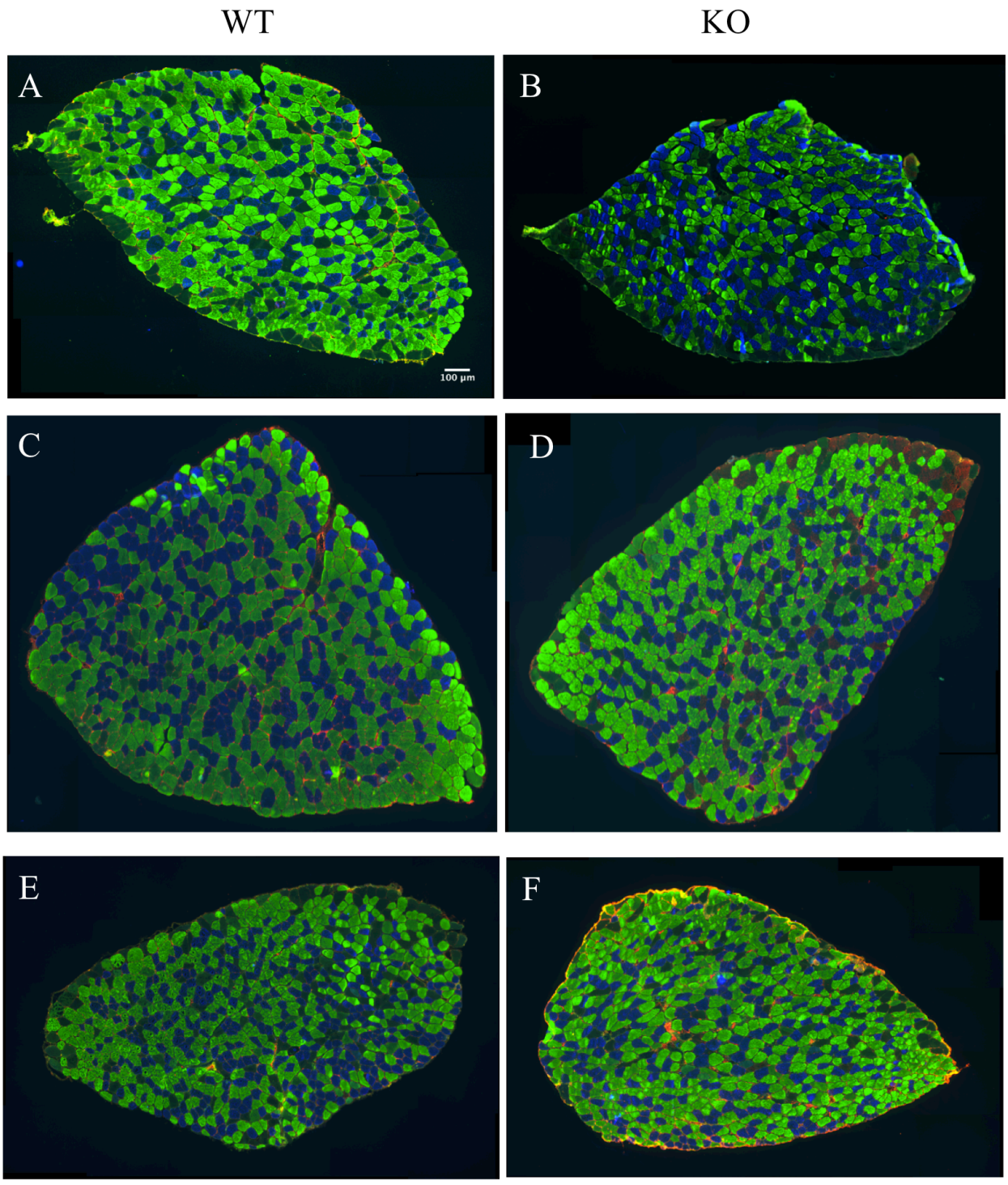

Figure 5. Representative immunohistochemical images of soleus muscle. A-F: Representative composite images of soleus whole-muscle cross-sections from wild type (WT) and ARC knockout (KO) animals treated with antibodies specific for the individual myosin heavy chain isoforms: type I (blue), type IIa (green), type IIb (red), and type IIx (unstained). A: 18 week WT, B: 18 week KO, C: 1 year WT, D: 1 year KO, E: 2 year WT, F: 2 year KO. Scale bar indicates 100 µm.

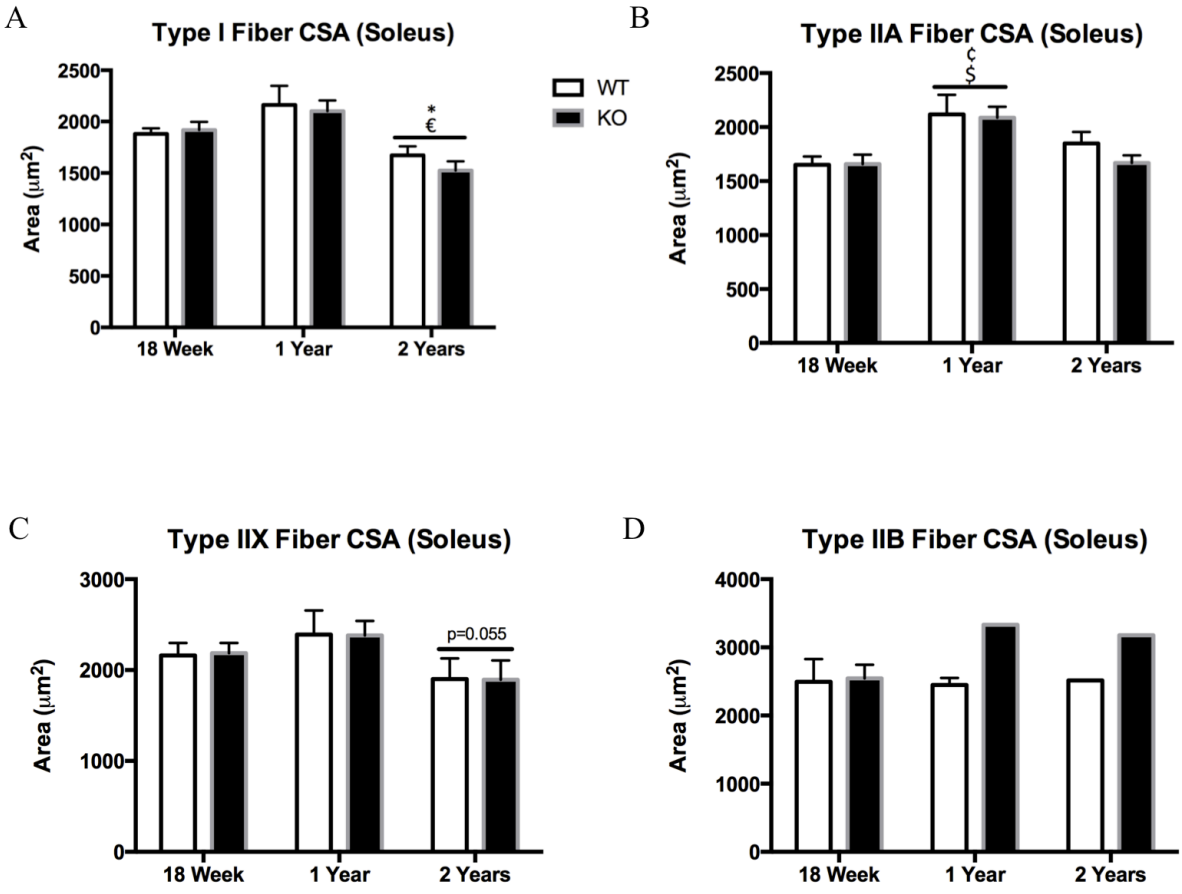

Figure 6. Immunohistochemical analysis of soleus muscle. A-D: Fiber type-specific cross-sectional area in soleus muscle of wild type (WT) and ARC knockout (KO) animals (n=11-12). Data are expressed as means ± SEM (* main effect $p<0.05$ vs. 18 week, € main effect $p<0.001$ vs. 1 year, ¢ main effect $p<0.01$ vs. 2 years, $ main effect $p<0.001$ vs. 18 week).

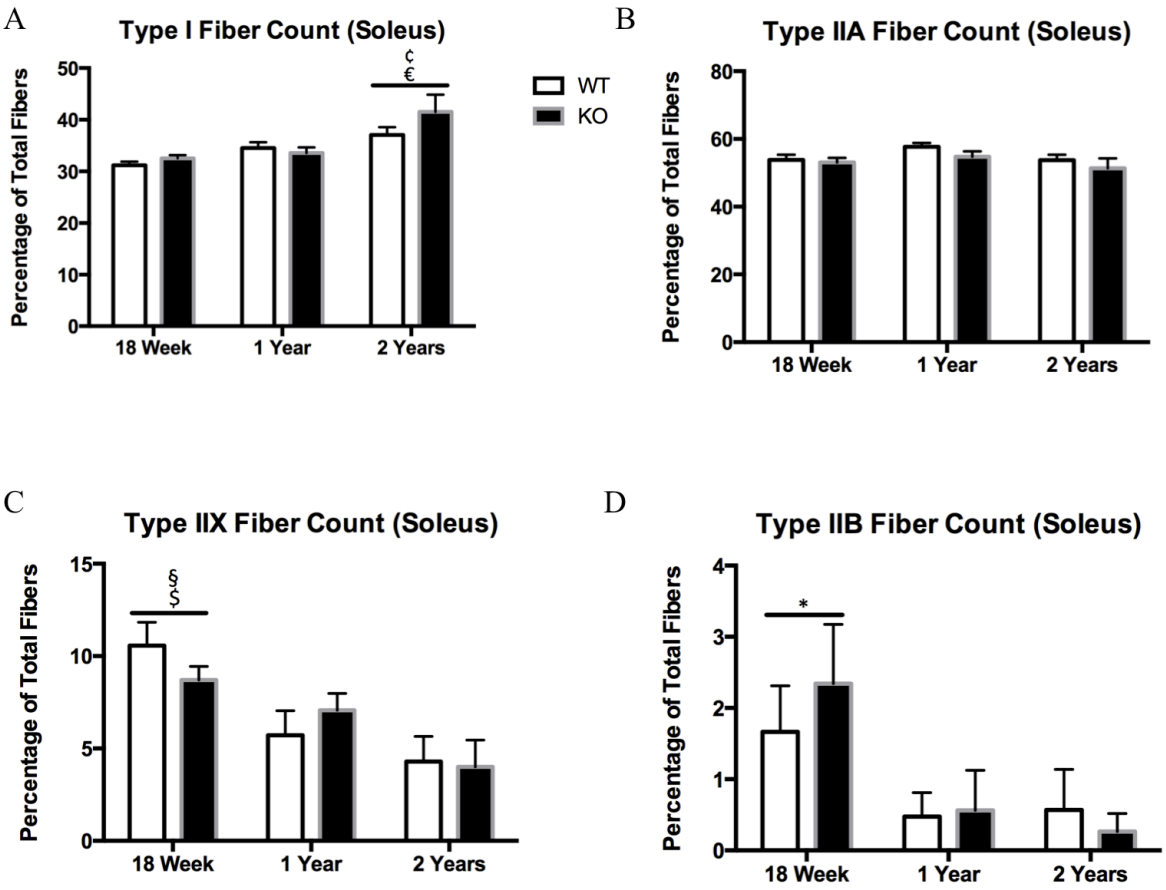

Figure 7. Immunohistochemical analysis of soleus muscle. A-D: Fiber type distribution (percentage of total fibers) in soleus of wild type (WT) and ARC knockout (KO) animals (n=11-12). Data are expressed as means ± SEM (¢ main effect $p<0.01$ vs. 1 year, € main effect $p<0.001$ vs. 18 week, § $p<0.05$ vs. 1 year, $ main effect $p<0.001$ vs. 2 years, * main effect $p<0.05$ vs. 1 and 2 years).

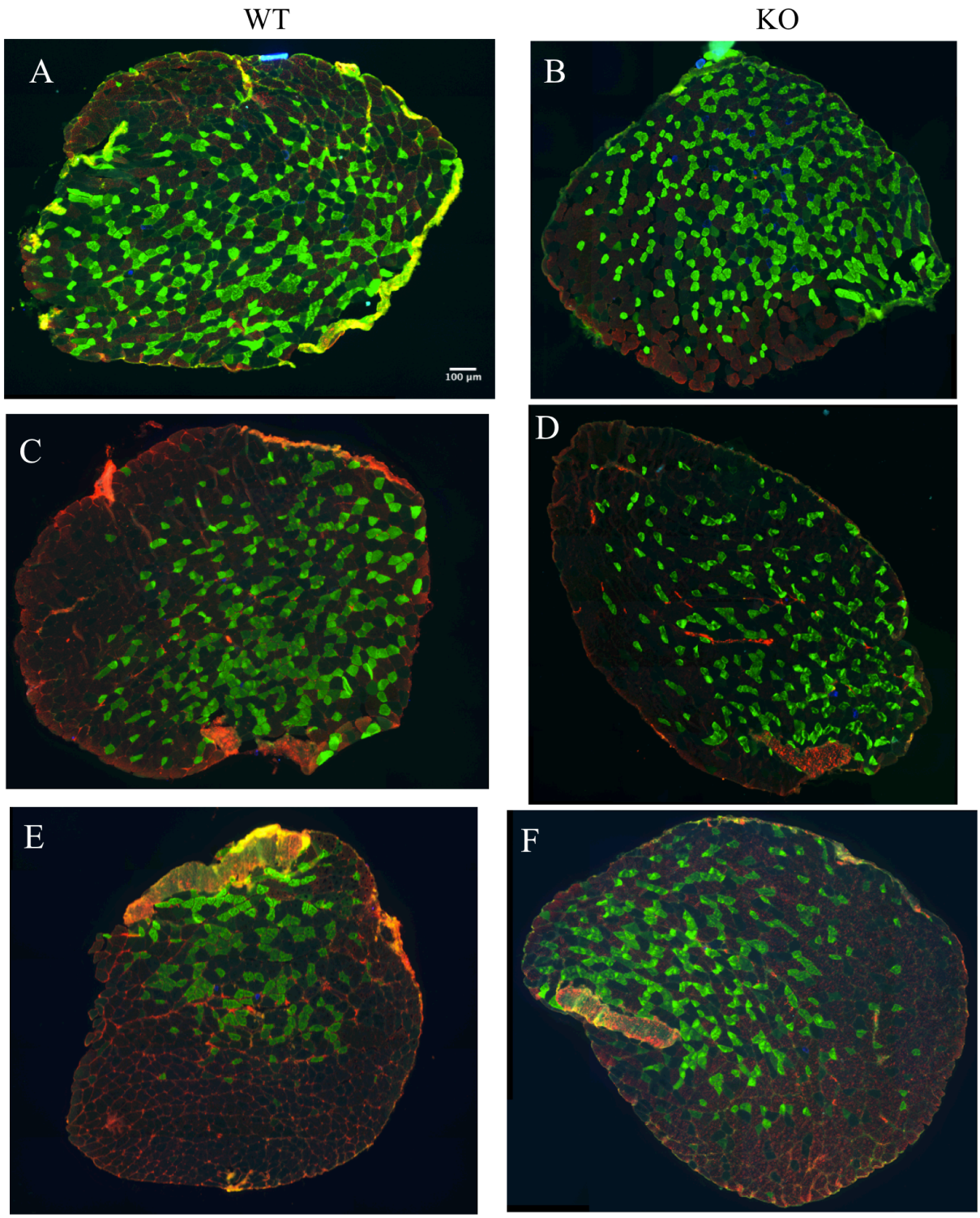

Figure 8. Representative immunohistochemical images of plantaris muscle. A-F: Representative composite images of plantaris whole-muscle cross-sections from wild type (WT) and ARC knockout (KO) animals treated with antibodies specific for the individual myosin heavy chain isoforms: type I (blue), type IIa (green), type IIb (red), and type IIx (unstained). A: 18 week WT, B: 18 week KO, C: 1 year WT, D: 1 year KO, E: 2 year WT, F: 2 year KO. Scale bar indicates 100 µm.

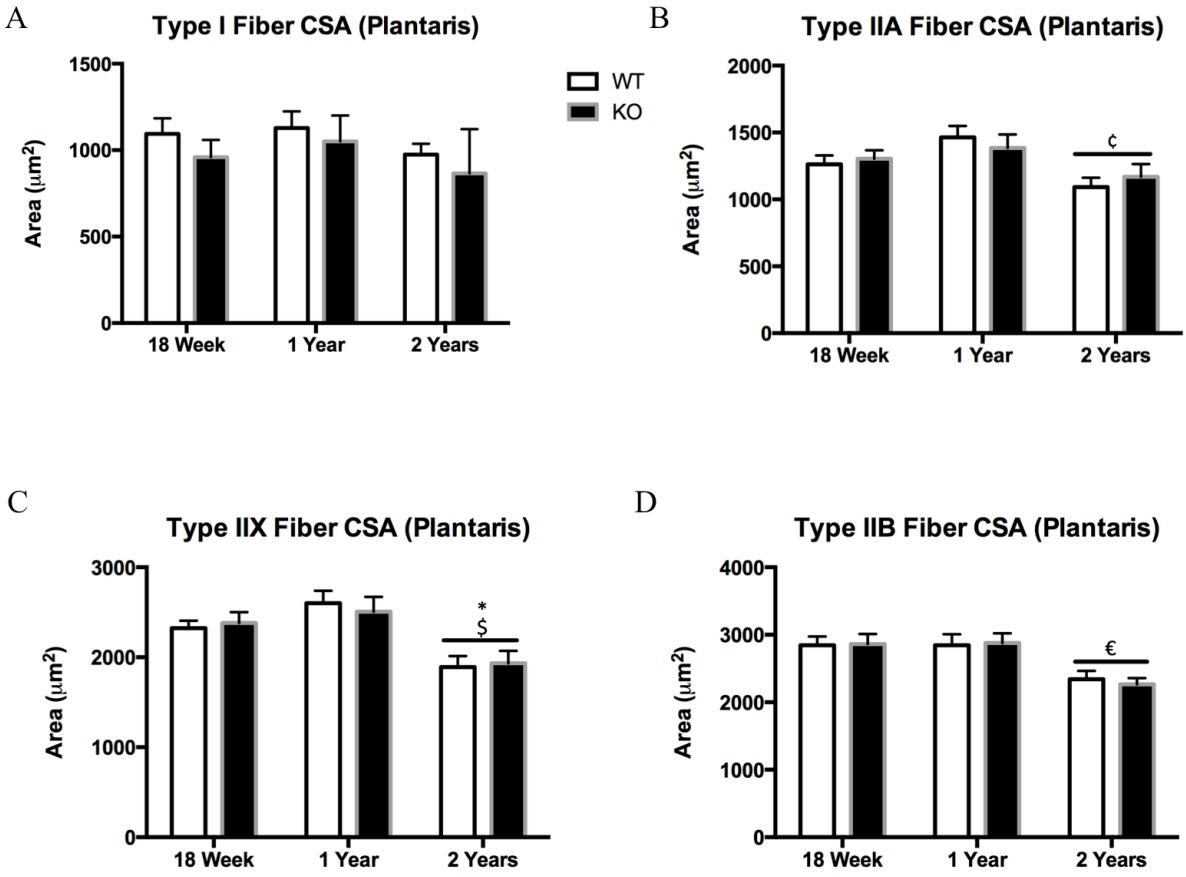

Figure 9. Immunohistochemical analysis of plantaris muscle. A-D: Fiber type-specific cross-sectional area in plantaris muscle of wild type (WT) and ARC knockout (KO) animals (n=11-12). Data are expressed as means ± SEM (¢ main effect $p<0.01$ vs. 1 year, € main effect $p<0.001$ vs. 18 week and 1 year, * main effect $p<0.01$ vs. 18 week, $ main effect $p<0.001$ vs. 1 year).

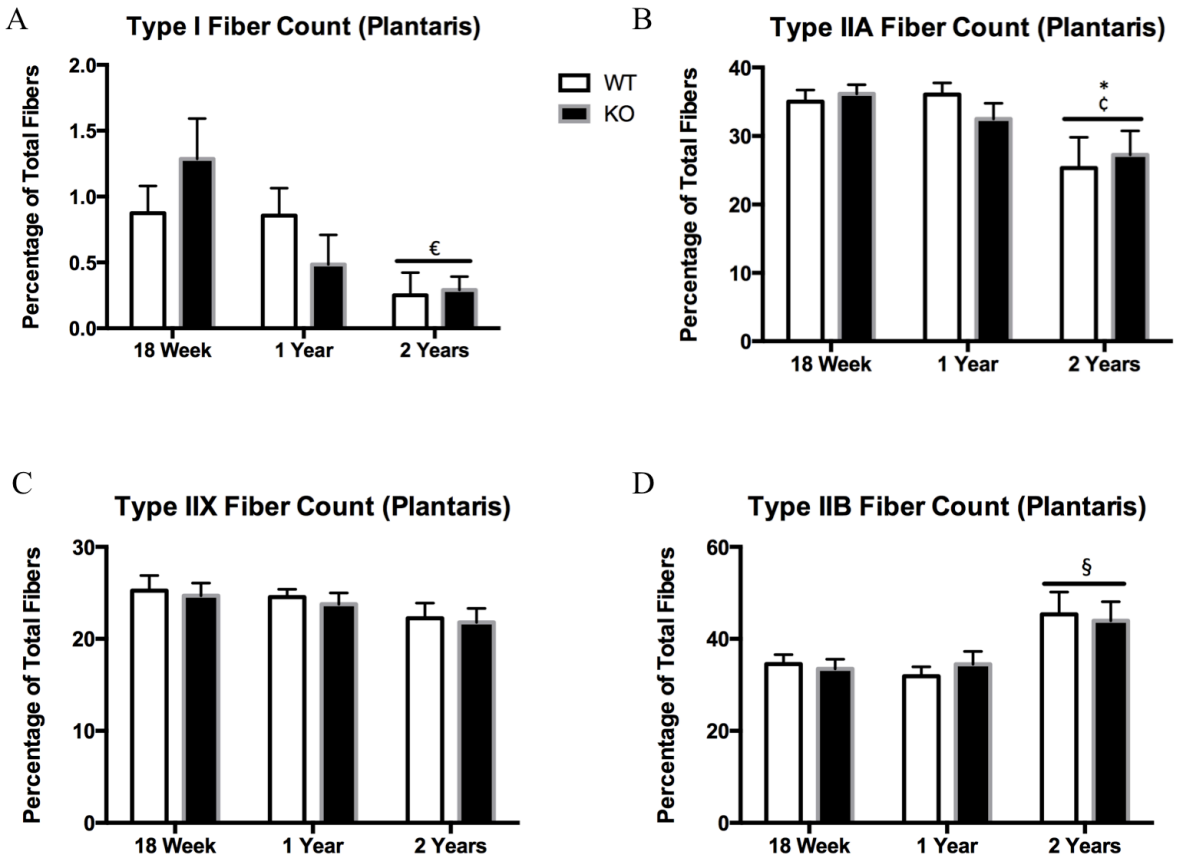

Figure 10. Immunohistochemical analysis of plantaris muscle. A-D: Fiber type distribution (percentage of total fibers) in plantaris of wild type (WT) and ARC knockout (KO) animals (n=11-12). Data are expressed as means ± SEM (€ main effect $p<0.001$ vs. 18 week, * main effect $p<0.05$ vs. 1 year, ¢ main effect $p<0.01$ vs. 18 week, § main effect $p<0.01$ vs. 18 week and 1 year).

Force Characteristics

In the soleus, there was no significant differences in force at 100 Hz, percent peak force remaining after 5 minutes of contraction, and number of contractions to 50% force reduction (Figure 11F, G, and H); however, the rate of twitch contraction showed a main effect of age ($p<0.01$), with the 2 year group demonstrating a significantly increased rate compared to the 18 week ($p<0.05$) and 1 year groups ($p<0.01$) (Figure 11A). The rate of twitch relaxation was significantly increased in the 2 year compared to the 18 week group ($p<0.05$) (Figure 11B). One-half relaxation time was significantly increased in the 2 year compared to the 18 week group ($p<0.05$) (Figure 11C). Time to peak tension was significantly increased in the 2 year compared to the 18 week group ($p<0.01$) (Figure 11D). Twitch to tetanus ratio was significantly increased in the 2 year compared to the 18 week and 1 year groups ($p<0.0001$) (Figure 11E). In the plantaris there were no significant differences in twitch to tetanus ratio, percent peak force remaining after 5 minutes of contraction, and the number of contractions to 50% force reduction (Figure 12E, G, and H). However, the rate of twitch contraction was significantly decreased in the 2 year compared to the 1 year group ($p<0.01$) (Figure 12A). The rate of twitch relaxation was significantly decreased in the 2 year compared to the 1 year group ($p<0.05$) (Figure 12B). One-half relaxation time was significantly increased in the 2 year compared to the 18 week group ($p<0.01$) (Figure 12C). Time to peak tension was significantly increased in the 2 year compared to the 18 week ($p<0.0001$) and 1 year groups ($p<0.05$) (Figure 12D). Lastly, there was a main effect of age ($p<0.05$) for force at 100 Hz (Figure 12F). Force-frequency curves were completed for both the soleus and plantaris (Appendix Figure 2).

(Next Page) Figure 11. Analysis of muscle contractility measurements. Analysis in the soleus of wild type (WT) and ARC knockout (KO) animals. A: Rate of contraction. B: Rate of relaxation. C: One half relaxation time. D: Time to peak tension. E: Twitch to tetanus ratio. F: Force at 100 Hz. G: Percent peak force remaining after five minutes of contraction. H: Number of contractions until 50% force reduction reached (n=5-8). Data are expressed as means ± SEM (* main effect $p<0.05$ vs. 18 week, ¢ main effect $p<0.01$ vs. 18 week, € main effect $p<0.001$ vs. 18 week and 1 year, § main effect $p<0.05$ vs. 18 week, # main effect $p<0.01$ vs. 1 year, $ main effect $p<0.05$ vs. 1 year).

(Next Page) Figure 12. Analysis of muscle contractility measurements. Analysis in the plantaris of wild type (WT) and ARC knockout (KO) animals. A: Rate of contraction. B: Rate of relaxation. C: One half relaxation time. D: Time to peak tension. E: Twitch to tetanus ratio. F: Force at 100 Hz. G: Percent peak force remaining after five minutes of contraction. H: Number of contractions until 50% force reduction reached (n=5-8). Data are expressed as means ± SEM (* main effect $p<0.05$ vs. 1 year, ¢ main effect $p<0.01$ vs. 18 week, € main effect $p<0.001$ vs. 18 week, § main effect $p<0.05$ vs. 1 year, # main effect $p<0.01$ vs. 1 year).

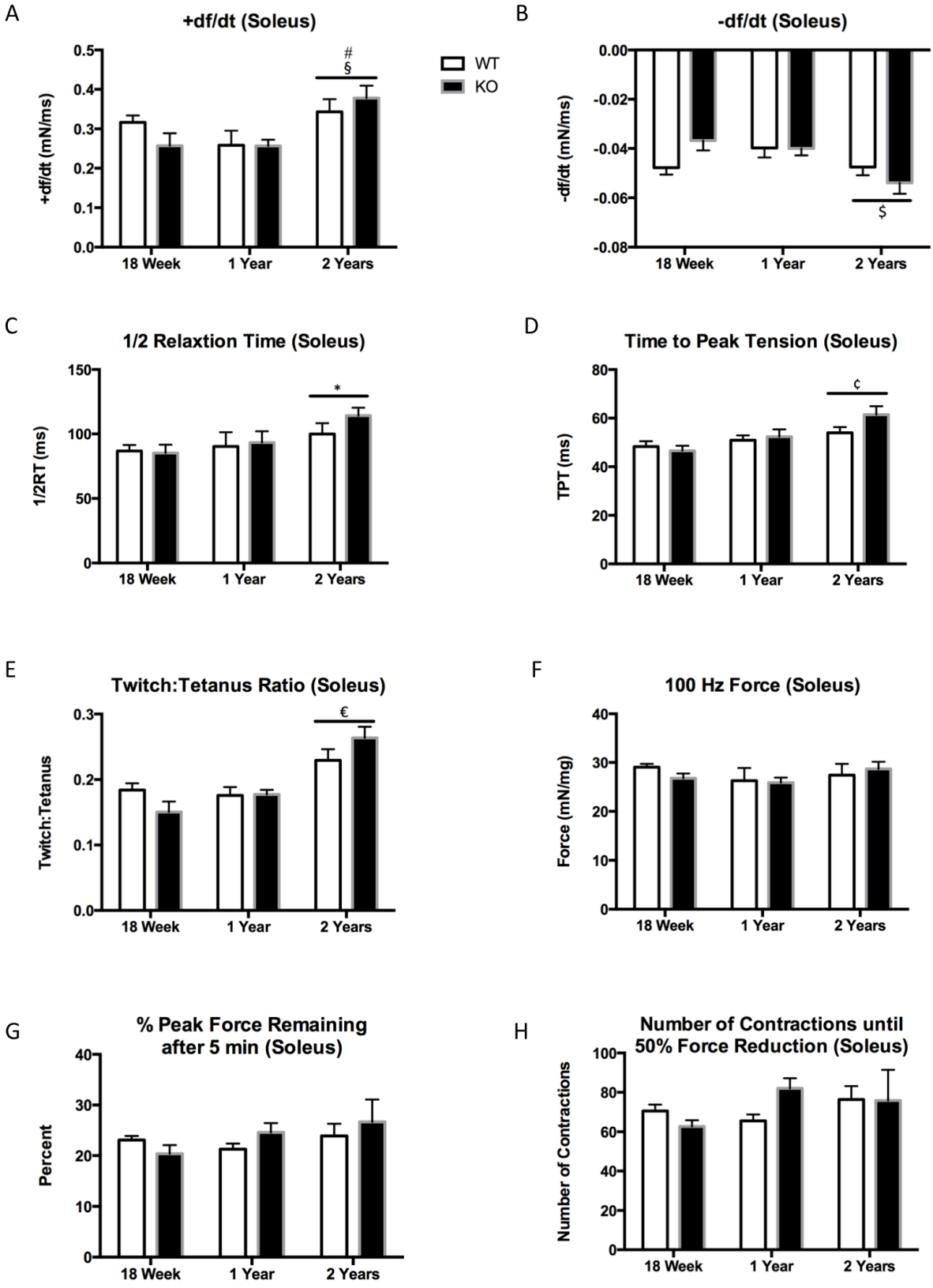
A
+df/dt (Soleus)
+df/dt (mN/ms)
0.5
0.4
0.3
0.2
0.1
0.0
#
§
18 Week
1 Year
2 Years
WT
KO
B
-df/dt (Soleus)
-df/dt (mN/ms)
0.00
-0.02
-0.04
-0.06
-0.08
$
18 Week
1 Year
2 Years
C
1/2 Relaxtion Time (Soleus)
1/2RT (ms)
150
100
50
0
*
18 Week
1 Year
2 Years
D
Time to Peak Tension (Soleus)
TPT (ms)
80
60
40
20
0
¢
18 Week
1 Year
2 Years
E
Twitch:Tetanus Ratio (Soleus)
Twitch:Tetanus
0.3
0.2
0.1
0.0
€
18 Week
1 Year
2 Years
F
100 Hz Force (Soleus)
Force (mN/mg)
40
30
20
10
0
18 Week
1 Year
2 Years
G
% Peak Force Remaining after 5 min (Soleus)
Percent
40
30
20
10
0
18 Week
1 Year
2 Years
H
Number of Contractions until 50% Force Reduction (Soleus)
Number of Contractions
100
80
60
40
20
0
18 Week
1 Year
2 Years

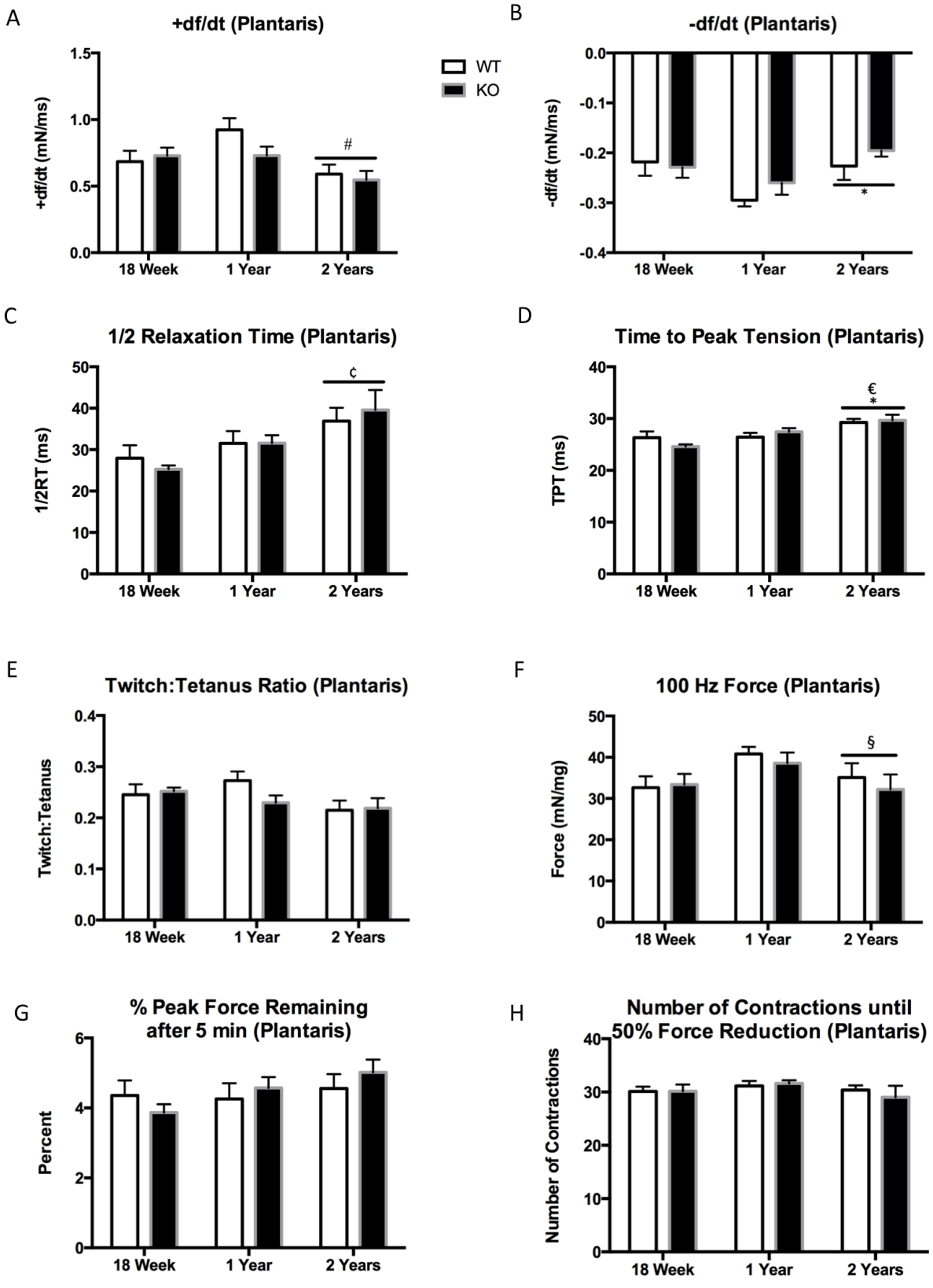
A
+df/dt (Plantaris)
+df/dt (mN/ms)
1.5
1.0
0.5
0.0
#
18 Week
1 Year
2 Years
WT
KO
B
-df/dt (Plantaris)
-df/dt (mN/ms)
0.0
-0.1
-0.2
-0.3
-0.4
*
18 Week
1 Year
2 Years
C
1/2 Relaxation Time (Plantaris)
1/2RT (ms)
50
40
30
20
10
0
¢
18 Week
1 Year
2 Years
D
Time to Peak Tension (Plantaris)
TPT (ms)
40
30
20
10
0
€
*
18 Week
1 Year
2 Years
E
Twitch:Tetanus Ratio (Plantaris)
Twitch:Tetanus
0.4
0.3
0.2
0.1
0.0
18 Week
1 Year
2 Years
F
100 Hz Force (Plantaris)
Force (mN/mg)
50
40
30
20
10
0
§
18 Week
1 Year
2 Years
G
% Peak Force Remaining after 5 min (Plantaris)
Percent
6
4
2
0
18 Week
1 Year
2 Years
H
Number of Contractions until 50% Force Reduction (Plantaris)
Number of Contractions
40
30
20
10
0
18 Week
1 Year
2 Years

Apoptotic Signaling and Protease Activity

No significant differences for age or genotype were found in either the red (Figure 13) or white gastrocnemius (Figure 14) muscle for total enzymatic activity (area under the curve; AUC) (data not shown) or maximal enzymatic activity for caspase-2, -3, -8, -9, and calpains.

Apoptotic Protein Expression

Total muscle content of mitochondrial housed proteins were measured in both soleus and plantaris muscles. Analysis of pro-apoptotic proteins in the soleus revealed a trend towards decreased Cyto-c with age ($p=0.095$) (Figure 15C). AIF and SMAC were not different between groups (Figure 15A and E). In the plantaris, there were no differences in AIF and SMAC (Figure 15B and F); however, Cyto-c was significantly increased in the 1 year compared to the 18 week group ($p<0.05$) (Figure 15D).

In the soleus, the 2 year WT group had significantly decreased ARC expression compared to the 18 week WT group ($p<0.05$) (Figure 16A). The 2 year group also had significantly increased expression of Bcl-2, Bcl-XL, Hsp-70, and XIAP compared to the 18 week and 1 year groups (Figure 16B, 16C, 16D, 18C). In the plantaris there were no significant differences in ARC or Hsp-70 between groups (Figure 17A and C). However, the 2 year group had significantly increased expression of Bcl-2, Bcl-XL, and XIAP compared to the 18 week and 1 year groups (Figure 17B, 17D, 19C).

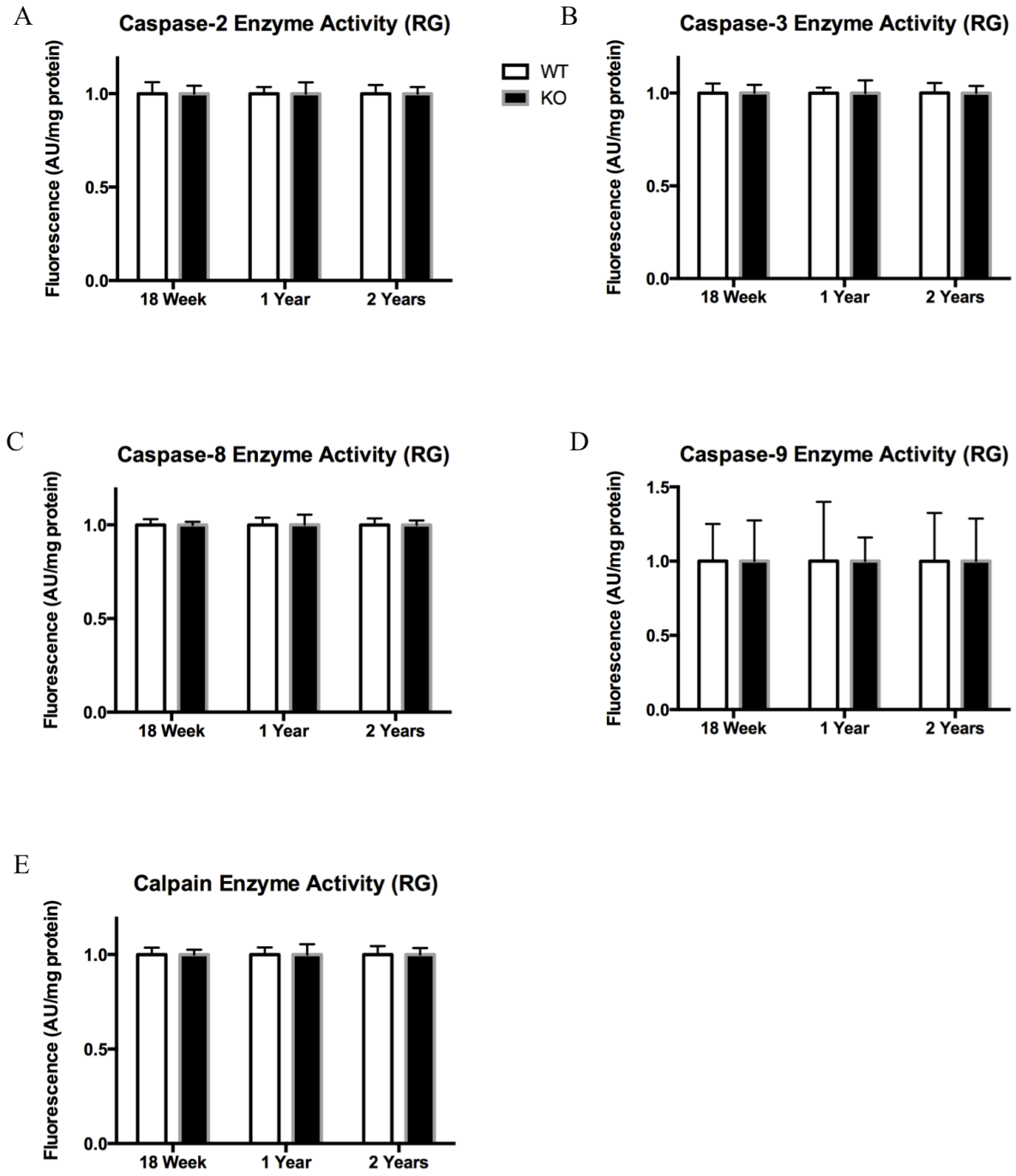

Figure 13. Proteolytic enzyme activity. A-E: Quantitative analysis of maximal caspase-2, -3, -8, -9, and calpain enzymatic activity in the red gastrocnemius (RG) of wild type (WT) and ARC knockout (KO) animals (n=8). Data are expressed as means ± SEM.

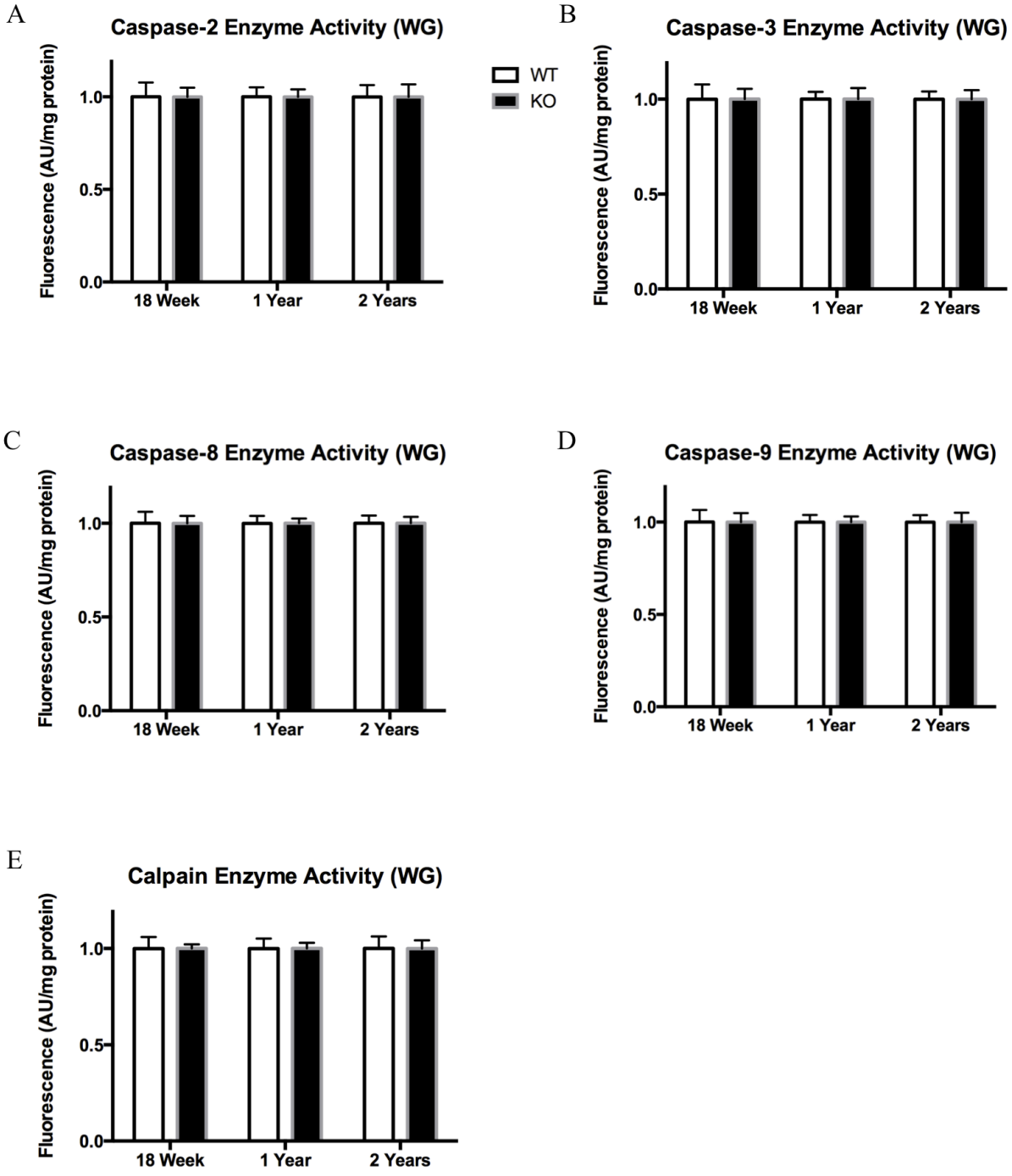

Figure 14. Proteolytic enzyme activity. A-E: Quantitative analysis of maximal caspase-2, -3, -8, -9, and calpain enzymatic activity in the white gastrocnemius (WG) of wild type (WT) and ARC knockout (KO) animals (n=8). Data are expressed as means ± SEM.

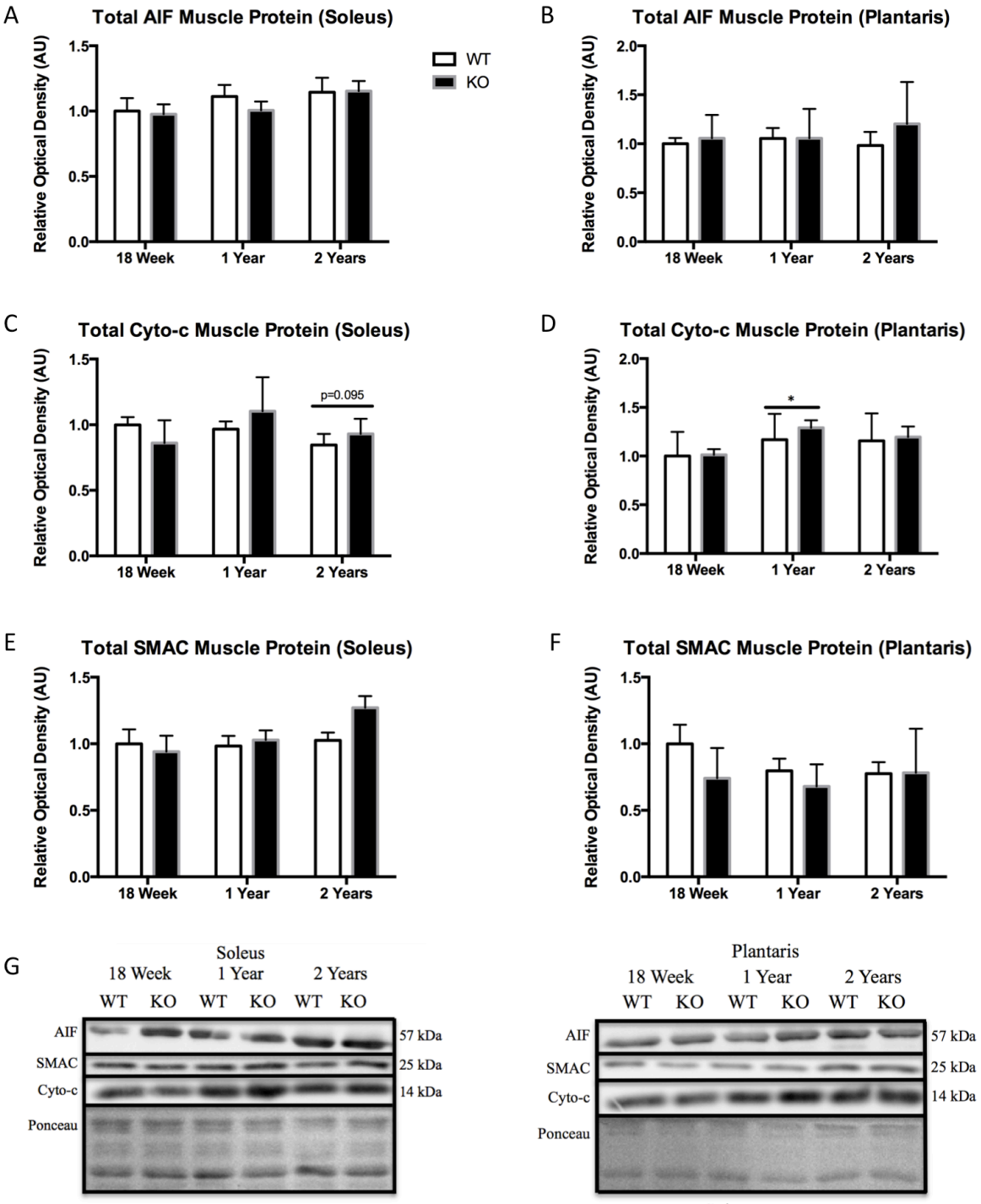

Figure 15. Expression of whole tissue mitochondrial housed pro-apoptotic proteins. A, C, and E: Quantification of AIF, Cyto-c, and SMAC protein expression in the soleus of wild type (WT) and ARC knockout (KO) animals. B, D, and F: Quantification of AIF, Cyto-c, and SMAC protein expression in the plantaris of WT and ARC KO animals (n=8). G: Representative immunoblots of AIF, SMAC, and Cyto-c in soleus and plantaris of WT and ARC KO animals. Ponceau stained membranes are shown as a loading control. Data are expressed as means ± SEM (* main effect $p<0.05$ vs. 18 week).

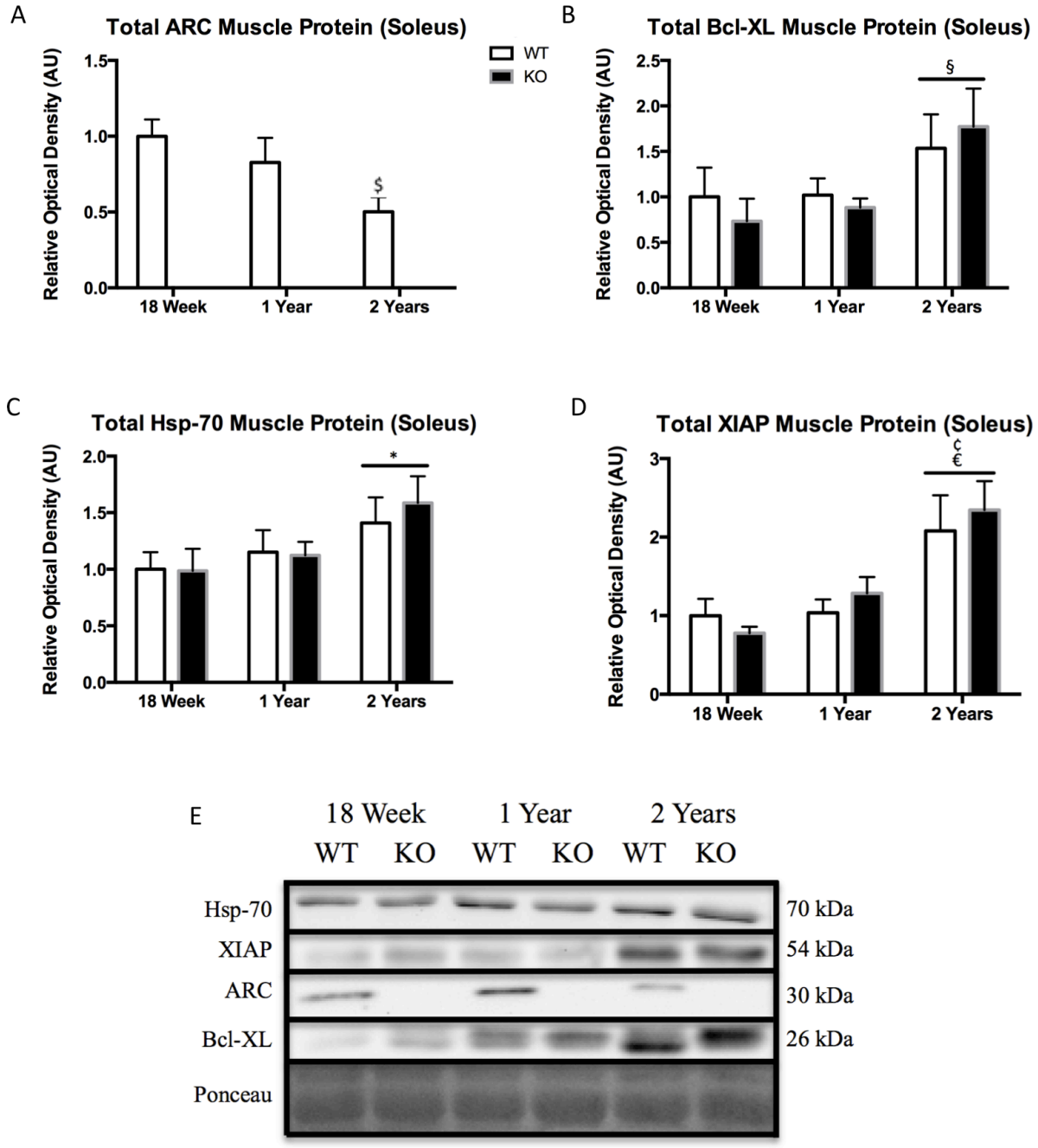

Figure 16. Expression of whole tissue anti-apoptotic proteins. A-D: Quantification of ARC, Bcl-XL, Hsp-70, and XIAP protein expression in the soleus of wild type (WT) and ARC knockout (KO) animals (n=8). E: Representative immunoblots of ARC, Bcl-XL, Hsp-70, and XIAP in soleus of WT and ARC KO animals. Ponceau stained membranes are shown as a loading control. Data are expressed as means ± SEM (* main effect $p<0.05$ vs. 18 weeks, ¢ main effect $p<0.01$ vs. 1 year, € main effect $p<0.001$ vs. 18 week, § main effect $p<0.05$ vs. 18 week, $ $p<0.05$ vs. 18 week).

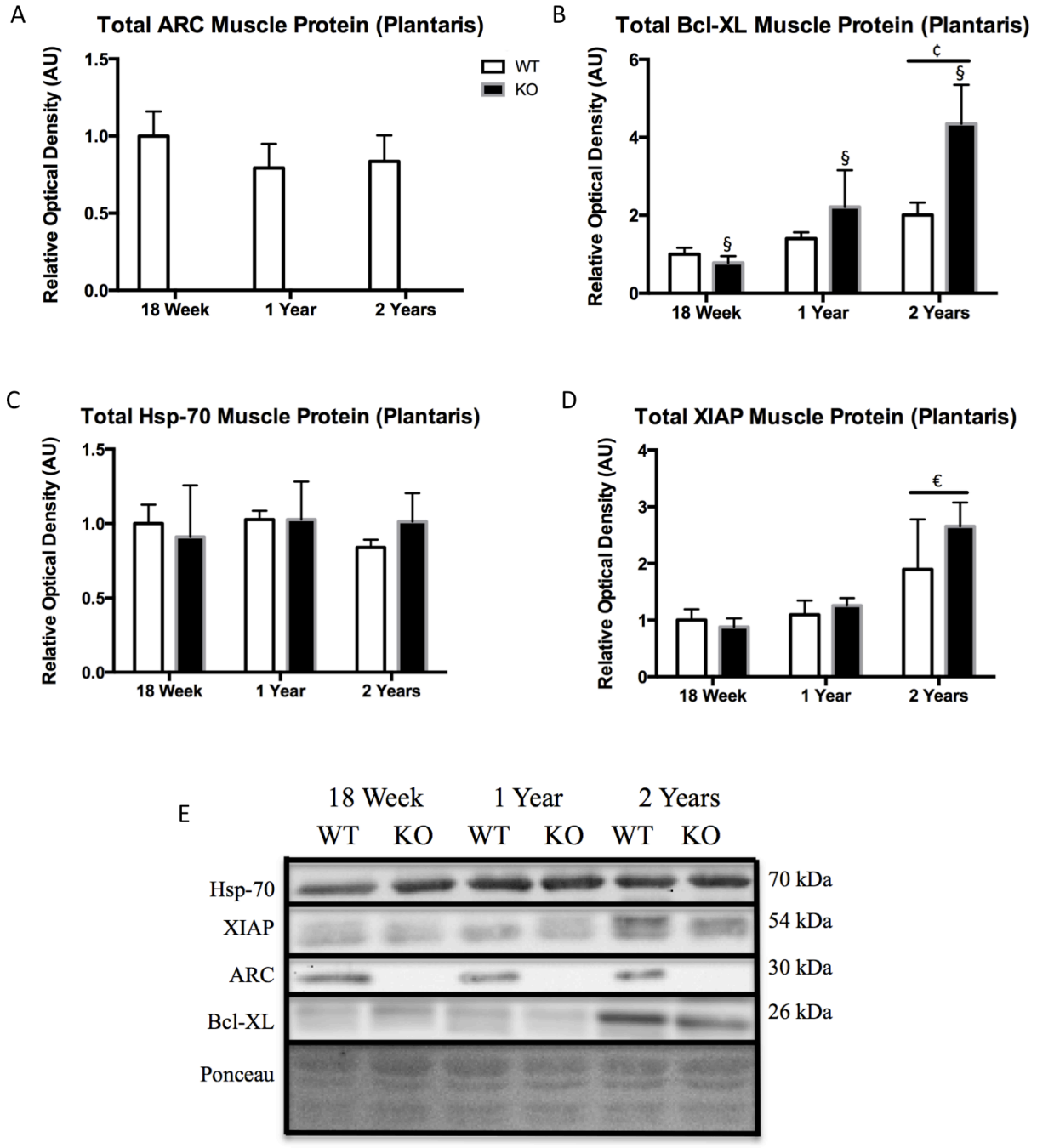

Figure 17. Expression of whole tissue anti-apoptotic proteins. A-D: Quantification of ARC, Bcl-XL, Hsp-70, and XIAP protein expression in the plantaris of wild type (WT) and ARC knockout (KO) animals (n=8). E: Representative immunoblots of ARC, Bcl-XL, Hsp-70, and XIAP in plantaris of WT and ARC KO animals. Ponceau stained membranes are shown as a loading control. Data are expressed as means ± SEM (¢ main effect $p<0.01$ vs. 18 week, € main effect $p<0.001$ vs. 18 week and 1 year, § main effect $p<0.05$ vs. WT).

The pro-apoptotic proteins Bax and Bid were not significantly different in the soleus between groups (Figure 18A and D). However, t-Bid was higher in the WT animals (Figure 18B). In the plantaris there was no significant differences in Bax, Bid, or t-Bid (Figure 19 A, B, and D). The Bax:Bcl-2 ratio in the soleus was significantly lower in the 2 year compared to the 18 week group ($p<0.05$) (Figure 18E). In the plantaris the Bax:Bcl-2 ratio was significantly higher in the 18 week compared to the 1 and 2 year groups ($p<0.01$) (Figure 19E).

Since ROS can influence cell death, antioxidants were examined. In the soleus there were no differences in CuZnSOD and Catalase (Figure 20A and C); however, MnSOD was significantly decreased in the 2 year compared to the 1 year group ($p<0.05$) (Figure 20E). In the plantaris, there were no differences in CuZnSOD or MnSOD (Figure 20D and F); however, there was a trend toward an increase in Catalase with age ($p=0.051$) (Figure 20B).

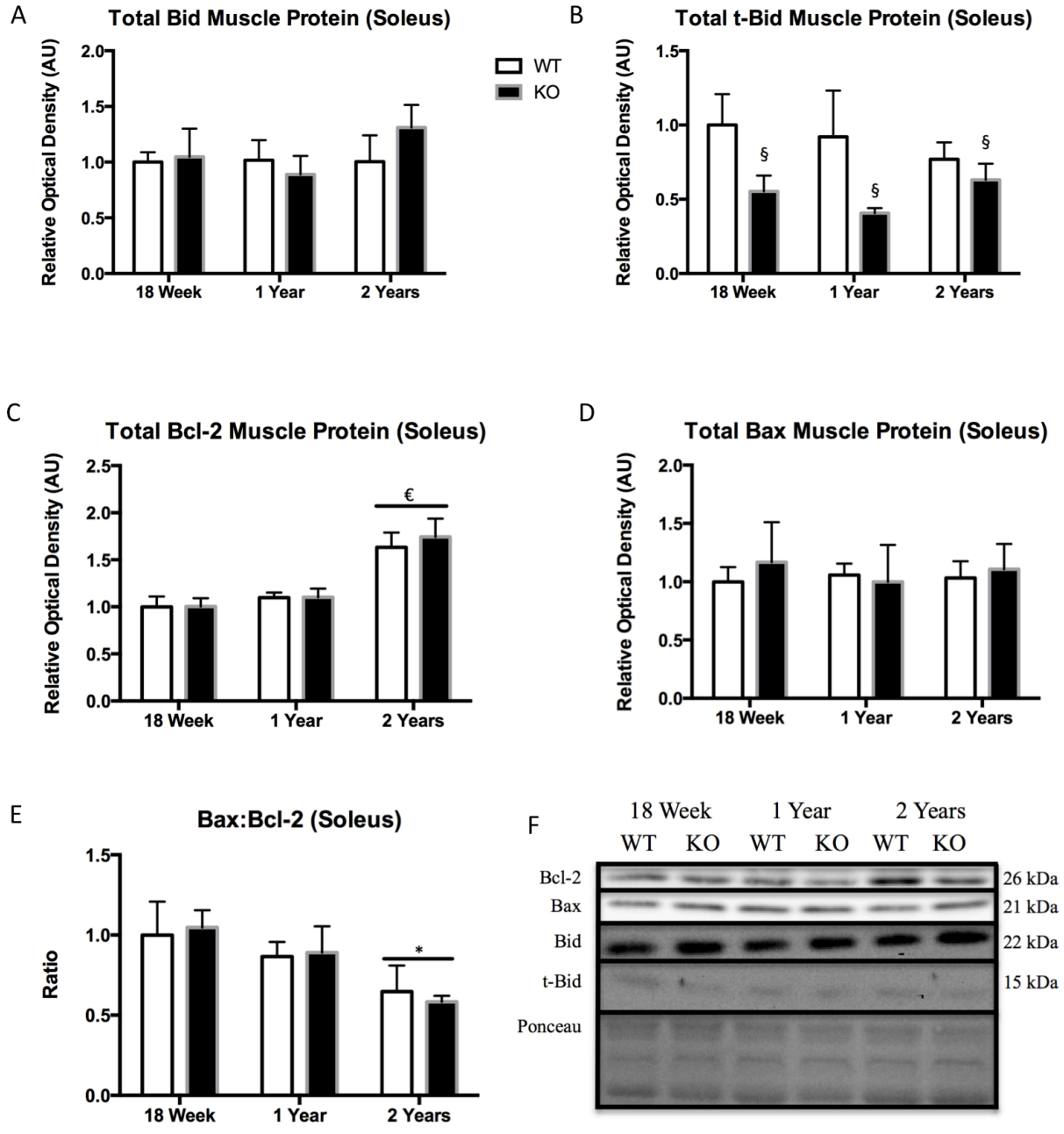

Figure 18. Expression of whole tissue apoptotic proteins. A-E: Quantification of Bid, t-Bid, Bcl-2, Bax, and Bax:Bcl-2 protein expression in the soleus of wild type (WT) and ARC knockout (KO) animals (n=8). F: Representative immunoblots of Bid, t-Bid, Bcl-2, Bax, and Bax:Bcl-2 in soleus of WT and ARC KO animals. Ponceau stained membranes are shown as a loading control. Data are expressed as means ± SEM (* main effect $p<0.05$ vs. 18 week, € $p<0.001$ vs. 18 week and 1 year, § main effect $p<0.05$ vs. WT).

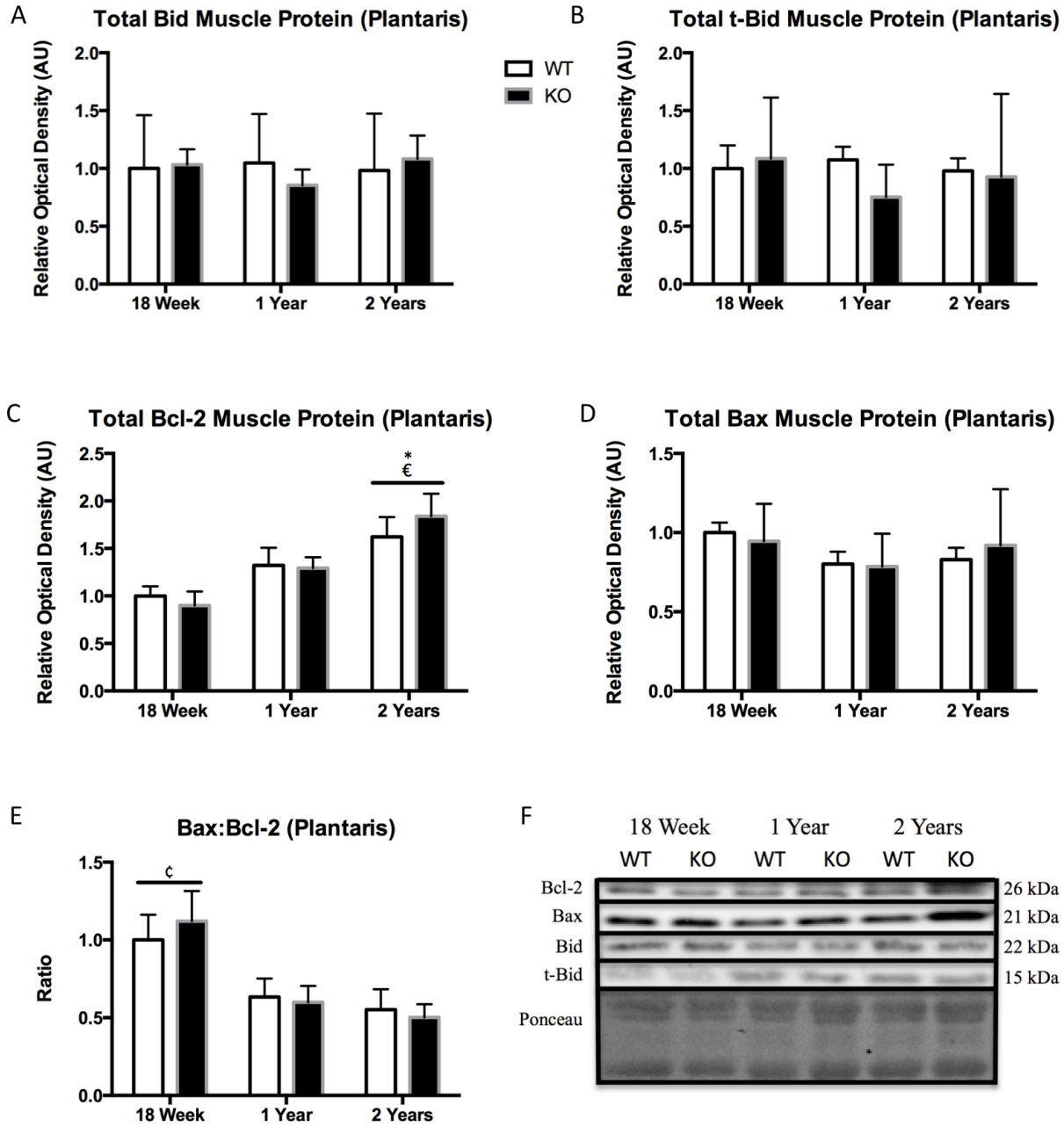

Figure 19. Expression of whole tissue apoptotic proteins. A-E: Quantification of Bid, t-Bid, Bcl-2, Bax, and Bax:Bcl-2 protein expression in the plantaris of wild type (WT) and ARC knockout (KO) animals (n=8). F: Representative immunoblots of Bid, t-Bid, Bcl-2, Bax, and Bax:Bcl-2 in plantaris of WT and ARC KO animals. Ponceau stained membranes are shown as a loading control. Data are expressed as means ± SEM (* main effect $p<0.05$ vs. 1 year, ¢ $p<0.01$ vs. 1 and 2 year, € $p<0.001$ vs. 18 week).

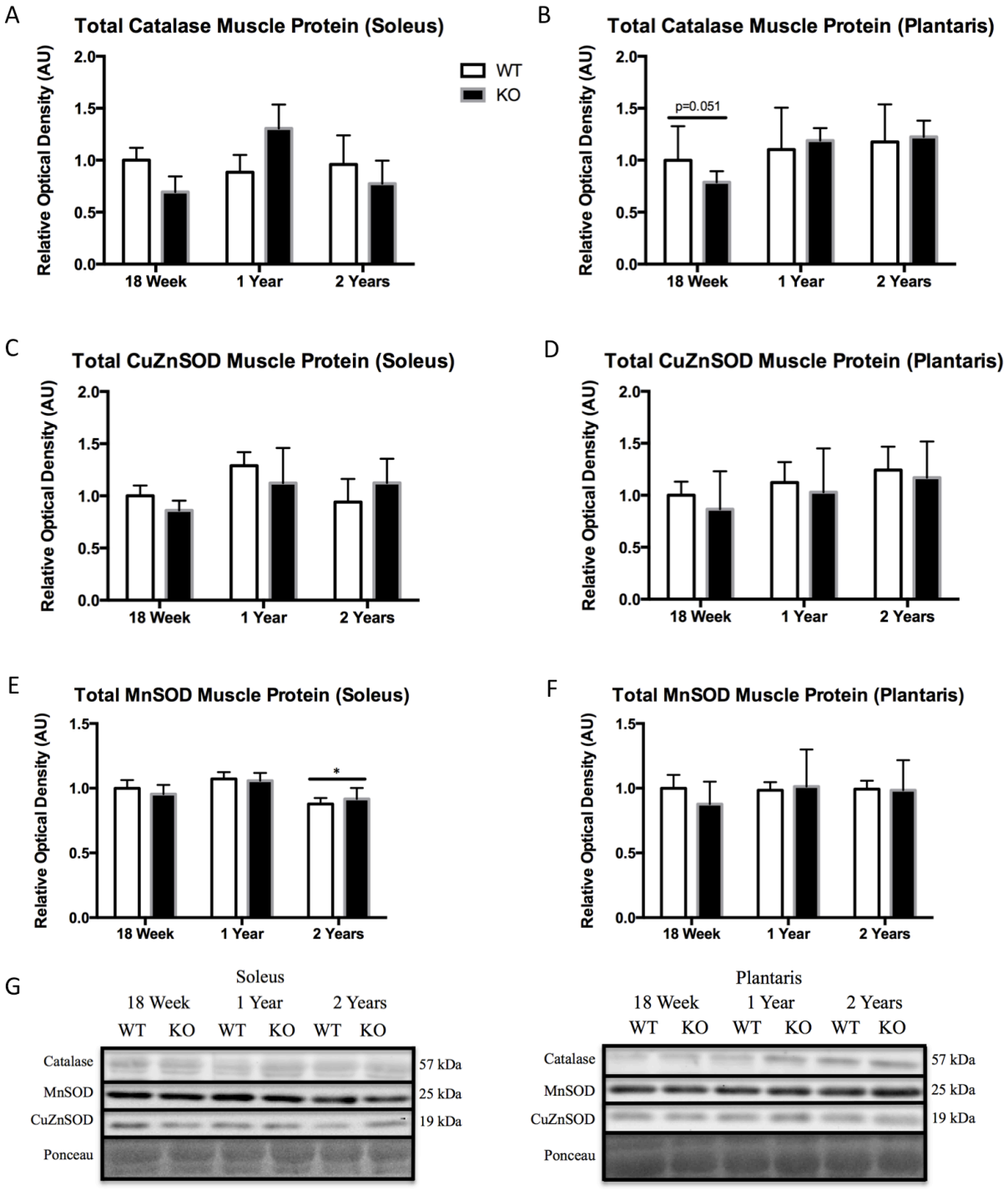

Figure 20. Expression of whole tissue anti-oxidant proteins. A, C, and E: Quantification of Catalase, CuZnSOD, and MnSOD protein expression in the soleus of wild type (WT) and ARC knockout (KO) animals. B, D, and F: Quantification of Catalase, CuZnSOD, and MnSOD protein expression in the plantaris of WT and ARC KO animals (n=8). G: Representative immunoblots of Catalase, CuZnSOD, and MnSOD in soleus and plantaris of WT and ARC KO animals. Ponceau stained membranes are shown as a loading control. Data are expressed as means ± SEM (* main effect $p<0.05$ vs 1 year).

Subfractionation analysis was conducted in red (RQ) and white (WQ) quadriceps muscle. In the cytosolic-enriched fractions of the RQ, no differences were observed in AIF, and Drp-1 (Figure 21A, and C); however, Cyto-c was significantly different in the 2 year ARC KO mice compared to the 2 year WT mice ($p<0.01$) (Figure 21B). In addition, the 2 year group had significantly increased cytosolic SMAC levels compared to the 1 year group ($p<0.01$) (Figure 21D). There were no differences in mitochondrial Drp-1 (Figure 23D); however, mitochondrial Bcl-2 was significantly different in the 2 year ARC KO mice compared to the 2 year WT mice ($p<0.05$) (Figure 23A). Further, mitochondrial Bax was significantly higher in the 18 week compared to the 1 year group ($p<0.01$) (Figure 23B). The mitochondrial Bax to Bcl-2 ratio was also significantly increased in 18 week compared to the 1 year ($p<0.01$) and 2 year ($p<0.05$) groups (Figure 23C). There were no differences in nuclear AIF between groups (Figure 25A).

There were no differences in cytosolic Cyto-c, and Drp-1 between groups in the WQ (Figure 22B, and C); however, AIF was significantly lower in the 18 week compared to the 1 and 2 year groups ($p<0.05$) (Figure 22A). Further, cytosolic SMAC was significantly increased in the 2 year compared to the 18 week and 1 year groups ($p<0.05$) (Figure 22D). There were no differences in mitochondrial Bax and Drp-1 (Figure 24B and D); however, Bcl-2 was significantly higher in the 2 year compared to the 18 week group ($p<0.05$) (Figure 24A). The mitochondrial Bax to Bcl-2 ratio was also significantly lower in the 2 year compared to the 18 week group ($p<0.01$) (Figure 24C). There were no differences in nuclear AIF between groups in the WQ (Figure 25B). Fraction purity was completed in cytosolic, mitochondrial, and nuclear-enriched fractions (Figure 26).

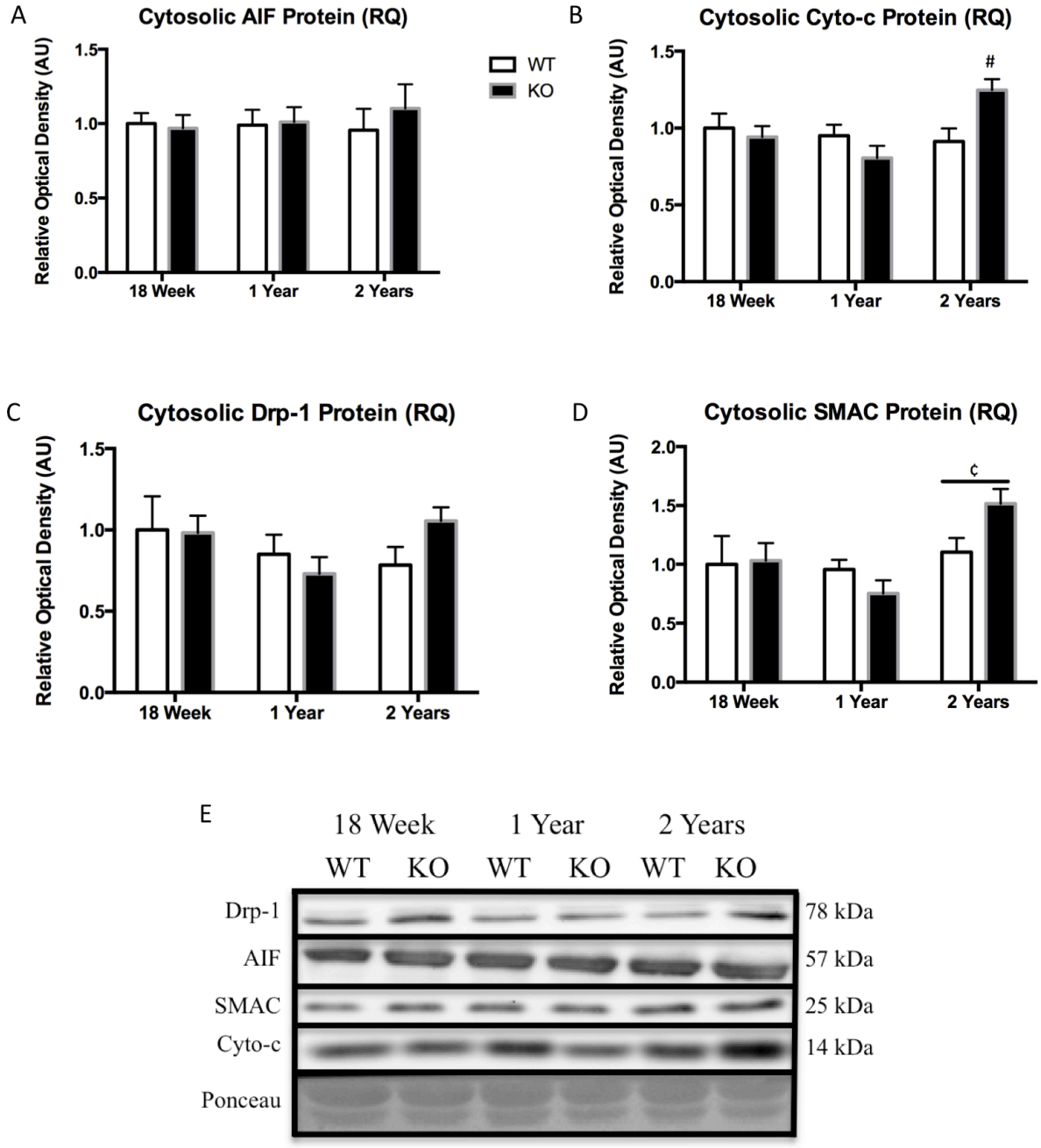

Figure 21. Expression of apoptotic markers in cytosolic subcellular fractions. A-D: Quantification of AIF, Cyto-c, Drp-1, and SMAC protein expression in the red quadriceps (RQ) of wild type (WT) and ARC knockout (KO) animals (n=8). E: Representative immunoblots of AIF, Cyto-c, Drp-1, and SMAC in RQ of WT and ARC KO animals. Ponceau stained membranes are shown as a loading control. Data are expressed as means ± SEM (¢ main effect $p<0.01$ vs. 1 year, # interaction effect $p<0.01$ vs. all).

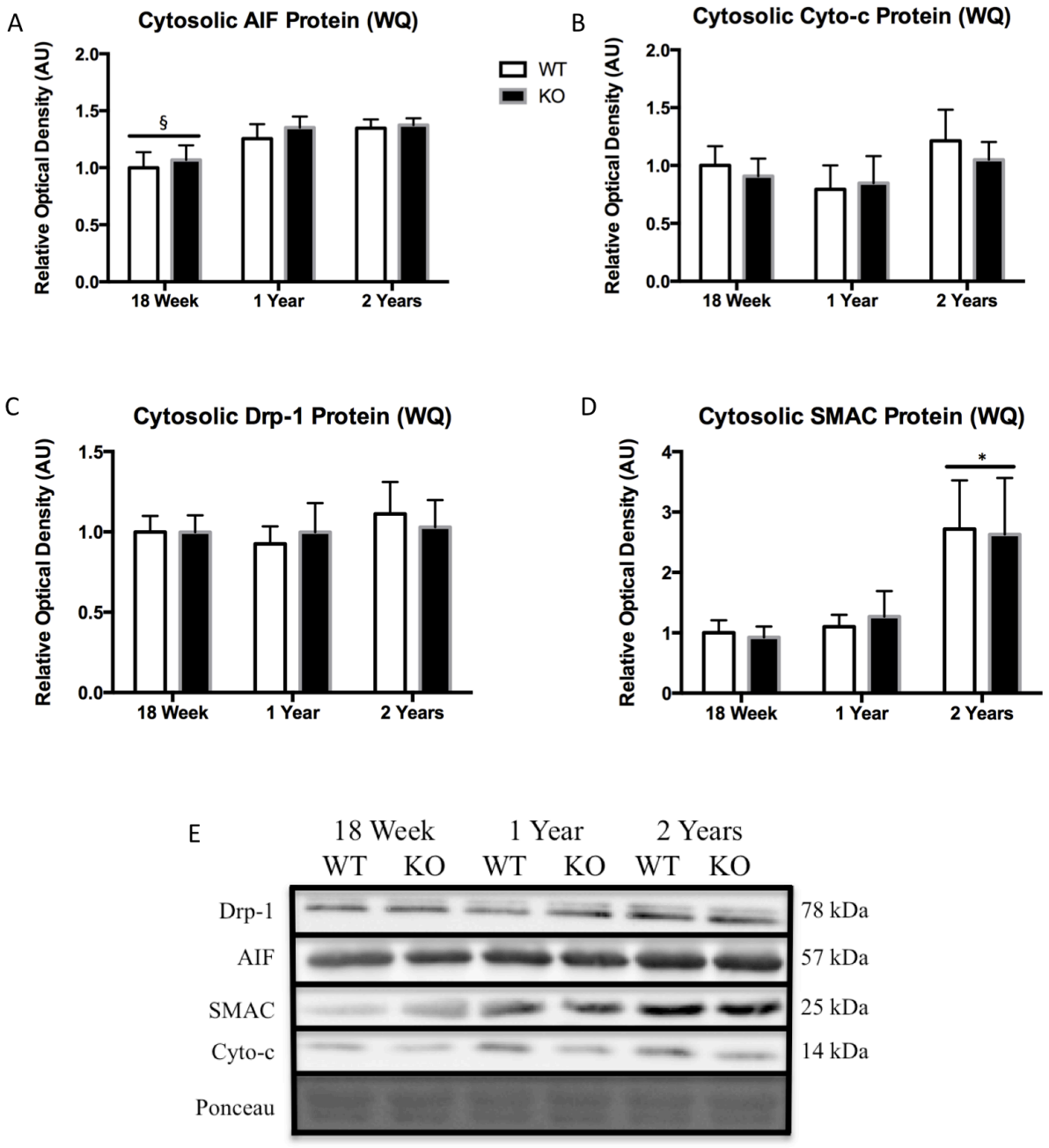

Figure 22. Expression of apoptotic markers in cytosolic subcellular fractions. A-D: Quantification of AIF, Cyto-c, Drp-1, and SMAC protein expression in the white quadriceps (WQ) of wild type (WT) and ARC knockout (KO) animals (n=7-8). E: Representative immunoblots of AIF, Cyto-c, Drp-1, and SMAC in WQ of WT and ARC KO animals. Ponceau stained membranes are shown as a loading control. Data are expressed as means ± SEM (* main effect $p<0.05$ vs. 18 week and 1 year, § main effect $p<0.05$ vs. 1 and 2 years).

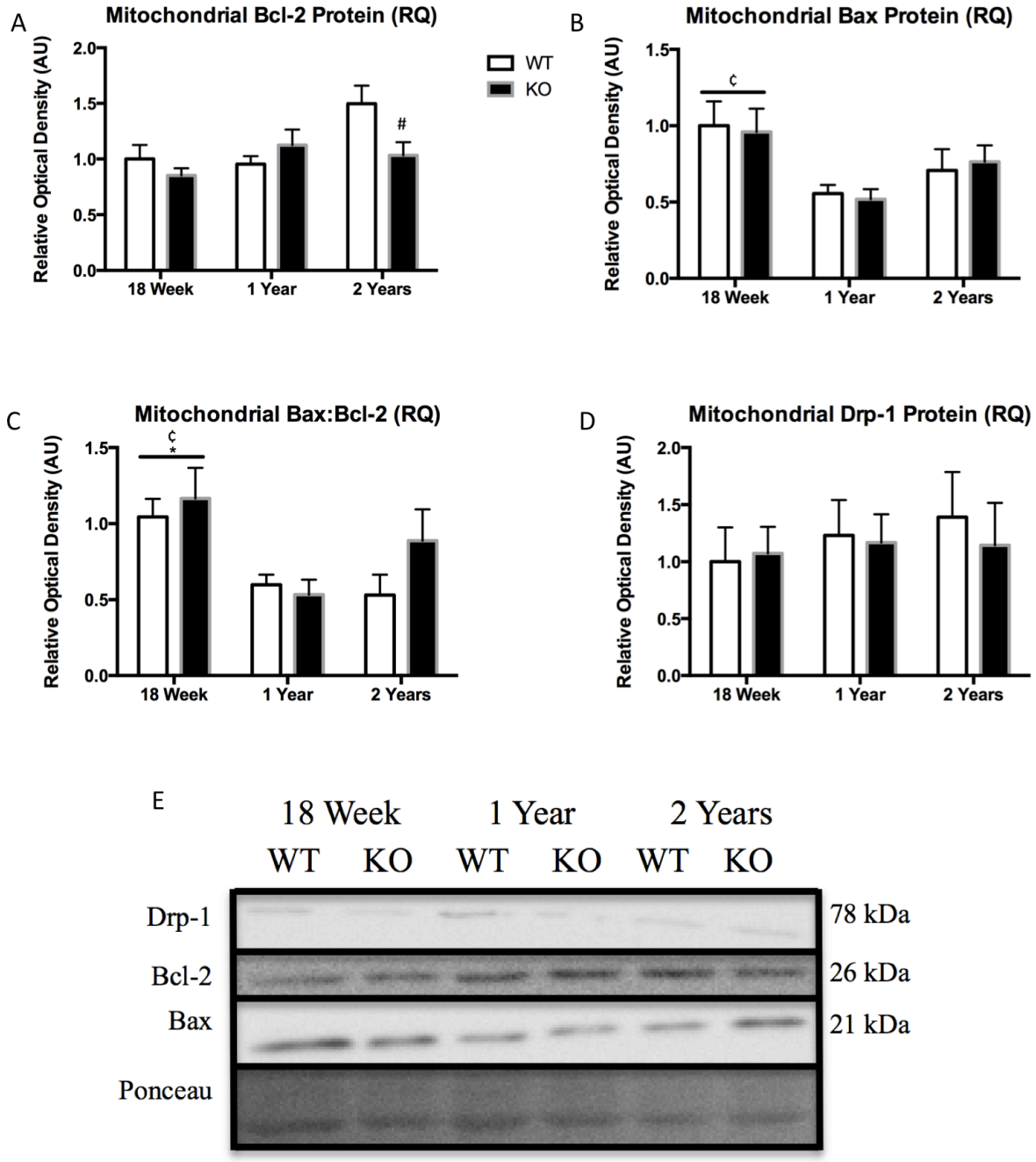

Figure 23. Expression of apoptotic markers in mitochondrial subcellular fractions. A-D: Quantification of Bcl-2, Bax, Bcl-2:Bax, and Drp-1 protein expression in the red quadriceps (RQ) of wild type (WT) and ARC knockout (KO) animals (n=8). E: Representative immunoblots of Bcl-2, Bax, Bax:Bcl-2, and Drp-1 in RQ of WT and ARC KO animals. Ponceau stained membranes are shown as a loading control. Data are expressed as means ± SEM (* main effect $p<0.05$ vs. 2 years, ¢ main effect $p<0.01$ vs. 1 year, # interaction effect $p<0.05$ vs. all).

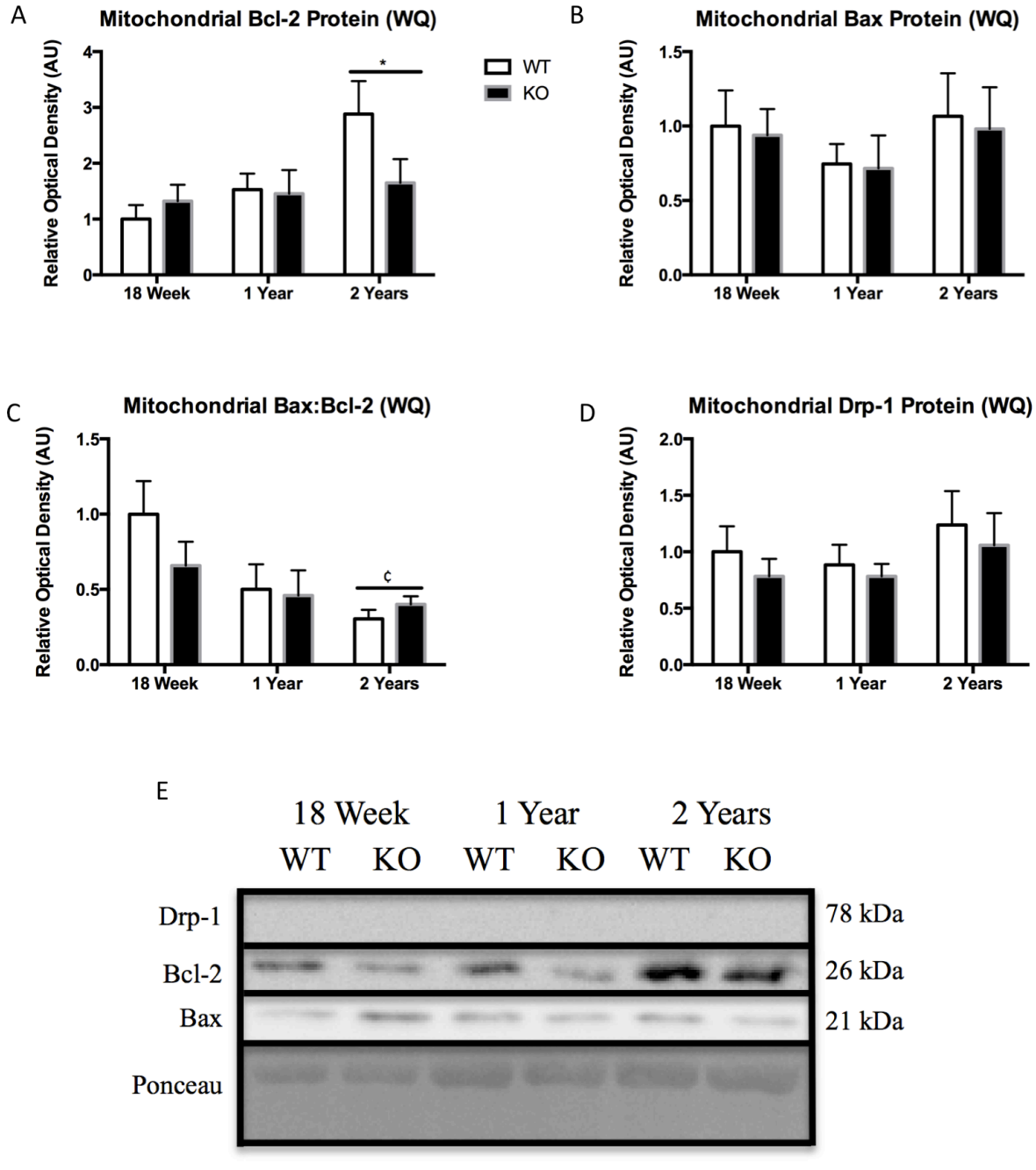

Figure 24. Expression of apoptotic markers in mitochondrial subcellular fractions. A-D: Quantification of Bcl-2, Bax, Bcl-2:Bax, and Drp-1 protein expression in the white quadriceps (WQ) of wild type (WT) and ARC knockout (KO) animals (n=7-8). Representative immunoblots of Bcl-2, Bax, Bax:Bcl-2, and Drp-1 in WQ of WT and ARC KO animals. Ponceau stained membranes are shown as a loading control. Data are expressed as means ± SEM (*$p<0.05$ vs. 18 week, ¢ main effect $p<0.01$ vs. 18 week).

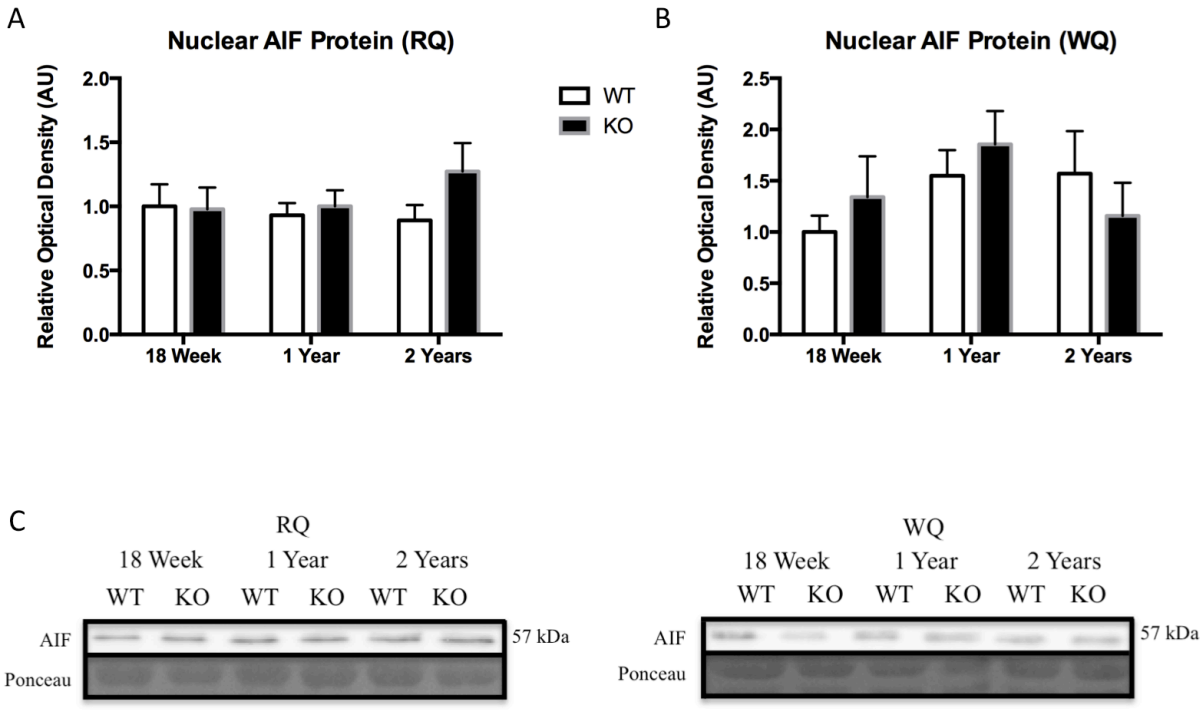

Figure 25. Expression of apoptotic markers in nuclear subcellular fractions. A: Quantification of AIF protein expression in the red quadriceps (RQ) of wild type (WT) and ARC knockout (KO) animals. B: Quantification of AIF protein expression in the white quadriceps (WQ) of WT and ARC KO animals (n=8). C: Representative immunoblots of AIF in RQ and WQ of WT and ARC KO animals. Ponceau stained membranes are shown as a loading control. Data are expressed as means ± SEM.

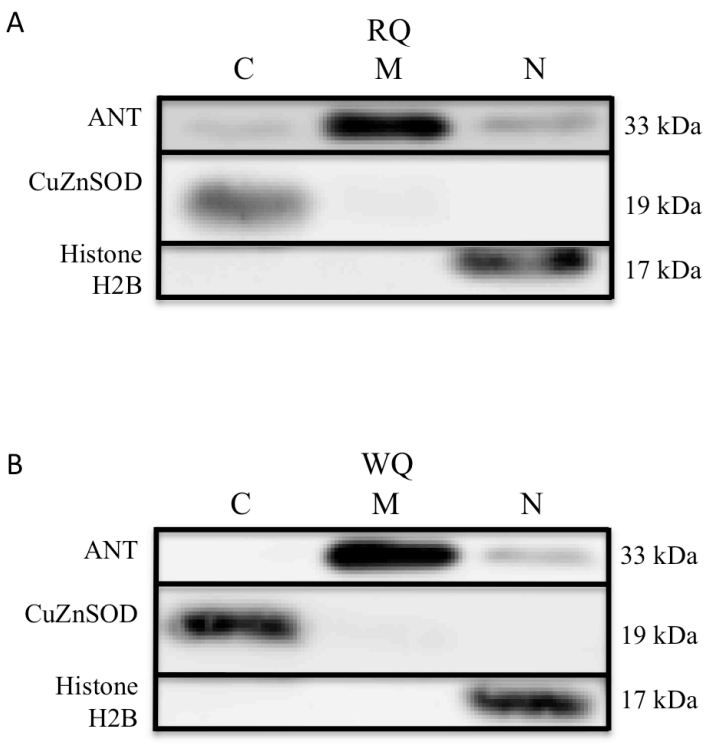

Figure 26. Subcellular fractionation procedure. A-B: Representative purity blots of cytosolic (C), mitochondrial (M), and nuclear (N) specific proteins following differential centrifugation in the red quadriceps (RQ) and white quadriceps (WQ) of wild type (WT) and ARC knockout (KO) animals. CuZnSOD represents a cytosolic marker, histone H2B a nuclear marker, and ANT a mitochondrial marker.

Discussion

The objective of this study was to examine morphological characteristics and apoptotic signaling measures in aging skeletal muscle and the role of apoptosis repressor with caspase recruitment domain (ARC). These measures were conducted in hindlimb skeletal muscle of young, middle age, and old WT and ARC-deficient (ARC KO) mice. Given that skeletal muscle atrophy occurs in aging, it was hypothesized that aged mice would display greater muscle wasting. Since increased atrophy is associated with an increase in apoptotic signaling, it was hypothesized that aged mice would also have a higher degree of apoptosis. Additionally, because ARC is a potent anti-apoptotic protein that regulates mitochondrial-mediated apoptotic signaling, it was hypothesized that the increased atrophy and apoptosis in the aged mice, would be exacerbated in the ARC KO mice and the increased apoptotic signaling would be mediated by the mitochondrial pathway. Further, we hypothesized that skeletal muscles and fibers with a higher ARC content would display greater atrophy in the ARC KO mice. Lastly, it was hypothesized that aged ARC KO mice would have decreased force production and fatigue resistance.

In the soleus, which has a relatively high ARC content, we expected that both morphological and apoptotic measures would be exacerbated. There were significant deceases in soleus weight, CSA, CSA in type I and IIA fibers, and a shift toward a slower phenotype in the 2 year animals. Along with the reduction in muscle size, contractility measures revealed higher rates of force development and relaxation rates in the 2 year animals, with no differences in fatigability. While caspase and calpain activity and whole tissue pro-apoptotic proteins were not altered in aged mice, expression of many anti-apoptotic proteins increased and mitochondrial release of pro-apoptotic proteins increased in the RQ. Surprisingly, the Bax:Bcl-2 ratio decreased

in the 2 year animals. Lastly, the effect of genotype on the soleus muscle was a decreased total fiber number and T-bid expression in ARC KO mice; however, 2 year KO mice displayed increased release of mitochondrial housed Cyto-c.

The plantaris is comprised mostly of type II glycolytic fibers and has a lower ARC content. We expected an attenuated response in both morphological and apoptotic changes in comparison to the soleus. There were significant decreases in weight, CSA, CSA in type IIA, IIX, and IIB fibers, and a shift toward a faster phenotype in the 2 year animals. Along with the increased atrophy and increased percentage of fast, glycolytic type IIB fibers, there were altered force characteristics in aged mice. The rate of force development and relaxation decreased, one-half relaxation time became longer, and the FFC decreased in aged mice. Similar to the soleus, anti-apoptotic protein expression increased and mitochondrial release of pro-apoptotic proteins increased in the WQ, Bax:Bcl-2 ratio decreased, and no differences were observed for caspase and calpain activity in the aged mice. As well, decreased plantaris weight and increased Bcl-XL expression were the only genotype effects observed in fast muscle of ARC KO mice.

Apoptotic Signaling in Skeletal Muscle

Through ARC's many interactions with apoptotic signaling proteins and molecules involved in the initiation of apoptosis, ARC is able to inhibit all three apoptotic signaling pathways. Several measurements from our results indicate the involvement of the mitochondrial-mediated apoptotic pathway in the 2 year animals as well as in ARC KO animals. Also, since we did not see any change in caspase-8 activity or calpain activity, this suggests no involvement of the death-receptor pathway or the ER-stress pathway.

ARC has been shown to inhibit the death-receptor pathway by directly binding to

caspase-2, and -8[42]. Nevertheless, the activity of caspase-2, and -8 were not different in both the RG and WG between ages or genotypes, suggesting a lack of involvement of this pathway. Additionally, activated caspase-8, is known to cleave Bid, resulting in its activation (truncated form, T-Bid), which can interact with the mitochondrial pathway by activating Bax[14]. In the soleus, T-Bid expression was decreased in KO animals, indicating decreased activation of this pathway. It has been well documented that levels of circulating cytokines, such as TNF-α, increase with age, which enhances binding to TNFR and activation of the death-receptor pathway[61]. These measurements were not conducted in this study, but none of our results indicate increased involvement of this pathway. As well, studies have suggested that caspase-independent cell death may play a larger role in aging than caspase-dependent pathways[37]. These results suggest no major differences in the involvement of the death-receptor pathway as a result of age or genotype.

ARC can inhibit the activation of the ER-stress pathway by binding to excess cytosolic Ca^{2+} thereby preventing calpain activation[42]. Overexpression ARC models have shown decreased Ca^{2+} transients, whereas decreasing ARC leads to Ca^{2+}-induced cell death[47]. Furthermore, increased resting cytosolic Ca^{2+} levels have been shown in the soleus and EDL of aged muscle, which could activate calpains[62]. Our results would indicate that the ER-stress pathway was not altered between ages or genotype; however, this was not a complete evaluation of this pathway as increased cytosolic Ca^{2+} can also activate caspase-12[20]. Additionally, skeletal muscle apoptosis can occur when elevated ER-stress activates CCAAT/enhancer-binding protein homologous protein (CHOP) [63]. Although none of our measures indicate an elevated level of apoptotic signaling through the ER-stress pathway between ages or genotype, previous work in our lab found no differences in calpain activity, yet the mitochondria were more susceptible to an

increased cytosolic Ca^{2+} level in 18 week ARC KO mice. Since increased Ca^{2+} levels can cause mPTP formation, and lead to mitochondrial-mediated apoptosis[15], elevated ER-stress still may be contributing to the altered morphology and apoptotic protein expression in the aged and ARC KO mice.

ARC directly and indirectly influences many signaling proteins involved in mitochondrial-mediated apoptosis. ARC can directly interact with Bax and inhibit pore formation at the mitochondria[43]. It was hypothesized that increased activation of this pathway would be seen in aged ARC KO animals; however, we only found a decreased mitochondrial Bax in the RQ of aged mice. Previous work in young ARC KO mice found increased Bax in the soleus, similar to what we saw in our 18 week group, with no change in Bcl-2. Given that Bcl-2 directly inhibits Bax activation, and we found increased Bcl-2 in the soleus, plantaris, and WQ mitochondrial fraction in the 2 year animals, this may suggest that Bax activity is attenuated in our aged mice. Additionally, previous work has shown cells become resistant to ROS and Ca^{2+} by overexpressing Bcl-2[64]. Bcl-2 can also interact with RyR allowing a slow Ca^{2+} leak from the SR, thereby attenuating a SR-stress mediated apoptotic insult[65]. Therefore, the increased Bcl-2 expression in the aged mice may be a compensatory mechanism to reduce the age-associated increase in resting Ca^{2+} and ROS production. Furthermore, there was a decreased mitochondrial Bcl-2 in the RQ in the 2 year KO vs. WT mice. Given that ARC is known to inhibit Bad and PUMA, both of which can inhibit Bcl-2[43], we speculate that a decrease in Bcl-2 activity might be seen in the aged ARC KO mice. As well, other studies in rats have shown that red skeletal muscle displays higher levels of pro- and anti-apoptotic proteins, ROS, and mitochondrial apoptosis[24], which would explain why the decreased Bcl-2 in the 2 year ARC KO mice was only seen in the RQ.

The Bax:Bcl-2 ratio is used as a marker of a cell's susceptibility to apoptosis, with earlier studies having found this ratio to be increased in the aged[31]. Previous work in our lab also found an increased Bax:Bcl-2 ratio in young ARC KO mice in the mitochondrial-enriched RQ (we also saw this in the 18 week ARC KO mice), as well as increased susceptibility to mitochondrial swelling and loss of membrane potential (two apoptotic events) after the addition of Ca^{2+}. Surprisingly, this ratio was lower in all tissues of the 2 year animals. Although an increased Bax:Bcl-2 ratio with aging has been shown in many studies, this is not always the case, and seem to depend on the muscle studied and the age of their 'old' animals[66]. One study found increased mitochondrial Bcl-2 and Bax expression yet no change in the Bax:Bcl-2 ratio in the gastrocnemius of 37 month old rats[37]. However, in this study there was a trend for the Bax:Bcl-2 ratio to decrease in aging. Whereas, another study found increased Bax and Bcl-2 expression in the EDL, yet in the soleus there was no change in Bax and increased Bcl-2 expression only in the 36 (not 30) month old rats[40]. Other studies have found increased Bcl-2 expression in both slow and fast muscle of aged rats[67]. In addition, this study found an increased Bcl-2 expression in gastrocnemius of 30 month old rats, with an further increase in Bcl-2 expression with an added stress, such as hindlimb suspension[67]. Thus, increased Bcl-2 expression may be a compensatory action in an attempt to counter the atrophy and apoptotic signaling occurring in skeletal muscle in aging.

Anti-apoptotic Proteins

To compensate for a lack of ARC, as well as to counter the increased apoptotic signaling and atrophy associated with aging, we believed there might be an increased expression of anti-apoptotic proteins. We found many of the anti-apoptotic proteins increased in the aged mice,

with fewer being influenced by genotype. In the soleus Bcl-XL, Hsp-70, and XIAP all increased in the 2 year animals, with ARC actually decreasing with age (in WT). Since these proteins have a higher expression in type I fibers, this increased protein expression may in part be caused by the shift towards a slower phenotype in aged mice. Although few studies have examined ARC expression over the lifespan, previous work found no differences in total ARC expression in gastrocnemius muscle of 30 month old rats[67], yet decreased cytosolic and increased mitochondrial ARC in gastrocnemius muscle of 26 month old rats[56]. ARC normally resides in the cytosol, but when phosphorylated by protein kinase CK2 at threonine-149, it translocates to the mitochondria, where it can exert its anti-apoptotic function[68]. However, under physiological conditions only a small amount of ARC is phosphorylated, inhibiting caspase activation[68]. Therefore, the previous study suggests an increased activation of ARC in aged rats. Although we did not measure ARC expression in subcellular fractions or phosphorylation status, we found no differences in total ARC expression in the plantaris of aged animals. Hsp-70 can inhibit Bax translocation to the mitochondria and AIF translocation to the nucleus, inhibit Apaf-1 from forming the apoptosome, prevent caspase-8 from activating Bid, as well as assisting in protein folding to alleviate ER-stress[69]. Additionally, XIAP can block caspase-9 activation[19]. Previous work has found increased expression of XIAP[56] and Hsp-70[31] in the gastrocnemius of rats 26 and 29 months old, respectively. These results suggest that an increased anti-apoptotic expression in aged mice may be an attempt to counteract the age-induced atrophy and apoptotic signaling. Interestingly no anti-apoptotic proteins were exclusively influenced by the lack of ARC in the soleus.

In the plantaris, the only anti-apoptotic protein alterations observed with age (2 year) were that of increased Bcl-XL, and XIAP. Interestingly, only the anti-apoptotic protein Bcl-XL

increased due to a lack of ARC protein in the plantaris. Bcl-XL is a mitochondrial transmembrane protein that prevents mPTP formation[70]. Without ARC inhibiting Bax activation, Bax can sequester Bcl-XL allowing pores to form[70]. In conditions of atrophy, such as denervation, Bcl-XL expression increases in rat facial muscle[71]. Therefore, it is likely that Bcl-XL expression increased to compensate for a lack of ARC in the KO animals, as well as to reduce apoptotic signaling seen in the 2 year animals.

Mitochondria are a major producer of free radicles, with increased ROS levels seen in the aged leading to increased oxidative damage, mDNA mutations[72], mitochondrial dysfunction, and apoptotic signaling[73]. In aging this could be attributed to decreased antioxidant defenses such as MnSOD and Catalase. Previous studies show mixed results, with increased enzyme activity [74] in aged rat muscle, whereas others show decreased activity in aged rat hearts[75], and decreased MnSOD protein content and activity in aged human vastus lateralis[76]. Additionally, transgenic mice lacking CuZnSOD display rapid aging, muscle atrophy, and increased oxidative modification to proteins[77]. In the soleus MnSOD protein expression was decreased in the 2 year animals, with no differences in the plantaris. Since we found no differences in the expression of the mitochondrial marker, ANT, in the 2 year animals, we can assume that the decreased MnSOD protein expression was not due to a decreased mitochondrial content. Although, other studies have found no differences in ANT in the gastrocnemius of 37 month old rats; however, an upward trend was found for Cyclophilin D with age[37]. Cyclophilin D resides within the mitochondrial matrix and contributes to mPTP formation. Thus, an increased Cyclophilin D content may reveal an increase in mitochondrial-mediated apoptotic signaling. This may suggest that increased ROS in aged mice without adequate increases in antioxidant proteins may lead to increased mitochondrial stress. Furthermore, aged animals display decreased mitochondrial

biogenesis[78], impaired clearance of damaged mitochondria, and increased fission[79]. Mitochondrial fission contributes to MOMP[80]. In H_2O_2-induced apoptosis, fission was prevented by overexpressing ARC in cardiomyocytes[81]. ARC inhibits PUMA, which is required for Drp-1 translocation and accumulation on the mitochondrial membrane to initiate fission[44]. We found no differences in cytosolic or mitochondrial Drp-1 between ages or genotypes.

Pro-apoptotic Proteins

Although the decreased Bax:Bcl-2 ratio seen in our aged mice suggests a diminished susceptibility of apoptotic signaling at the mitochondria, which has been suggested in a few studies[56], other measures performed in this study do not support this notion. In response to mitochondrial-mediated apoptotic signaling, mitochondrial housed AIF can be released into the cytosol, translocate to the nucleus, and cause DNA fragmentation independent of caspase activation[17]. Previous studies have shown increased cytosolic and nuclear levels of AIF in gastrocnemius of 29 and 37 month old rats[37]; however, others have shown only increased cytosolic, but not nuclear AIF in the gastrocnemius of 26 month old rats[56], as well as no increase in cytosolic or nuclear AIF in the gastrocnemius of 30 month old rats[67]. Since our aged mice showed increased Hsp-70 expression, which is known to inhibit AIF translocation from the cytosol to the nucleus, this may explain why we only observed an increased cytosolic, but not nuclear AIF in the WQ in aged mice. In addition to its role in apoptotic signaling, AIF has a role mitochondrial function and dysfunction[82]. AIF has been suggested to have a role in mitochondrial energy metabolism as well as in preventing ROS generation[83]. For example, in mouse muscle, tissue-specific deletion of AIF results in impaired oxidative phosphorylation and functional deficits in complex 1 activity and content[82]. Thus, if AIF is being released into the

cytosol, mitochondrial electron transport may be affected, leading to reduced mitochondria function and ROS generation. Previous work in our lab found an increased cytosolic AIF in the RQ in young ARC KO mice, with our 18 week KO mice displaying increased cytosolic AIF in the WQ. Overall our findings show a slight increase in caspase-independent apoptotic signaling in fast muscle of aged mice.

Differences were also observed in our study with caspase-dependent signaling. Increased[67] cytosolic Cyto-c content has been found in the gastrocnemius of 30 month old rats. However, decreased[56] cytosolic Cyto-c levels were also found in the gastrocnemius of 26 month old rats. Additionally, a transient increase in caspase-9 activity over the lifespan was reported[37]. We found a similar result with total Cyto-c in the plantaris increasing in the 1 year vs. 18 week animals, with a decline at 2 years. This may be due to an increased mitochondrial content in the 1 year animals and a decreased content in the 2 year animals. However, as stated before, we found no differences in ANT expression in the 2 year animals; therefore, this is likely do to specific alterations in Cyto-c expression. In the RQ and WQ there was increased cytosolic SMAC in the 2 year animals. An increase in SMAC would block the inhibitory actions of XIAP[19]. In agreement with our results, increased SMAC was shown in the gastrocnemius of 30 month old rats[67]. Furthermore, examination of the 2 year ARC KO mice vs. WT revealed an increased Bax:Bcl-2 ratio, nuclear AIF, cytosolic Cyto-c, and cytosolic SMAC in the RQ. Given that ARC is able to inhibit Bax, preventing the release of pro-apoptotic proteins from the mitochondria, this coincides with our hypothesis that the 2 year ARC KO animals would display an increased mitochondrial-mediated apoptotic signaling.

Skeletal Muscle Morphological and Phenotypic Changes

Advancing age is associated with skeletal muscle atrophy, decreased fiber CSA and number, as well as a shift toward a slower phenotype[32]. Previous work on young ARC KO mice showed altered CSA and fiber distribution in both the soleus and plantaris. We found both morphological differences, in muscle CSA, as well as phenotypic differences, in fiber type distribution in both soleus and plantaris muscle. Numerous other apoptotic proteins are involved in the regulation of skeletal muscle size during development and formation. For example, skeletal muscle differentiation is reduced in cultured myoblasts by overexpressing Bcl-XL, preventing increases in caspase-3[84]. Additionally, myotubes display enhanced apoptotic cell death when differentiated from low Bcl-2 expressing C2C12 cells[85]. Furthermore, under conditions of stress, such as immobilization, caspase-3 KO mice show attenuated decreases in muscle mass in both the soleus and gastrocnemius[86]. Additionally, one study examined muscle-specific overexpression of the anti-apoptotic Hsp-70 in adult mice and surprisingly found a decrease in both body and muscle mass[87]. Whereas, another study of overexpression found that after 7 days of immobilization there was decreased CSA of type II fibers in the EDL and type I and II fibers from soleus; however, after 7 days of recovering only the mice overexpressing Hsp-70 recovered muscle size[88]. Together, these studies suggest that apoptotic signaling proteins alter skeletal muscle morphology, with their expression changing in development and under conditions of stress. These factors may contribute to alterations in force development in both the aging process, as well as a result of a lack of ARC protein.

Changes in Cross-Sectional Area

Total CSA decreased in the 2 year animals in both the soleus and plantaris, with a trend

towards a decrease in KO animals in the soleus. Since ARC is higher in type I and IIA fibers which comprises around 80% of the soleus, it was expected that total CSA would be lower in KO animals. As well, previous work in our lab found a smaller soleus CSA, but a larger plantaris CSA in young ARC KO mice, with our results revealing similar findings in 18 week KO mice. Therefore, it is not surprising that the total CSA of the plantaris did not decrease in our ARC KO animals. In the soleus type I, IIA, and IIX fiber CSA decreased in the 2 year animals, whereas a decrease was seen in CSA of type IIA, IIX, and IIB fibers in the plantaris. Similar to our plantaris results, aging studies demonstrate atrophy of type II fibers with little change in type I[32]. Furthermore, there appeared to be a wide range of both large and very small fiber sizes in the 2 year animals, which may not have been represented in the averages of specific fiber type CSA. Literature has shown large variations in fiber sizes among individuals with this being exacerbated with age[89]. It has been speculated that this results from the denervation-reinnervation in the aged[90], allowing denervated fibers to atrophy while others may hypertrophy to compensate[91]. Furthermore, conditions of stress, other than aging, can result in specific fibers atrophying. One such condition being inactivity, which causes a decrease in CSA of type I and IIA fibers[92]. Although this was not a study of inactivity or of forced disuse, such as hindlimb suspension, the mice were cage bound with no access to a running wheel over their lifespan. Since the literature has shown that C57/B6 mice with access to a running wheel run an average of 4 km per day[93], our model could lead to a more sedentary lifestyle (and be a chronic model of inactivity), possibly influencing the differences seen in fiber-specific CSA. This may have blunted the effects of aging on a lack of ARC, resulting in a larger decrease in type I and IIA CSA then would usually be seen in aging. There were no differences in specific fiber CSA with respect to genotype. As well, previous work in our lab showed a decreased CSA of type I and

IIA fibers in the soleus of young ARC KO mice; however we did not see this in our 18 week KO mice. As well, in the plantaris of young ARC KO mice previous work found an increase in type IIB fiber CSA; however we saw a decreased type I fiber CSA in 18 week KO mice. Overall, we found a decrease in the CSA of all type II fibers in the 2 year animals, reflecting what is seen in aging, as well as a decrease in type I CSA in the soleus during aging.

Changes in Skeletal Muscle Fiber Type

Along with alterations in CSA, we also found shifts in fiber type distribution with aging. In the soleus, aged mice display a higher percentage of type I fibers and a decreased percentage of type IIX and IIB fibers, resulting in a shift towards a slower phenotype. In the plantaris, aged mice display a lower percentage of type I and type IIA fibers, and an increased percentage of type IIB fibers, resulting in a shift towards a faster phenotype. Even though there was an increase in type IIB fiber percentage, the CSA of those fibers were smaller. One study on aged C57/B6 mice found similar results with a shift toward a slower phenotype in the soleus and a faster phenotype in the EDL[94]. A number of conditions result in fiber type switching[95]. Aging results in a shift towards a slower phenotype, whereas inactivity is associated with a slow to fast shift[96]. Although this study was not an inactivity model as stated before, these animals were cage-bound their entire life, possibly influencing the shift in fiber types[93]. Therefore the shift towards a slower MHC in aging may have been blunted, resulting in a heightened shift towards a faster MHC, increasing the influence of a lack of ARC. Thus, the soleus revealed a shift towards a slower fiber type composition, commonly seen in aging, yet the faster shift in the plantaris more closely resembles an inactive model. The fiber type shift in our aged ARC KO mice likely reflects a balance between a slower phenotype shift in aging, and a faster phenotype shift due to

ARC-deficiency, as seen previously in young ARC KO mice in our lab as well as in the soleus of our 18 week ARC KO mice. Although we found no effect of genotype in either muscle, the dramatic fiber type switching in normal aging may "washout" any effects of a lack of ARC protein.

In addition to ARC's anti-apoptotic role in skeletal muscle maintenance, ARC also has an important role in skeletal muscle development, remodeling with exercise and in disease. Previous work in our lab and others have demonstrated ARC's role in skeletal muscle differentiation[58]. ARC protein content was found to be low in myoblasts but becomes upregulated during differentiation into myotubes[58]. Whereas, overexpression of ARC in pre-differentiated H9c2 cells, prevented these cells from differentiating[57]. Therefore, ARC has a central role in the formation of healthy muscle during development. Furthermore, ARC also has an important role in adaptations to exercise. For example, ARC becomes upregulated in response to exercise training in rat soleus muscle[97], with exercise also known to decrease apoptosis. Additionally, ARC expression has been shown to change in disease states. For example, ARC localization changes in muscular dystrophy[98], whereas ARC expression decreases in hypoxia[50], and ischemia-reperfusion injury[49]. Transgenic overexpression of ARC in dystrophic muscles of 6 week old mice was found not to be protective, possibly resulting from a functional saturation of ARC[99]. Whereas, ARC deficiency in dystrophic muscle resulted in increased Bax, elevated Ca^{2+}, and a lower threshold of the mPTP[98]. Thus, these studies show that under various conditions of stress, that the regulation and expression of ARC differs, with our aging study showing a decrease in the expression of ARC in the soleus of our 2 year WT mice despite the shift to a slower phenotype.

Changes in Force Characteristics

There is a progressive decline in both muscle mass and function with increasing age. Studies have shown that in addition to a decreased fiber size and number with aging[94], increasing age results in fiber denervation (especially of fast α-motorneurons) and reinnervation[100], structural alterations, and a decrease in force generating capacity[66]. The decline in force generating capacity is around a 40% decrease from age 20 to 80 years in humans[101], although in mice the decrease is about 20%[66]. Our results revealed a higher rate of both contraction and relaxation and twitch:tetanus ratio in the soleus of the 2 year animals, indicating an increased twitch force and smaller tetanic contraction in aged mice. The plantaris revealed slower contraction and relaxation rates, decreased tetanic contraction, as well as the force-frequency curve was shifted downwards in the 2 year animals. This is likely due to a decreased CSA of type IIB fibers, as well as a decrease in whole muscle CSA. Decreased tetanic force with age has been documented in previous studies[102]. With age, the decline in force may not just be due to atrophy, but a loss of force per unit cross-sectional area, resulting from extracellular non-contractile tissue in muscle[103]. As well, the specific force of individual fibers decreases with age, which may be from changes in excitation contraction coupling and/or alterations to myosin and actin[104]. This can result from increased damage to the mitochondria and ER, by increased ROS[105], and apoptotic changes, such as an increase in enzymes that can cleave structural and contractile proteins. For example, in mice the overexpression of the antioxidant catalase in the mitochondria reduced the normal age decline in force generating capacity[106]. Both the soleus and plantaris demonstrated slower one-half relaxation rates, with the soleus also having slower time to peak tension in the 2 year animals. This could be the result of a higher percentage of slow type I fibers in the soleus, as well as slower uptake of Ca^{2+} into the SR by the sarco/endoplasmic

reticulum Ca^{2+} ATPase (SERCA) in increasing age, in both muscles[106]. However, measures of fatigue were not different between groups. Previous work also found no differences in the EDL of aged mice[107]. We can speculate that the lack of differences in fatigability of both soleus and plantaris muscles in our study, may be due to motor unit switching or a decreased proportion of fiber area from type IIB fibers in the soleus. Additionally, there is evidence that the increased fatigue, usually seen in aged humans[108] and mice[109], is central fatigue. Since we used isolated muscles we were not able to test or to attribute differences to either central or peripheral fatigue. In our measures, we found no significant effect with respect to genotype. Previous work in 18 week ARC KO mice found that maximum twitch contraction rates were decreased in the soleus, and that the plantaris showed decreased fatigability. We found similar results when only comparing our 18 week animals. Differences in apoptotic signaling and skeletal muscle morphology were minimal between genotypes in the aged mice, which may have resulted in the lack of an effect seen in the contractile measures. Also, since age has a dramatic effect on muscle function, any significant differences in genotype may have been 'washed out' by the effects of age, if any changes did occur. Overexpression of other apoptotic proteins in mice has shown improvements in contractile function with age. For example, when aged mice were given damaging lengthening contractions, muscle-specific overexpression of Hsp-70 resulted in faster recovery, better Ca^{2+} handling, and maintenance of specific force, in overexpressing mice[87]. Although these mice still demonstrated age-related skeletal muscle atrophy, they were able to maintain the same force per unit of cross-sectional area. Overall, although studies on young ARC KO mice found an effect of genotype, we did not observe the same effects over the lifespan; however, we demonstrated significant age-related alterations in force generating capacity and rate, with no differences in fatigability.

Satellite cell content has been reported to decrease in the aged[35], and this correlates with a decreased regenerative ability[110]. This loss of satellite cells in sarcopenia is also greater in type II fibers[111]. There is speculation that the myonuclear domain size changes in aging[112]. Some suggest that in aged a decrease in satellite cell number, slowed activation, and decreased proliferation leads to nuclei not being replaced and an increase[113] or decrease[114] in myonuclear domain size. Since the myonuclear domain supports protein synthesis and gene maintenance within the muscle, changes in size may impact function. Regardless, aged muscles display decreased regenerative ability, increased protein degradation, and an attenuated rate of protein synthesis. These combination of factors than ultimately lead to atrophy and functional alterations.

Conclusion

There is significant skeletal muscle mass and strength loss in the elderly resulting in impaired mobility. Elucidating the mechanisms that influence muscle loss over the lifespan may lead to improved function and health. Using an ARC KO mouse model at three different ages we examined the role of ARC in the maintenance of skeletal muscle over the lifespan. Specifically we found alterations in skeletal muscle morphology in both fast and slow muscle, including differences in muscle size and fiber distribution during the aging process. Furthermore, we also found alterations in force production, an upregulation of proteins involved in apoptotic signaling, but no differences in proteolytic enzymes in aged mice. Although differences were seen from a lack of ARC over the lifespan, the morphological and apoptotic alterations seen in aging were more overt, suggesting ARC may have a larger influence during skeletal muscle development rather than during aging, and possibly in situations with greater additional stress. Overall, this study illustrates the morphological, apoptotic, and functional alterations in skeletal muscle of aged mice, with only a few differences in aged ARC KO mice.

Limitations

The transgenic ARC KO mouse model used in this study was a global KO and therefore it was not specific to only skeletal muscle. This may have affected the regulation of other tissues within the body, which may have influenced these results. ARC is primarily in skeletal muscle, cardiac muscle, and brain; therefore, the resulting effects from these tissues may have had an influence on our outcomes.

The soleus and plantaris muscles were used for morphological measures and protein expression, but due to their small size, other representative slow (red gastrocnemius and quadriceps) and fast (white gastrocnemius and quadriceps) muscles were used for measures of protein expression in subcellular fractions and enzymatic activity. These muscles have different fiber type compositions and may have lead to discrepancies when making muscle comparisons. Additionally, whole muscle homogenates were used which are a heterogeneous mixture of fiber types, thereby conclusions about fiber type-specific protein expression cannot be conducted from our results. Also, changes in fiber type composition could affect the protein expression of other apoptotic factors. Furthermore, atrophy, denoted by decreased fiber type-specific CSA, did not occur in all fiber types. Therefore, we cannot infer that all fiber types may be contributing to the altered apoptotic signaling in skeletal muscle.

Future Directions

While some differences were found as a result of a lack of ARC protein over the aging process, future work is needed to further examine the role of ARC over the lifespan. Firstly, the mice had no access to a running wheel in their cages possibly producing a more sedentary lifestyle than would be normal. This could be avoided by allowing the mice access to a running wheel. Additionally, by employing a forced disuse model (hindlimb suspension or denervation), we could determine whether these phenotypic differences become exacerbated in the skeletal muscle of aged mice. Furthermore, an exercise study could be of interest, since exercise is associated with a decrease in apoptotic signaling and an increase in ARC expression[97]. Determining if the protective effects of exercise are mediated through ARC by using an ARC KO mouse model in an exercise training study would help to further elucidate the role of ARC under different conditions of stress.

Secondly, an ARC overexpression study in mice would be of interest to determine if increased ARC expression can attenuate the age associated decrease in skeletal muscle mass. Previous work has found that overexpression of other anti-apoptotic proteins results in decreased apoptotic signaling and attenuated decreases in force production with age[87].

Lastly, previous aging studies implementing caloric restriction have demonstrated protective effects against increases in apoptotic signaling, as well as muscle atrophy. One study showed that lifelong caloric restriction increased ARC expression, thereby decreasing mitochondrial-mediated apoptotic signaling[55]. Therefore, combining caloric restriction with an ARC KO mouse model may be of importance for future studies. These experiments would increase the knowledge of ARC's role in the regulation of fiber-specific muscle morphology, adaptation to exercise, and apoptotic signaling in disease.

References

1. Portt L, Norman G, Clapp C, Greenwood M, Greenwood MT. Anti-apoptosis and cell survival: A review. *Biochimica et Biophysica Acta - Molecular Cell Research*. 2011;1813(1):238-259.

2. Saikumar P, Dong Z, Mikhailov V, Denton M, Weinberg JM, Venkatachalam MA. Apoptosis: Definition, mechanisms, and relevance to disease. *Am J Med*. 1999;107(5):489-506.

3. Dominov JA, Dunn JJ, Miller JB. Bcl-2 expression identifies an early stage of myogenesis and promotes clonal expansion of muscle cells. *J Cell Biol*. 1998;142(2):537-544.

4. Zermati Y, Garrido C, Amsellem S, et al. Caspase activation is required for terminal erythroid differentiation. *J Exp Med*. 2001;193(2):247-254.

5. Medina-Ramirez CM, Goswami S, Smirnova T, et al. Apoptosis inhibitor ARC promotes breast tumorigenesis, metastasis, and chemoresistance. *Cancer Res*. 2011;71(24):7705-7715.

6. Li Y, Ge X, Liu X. The cardioprotective effect of postconditioning is mediated by ARC through inhibiting mitochondrial apoptotic pathway. *Apoptosis*. 2009;14(2):164-172.

7. Reed JC. Apoptosis-based therapies. *Nature Reviews Drug Discovery*. 2002;1(2):111-121.

8. Dupont-Versteegden EE. Apoptosis in muscle atrophy: Relevance to sarcopenia. *Exp Gerontol*. 2005;40(6):473-481.

9. McKimpson WM, Weinberger J, Czerski L, et al. The apoptosis inhibitor ARC alleviates the ER stress response to promote ß-cell survival. *Diabetes*. 2013;62(1):183-193.

10. Fan T-, Han L-, Cong R-, Liang J. Caspase family proteases and apoptosis. *Acta Biochimica et Biophysica Sinica*. 2005;37(11):719-727.

11. Ola MS, Nawaz M, Ahsan H. Role of bcl-2 family proteins and caspases in the regulation of apoptosis. *Mol Cell Biochem*. 2011;351(1-2):41-58.

12. Krysko DV, Vanden Berghe T, D'Herde K, Vandenabeele P. Apoptosis and necrosis: Detection, discrimination and phagocytosis. *Methods*. 2008;44(3):205-221.

13. Quadrilatero J, Alway SE, Dupont-Versteegden E. Skeletal muscle apoptotic response to physical activity: Potential mechanisms for protection. *Applied Physiology, Nutrition and Metabolism*. 2011;36(5):608-617.

14. Tait SWG, Green DR. Mitochondria and cell death: Outer membrane permeabilization and beyond. *Nature Reviews Molecular Cell Biology*. 2010;11(9):621-632.

15. Kroemer G, Galluzzi L, Brenner C. Mitochondrial membrane permeabilization in cell death. *Physiol Rev*. 2007;87(1):99-163.

16. Morselli E, Galluzzi L, Kroemer G. Mechanisms of p53-mediated mitochondrial membrane permeabilization. *Cell Res*. 2008;18(7):708-710.

17. Wang C, Youle RJ, eds. *The role of mitochondria in apoptosis*. ; 2009Annual Review of Genetics; No. 43.

18. Bao Q, Shi Y. Apoptosome: A platform for the activation of initiator caspases. *Cell Death Differ*. 2007;14(1):56-65.

19. Du C, Fang M, Li Y, Li L, Wang X. Smac, a mitochondrial protein that promotes cytochrome c-dependent caspase activation by eliminating IAP inhibition. *Cell*. 2000;102(1):33-42.

20. Boyce M, Yuan J. Cellular response to endoplasmic reticulum stress: A matter of life or death. *Cell Death Differ*. 2006;13(3):363-373.

21. Xu C, Bailly-Maitre B, Reed JC. Endoplasmic reticulum stress: Cell life and death decisions. *J Clin Invest*. 2005;115(10):2656-2664.

22. Vannuvel K, Renard P, Raes M, Arnould T. Functional and morphological impact of ER stress on mitochondria. *J Cell Physiol*. 2013;228(9):1802-1818.

23. Rasheva VI, Domingos PM. Cellular responses to endoplasmic reticulum stress and apoptosis. *Apoptosis*. 2009;14(8):996-1007.

24. McMillan EM, Quadrilatero J. Differential apoptosis-related protein expression, mitochondrial properties, proteolytic enzyme activity, and DNA fragmentation between skeletal muscles. *American Journal of Physiology - Regulatory Integrative and Comparative Physiology*. 2011;300(3):R531-R543.

25. Allen DL, Roy RR, Reggie Edgerton V. Myonuclear domains in muscle adaptation and disease. *Muscle and Nerve*. 1999;22(10):1350-1360.

26. Alway SE, Siu PM. Nuclear apoptosis contributes to sarcopenia. *Exerc Sport Sci Rev*. 2008;36(2):51-57.

27. Zierath JR, Hawley JA. Skeletal muscle fiber type: Influence on contractile and metabolic properties. *PLoS Biology*. 2004;2(10).

28. Dam AD, Mitchell AS, Rush JWE, Quadrilatero J. Elevated skeletal muscle apoptotic signaling following glutathione depletion. *Apoptosis*. 2012;17(1):48-60.

29. Cruz-Jentoft AJ, Baeyens JP, Bauer JM, et al. Sarcopenia: European consensus on definition and diagnosis. *Age Ageing*. 2010;39(4):412-423.

30. Buford TW, Anton SD, Judge AR, et al. Models of accelerated sarcopenia: Critical pieces for solving the puzzle of age-related muscle atrophy. *Ageing Research Reviews*. 2010;9(4):369-383.

31. Chung L, Ng Y-. Age-related alterations in expression of apoptosis regulatory proteins and heat shock proteins in rat skeletal muscle. *Biochimica et Biophysica Acta - Molecular Basis of Disease*. 2006;1762(1):103-109.

32. Nilwik R, Snijders T, Leenders M, et al. The decline in skeletal muscle mass with aging is mainly attributed to a reduction in type II muscle fiber size. *Exp Gerontol*. 2013;48(5):492-498.

33. Cai D, Lee KKH, Li M, Tang MK, Chan KM. Ubiquitin expression is up-regulated in human and rat skeletal muscles during aging. *Arch Biochem Biophys*. 2004;425(1):42-50.

34. Calvani R, Joseph A-, Adhihetty PJ, et al. Mitochondrial pathways in sarcopenia of aging and disuse muscle atrophy. *Biol Chem*. 2013;394(3):393-414.

35. Alway SE, Myers MJ, Mohamed JS. Regulation of satellite cell function in sarcopenia. *Frontiers in Aging Neuroscience*. 2014;6(SEP).

36. Dirks A, Leeuwenburgh C. Apoptosis in skeletal muscle with aging. *Am J Physiol -Regul Integr Comp Physiol*. 2002;282(2):R519-R527.

37. Marzetti E, Wohlgemuth SE, Lees HA, Chung H-, Giovannini S, Leeuwenburgh C. Age-related activation of mitochondrial caspase-independent apoptotic signaling in rat gastrocnemius muscle. *Mech Ageing Dev*. 2008;129(9):542-549.

38. Pistilli EE, Jackson JR, Alway SE. Death receptor-associated pro-apoptotic signaling in aged skeletal muscle. *Apoptosis*. 2006;11(12):2115-2126.

39. Leeuwenburgh C, Gurley CM, Strotman BA, Dupont-Versteegden EE. Age-related differences in apoptosis with disuse atrophy in soleus muscle. *American Journal of Physiology - Regulatory Integrative and Comparative Physiology*. 2005;288(5 57-5):R1288-R1296.

40. Rice KM, Blough ER. Sarcopenia-related apoptosis is regulated differently in fast- and slow-twitch muscles of the aging F344/N × BN rat model. *Mech Ageing Dev*. 2006;127(8):670-679.

41. Nam Y-, Mani K, Ashton AW, et al. Inhibition of both the extrinsic and intrinsic death pathways through nonhomotypic death-fold interactions. *Mol Cell*. 2004;15(6):901-912.

42. Ludwig-Galezowska AH, Flanagan L, Rehm M. Apoptosis repressor with caspase recruitment domain, a multifunctional modulator of cell death. *J Cell Mol Med*. 2011;15(5):1044-1053.

43. Li Y-, Lu D-, Tan W-, Wang J-, Li P-. p53 initiates apoptosis by transcriptionally targeting the antiapoptotic protein ARC. *Mol Cell Biol*. 2008;28(2):564-574.

44. Wang J-, Li Q, Li P-. Apoptosis repressor with caspase recruitment domain contributes to chemotherapy resistance by abolishing mitochondrial fission mediated by dynamin-related protein-1. *Cancer Res*. 2009;69(2):492-500.

45. Foo RS-, Nam Y-, Ostreicher MJ, et al. Regulation of p53 tetramerization and nuclear export by ARC. *Proc Natl Acad Sci U S A*. 2007;104(52):20826-20831.

46. Foo RS-, Chan LKW, Kitsis RN, Bennett MR. Ubiquitination and degradation of the anti-apoptotic protein ARC by MDM2. *J Biol Chem*. 2007;282(8):5529-5535.

47. Jo D-, Jun J-, Chang J-, et al. Calcium binding of ARC mediates regulation of caspase 8 and cell death. *Mol Cell Biol*. 2004;24(22):9763-9770.

48. Quadrilatero J, Bloemberg D. Apoptosis repressor with caspase recruitment domain is dramatically reduced in cardiac, skeletal, and vascular smooth muscle during hypertension. *Biochem Biophys Res Commun*. 2010;391(3):1437-1442.

49. Donath S, Li P, Willenbockel C, et al. Apoptosis repressor with caspase recruitment domain is required for cardioprotection in response to biomechanical and ischemic stress. *Circulation*. 2006;113(9):1203-1212.

50. Wang M, Qanungo S, Crow MT, Watanabe M, Nieminen A-. Apoptosis repressor with caspase recruitment domain (ARC) is expressed in cancer cells and localizes to nuclei. *FEBS Lett*. 2005;579(11):2411-2415.

51. An J, Harms C, Lättig-Tünnemann G, et al. TAT-apoptosis repressor with caspase recruitment domain protein transduction rescues mice from fulminant liver failure. *Hepatology*. 2012;56(2):715-726.

52. Zhang Y-, Herman B. Expression and modification of ARC (apoptosis repressor with a CARD domain) is distinctly regulated by oxidative stress in cancer cells. *J Cell Biochem*. 2008;104(3):818-825.

53. Gustafsson ÅB, Sayen MR, Williams SD, Crow MT, Gottlieb RA. TAT protein transduction into isolated perfused hearts: TAT-apoptosis repressor with caspase recruitment domain is cardioprotective. *Circulation*. 2002;106(6):735-739.

54. Li Q, Ren J. Influence of cardiac-specific overexpression of insulin-like growth factor 1 on lifespan and aging-associated changes in cardiac intracellular Ca2+ homeostasis, protein damage and apoptotic protein expression. *Aging Cell*. 2007;6(6):799-806.

55. Shelke RR, Leeuwenburgh C. Lifelong caloric restriction increases expression of apoptosis repressor with a caspase recruitment domain (ARC) in the brain. *The FASEB journal : official publication of the Federation of American Societies for Experimental Biology*. 2003;17(3):494-496.

56. Dirks AJ, Leeuwenburgh C. Aging and lifelong calorie restriction result in adaptations of skeletal muscle apoptosis repressor, apoptosis-inducing factor, X-linked inhibitor of apoptosis, caspase-3, and caspase-12. *Free Radical Biology and Medicine*. 2004;36(1):27-39.

57. Hunter AL, Zhang J, Chen SC, et al. Apoptosis repressor with caspase recruitment domain (ARC) inhibits myogenic differentiation. *FEBS Lett*. 2007;581(5):879-884.

58. Xiao R, Ferry AL, Dupont-Versteegden EE. Cell death-resistance of differentiated myotubes is associated with enhanced anti-apoptotic mechanisms compared to myoblasts. *Apoptosis*. 2011;16(3):221-234.

59. Quadrilatero J, Rush JWE. Increased DNA fragmentation and altered apoptotic protein levels in skeletal muscle of spontaneously hypertensive rats. *J Appl Physiol*. 2006;101(4):1149-1161.

60. Bloemberg D, Quadrilatero J. Rapid determination of myosin heavy chain expression in rat, mouse, and human skeletal muscle using multicolor immunofluorescence analysis. *PLoS ONE*. 2012;7(4).

61. Brüünsgaard H, Pedersen BK. Age-related inflammatory cytokines and disease. *Immunology and Allergy Clinics of North America*. 2003;23(1):15-39.

62. Fraysse B, Desaphy J-, Rolland J-, et al. Fiber type-related changes in rat skeletal muscle calcium homeostasis during aging and restoration by growth hormone. *Neurobiol Dis*. 2006;21(2):372-380.

63. Nishitoh H. CHOP is a multifunctional transcription factor in the ER stress response. *J Biochem*. 2012;151(3):217-219.

64. Hockenbery D, Niñez G, Milliman C, Schreiber RD, Korsmeyer SJ. Bcl-2 is an inner mitochondrial membrane protein that blocks programmed cell death. *Nature*. 1990;348(6299):334-336.

65. Pinton P, Rizzuto R. Bcl-2 and Ca2+ homeostasis in the endoplasmic reticulum. *Cell Death Differ*. 2006;13(8):1409-1418.

66. Ballak SB, Degens H, de Haan A, Jaspers RT. Aging related changes in determinants of muscle force generating capacity: A comparison of muscle aging in men and male rodents. *Ageing Research Reviews*. 2014;14(1):43-55.

67. Siu PM, Pistilli EE, Alway SE. Apoptotic responses to hindlimb suspension in gastrocnemius muscles from young adult and aged rats. *American Journal of Physiology - Regulatory Integrative and Comparative Physiology*. 2005;289(4 58-4):R1015-R1026.

68. Li P-, Li J, Müller E-, Otto A, Dietz R, Von Harsdorf R. Phosphorylation by protein kinase CK2: A signaling switch for the caspase-inhibiting protein ARC. *Mol Cell*. 2002;10(2):247-258.

69. Beere HM. Death versus survival: Functional interaction between the apoptotic and stress-inducible heat shock protein pathways. *J Clin Invest*. 2005;115(10):2633-2639.

70. Finucane DM, Bossy-Wetzel E, Waterhouse NJ, Cotter TG, Green DR. Bax-induced caspase activation and apoptosis via cytochrome c release from mitochondria is inhibitable by bcl-xL. *J Biol Chem*. 1999;274(4):2225-2233.

71. Tews DS, Goebel HH, Schneider I, Gunkel A, Stennert E, Neiss WF. DNA-fragmentation and expression of apoptosis-related proteins in experimentally denervated and reinnervated rat facial muscle. *Neuropathol Appl Neurobiol*. 1997;23(2):141-149.

72. Kujoth GC, Leeuwenburgh C, Prolla TA. Mitochondrial DNA mutations and apoptosis in mammalian aging. *Cancer Res*. 2006;66(15):7386-7389.

73. Chabi B, Ljubicic V, Menzies KJ, Huang JH, Saleem A, Hood DA. Mitochondrial function and apoptotic susceptibility in aging skeletal muscle. *Aging Cell*. 2008;7(1):2-12.

74. Ji LL, Dillon D, Wu E. Alteration of antioxidant enzymes with aging in rat skeletal muscle and liver. *American Journal of Physiology - Regulatory Integrative and Comparative Physiology*. 1990;258(4 27-4):R918-R923.

75. Xia E, Rao G, Van Remmen H, Heydari AR, Richardson A. Activities of antioxidant enzymes in various tissues of male fischer 344 rats are altered by food restriction. *J Nutr*. 1995;125(2):195-201.

76. Safdar A, Hamadeh MJ, Kaczor JJ, Raha S, deBeer J, Tarnopolsky MA. Aberrant mitochondrial homeostasis in the skeletal muscle of sedentary older adults. *PLoS ONE*. 2010;5(5).

77. Muller FL, Song W, Liu Y, et al. Absence of CuZn superoxide dismutase leads to elevated oxidative stress and acceleration of age-dependent skeletal muscle atrophy. *Free Radical Biology and Medicine*. 2006;40(11):1993-2004.

78. Reznick RM, Zong H, Li J, et al. Aging-associated reductions in AMP-activated protein kinase activity and mitochondrial biogenesis. *Cell Metabolism*. 2007;5(2):151-156.

79. Brunk UT, Terman A. The mitochondrial-lysosomal axis theory of aging: Accumulation of damaged mitochondria as a result of imperfect autophagocytosis. *European Journal of Biochemistry*. 2002;269(8):1996-2002.

80. Frank S, Gaume B, Bergmann-Leitner ES, et al. The role of dynamin-related protein 1, a mediator of mitochondrial fission, in apoptosis. *Developmental Cell*. 2001;1(4):515-525.

81. Li J, Li Y, Qin D, Von Harsdorf R, Li P. Mitochondrial fission leads to smac/DIABLO release quenched by ARC. *Apoptosis*. 2010;15(10):1187-1196.

82. Joza N, Oudit GY, Brown D, et al. Muscle-specific loss of apoptosis-inducing factor leads to mitochondrial dysfunction, skeletal muscle atrophy, and dilated cardiomyopathy. *Mol Cell Biol*. 2005;25(23):10261-10272.

83. Joza N, Pospisilik JA, Hangen E, et al, eds. *AIF: Not just an apoptosis-inducing factor*. ; 2009Annals of the New York Academy of Sciences; No. 1171.

84. Murray TVA, McMahon JM, Howley BA, et al. A non-apoptotic role for caspase-9 in muscle differentiation. *J Cell Sci*. 2008;121(22):3786-3793.

85. Schöneich C, Dremina E, Galeva N, Sharov V. Apoptosis in differentiating C2C12 muscle cells selectively targets bcl-2-deficient myotubes. *Apoptosis*. 2014;19(1):42-57.

86. Zhu S, Nagashima M, Khan MAS, Yasuhara S, Kaneki M, Martyn JAJ. Lack of caspase-3 attenuates immobilization-induced muscle atrophy and loss of tension generation along with mitigation of apoptosis and inflammation. *Muscle and Nerve*. 2013;47(5):711-721.

87. McArdle A, Dillmann WH, Mestril R, Faulkner JA, Jackson MJ. Overexpression of HSP70 in mouse skeletal muscle protects against muscle damage and age-related muscle dysfunction. *The FASEB journal : official publication of the Federation of American Societies for Experimental Biology*. 2004;18(2):355-357.

88. Miyabara EH, Nascimento TL, Rodrigues DC, et al. Overexpression of inducible 70-kDa heat shock protein in mouse improves structural and functional recovery of skeletal muscles from atrophy. *Pflugers Archiv European Journal of Physiology*. 2012;463(5):733-741.

89. Degens H, Morse CI, Hopman MTE, eds. *Heterogeneity of capillary spacing in the hypertrophied plantaris muscle from young-adult and old rats*. ; 2009Advances in Experimental Medicine and Biology; No. 645.

90. Larsson L, Ansved T. Effects of ageing on the motor unit. *Prog Neurobiol*. 1995;45(5):397-415,417-421,423-458.

91. Degens H, Korhonen MT. Factors contributing to the variability in muscle ageing. *Maturitas*. 2012;73(3):197-201.

92. Zhong H, Roy RR, Siengthai B, Edgerton VR. Effects of inactivity on fiber size and myonuclear number in rat soleus muscle. *J Appl Physiol*. 2005;99(4):1494-1499.

93. Lightfoot JT, Turner MJ, Daves M, Vordermark A, Kleeberger SR. Genetic influence on daily wheel running activity level. *Physiological Genomics*. 2005;19:270-276.

94. Sheard PW, Anderson RD. Age-related loss of muscle fibres is highly variable amongst mouse skeletal muscles. *Biogerontology*. 2012;13(2):157-167.

95. Nakatani T, Nakashima T, Kita T, et al. Fiber type distribution, cross-sectional area, and succinate dehydrogenase activity of soleus and extensor digitorum longus muscles in spontaneously hypertensive rats. *Acta Histochem Cytochem*. 2002;35(4):315-322.

96. Talmadge RJ. Myosin heavy chain isoform expression following reduced neuromuscular activity: Potential regulatory mechanisms. *Muscle and Nerve*. 2000;23(5):661-679.

97. Siu PM, Bryner RW, Murlasits Z, Alway SE. Response of XIAP, ARC, and FLIP apoptotic suppressors to 8 wk of treadmill running in rat heart and skeletal muscle. *J Appl Physiol*. 2005;99(1):204-209.

98. Davis J, Kwong JQ, Kitsis RN, Molkentin JD. Apoptosis repressor with a CARD domain (ARC) restrains bax-mediated pathogenesis in dystrophic skeletal muscle. *PLoS ONE*. 2013;8(12).

99. Abmayr S, Crawford RW, Chamberlain JS. Characterization of ARC, apoptosis repressor interacting with CARD, in normal and dystrophin-deficient skeletal muscle. *Hum Mol Genet*. 2004;13(2):213-221.

100. Rowan SL, Rygiel K, Purves-Smith FM, Solbak NM, Turnbull DM, Hepple RT. Denervation causes fiber atrophy and myosin heavy chain co-expression in senescent skeletal muscle. *PLoS ONE*. 2012;7(1).

101. Doherty TJ. Invited review: Aging and sarcopenia. *J Appl Physiol*. 2003;95(4):1717-1727.

102. Degens H, Alway SE. Skeletal muscle function and hypertrophy are diminished in old age. *Muscle and Nerve*. 2003;27(3):339-347.

103. Payne AM, Dodd SL, Leeuwenburgh C. Life-long calorie restriction in fischer 344 rats attenuates age-related loss in skeletal muscle-specific force and reduces extracellular space. *J Appl Physiol*. 2003;95(6):2554-2562.

104. Lowe DA, Surer JT, Thomas DD, Thompson LV. Electron paramagnetic resonance reveals age-related myosin structural changes in rat skeletal muscle fibers. *American Journal of Physiology - Cell Physiology*. 2001;280(3 49-3):C540-C547.

105. Andersson DC, Betzenhauser MJ, Reiken S, et al. Ryanodine receptor oxidation causes intracellular calcium leak and muscle weakness in aging. *Cell Metabolism*. 2011;14(2):196-207.

106. Umanskaya A, Santulli G, Xie W, Andersson DC, Reiken SR, Marks AR. Genetically enhancing mitochondrial antioxidant activity improves muscle function in aging. *Proc Natl Acad Sci U S A*. 2014;111(42):15250-15255.

107. Chan S, Head SI. Age- and gender-related changes in contractile properties of non-atrophied EDL muscle. *PLoS ONE*. 2010;5(8).

108. Yoon T, De-Lap BS, Griffith EE, Hunter SK. Age-related muscle fatigue after a low-force fatiguing contraction is explained by central fatigue. *Muscle and Nerve*. 2008;37(4):457-466.

109. Pagala MK, Ravindran K, Namba T, Grob D. Skeletal muscle fatigue and physical endurance of young and old mice. *Muscle and Nerve*. 1998;21(12):1729-1739.

110. Jang YC, Sinha M, Cerletti M, Dall'osso C, Wagers AJ, eds. *Skeletal muscle stem cells: Effects of aging and metabolism on muscle regenerative function*. ; 2011Cold Spring Harbor Symposia on Quantitative Biology; No. 76.

111. Verdijk LB, Snijders T, Drost M, Delhaas T, Kadi F, Van Loon LJC. Satellite cells in human skeletal muscle; from birth to old age. *Age*. 2014;36(2):545-557.

112. Wada KI, Katsuta S, Soya H. Natural occurrence of myofiber cytoplasmic enlargement accompanied by decrease in myonuclear number. *Jpn J Physiol*. 2003;53(2):145-150.

113. Brack AS, Bildsoe H, Hughes SM. Evidence that satellite cell decrement contributes to preferential decline in nuclear number from large fibres during murine age-related muscle atrophy. *J Cell Sci*. 2005;118(20):4813-4821.

114. Gallegly JC, Turesky NA, Strotman BA, Gurley CM, Peterson CA, Dupont-Versteegden EE. Satellite cell regulation of muscle mass is altered at old age. *J Appl Physiol*. 2004;97(3):1082-1090.

115. Mitchell AS, Smith IC, Gamu D, von Harsdorf R, Donath S, Tupling AR, Quadrilatero J. Functional, morphological, and apoptotic alterations in skeletal muscle of ARC deficient mice. *In press*.

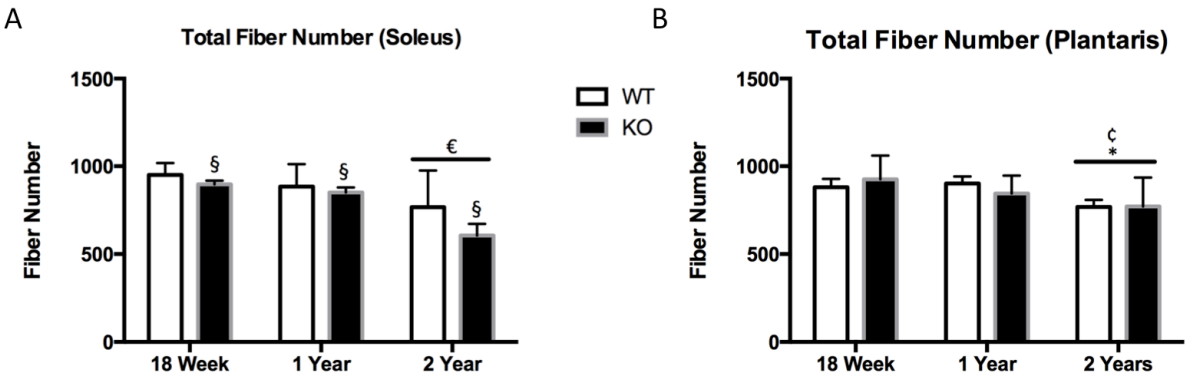

Appendix Figure 1. Total skeletal muscle fiber number. A-B: Total muscle fiber number in the soleus and plantaris of wild type (WT) and ARC knockout (KO) animals (n=11-12). Data are expressed as means ± SEM (* main effect $p<0.05$ vs. 1 year, ¢ main effect $p<0.01$ vs. 18 week, € main effect $p<0.001$ vs. 18 week and 1 year, § main effect $p<0.05$ vs. WT).

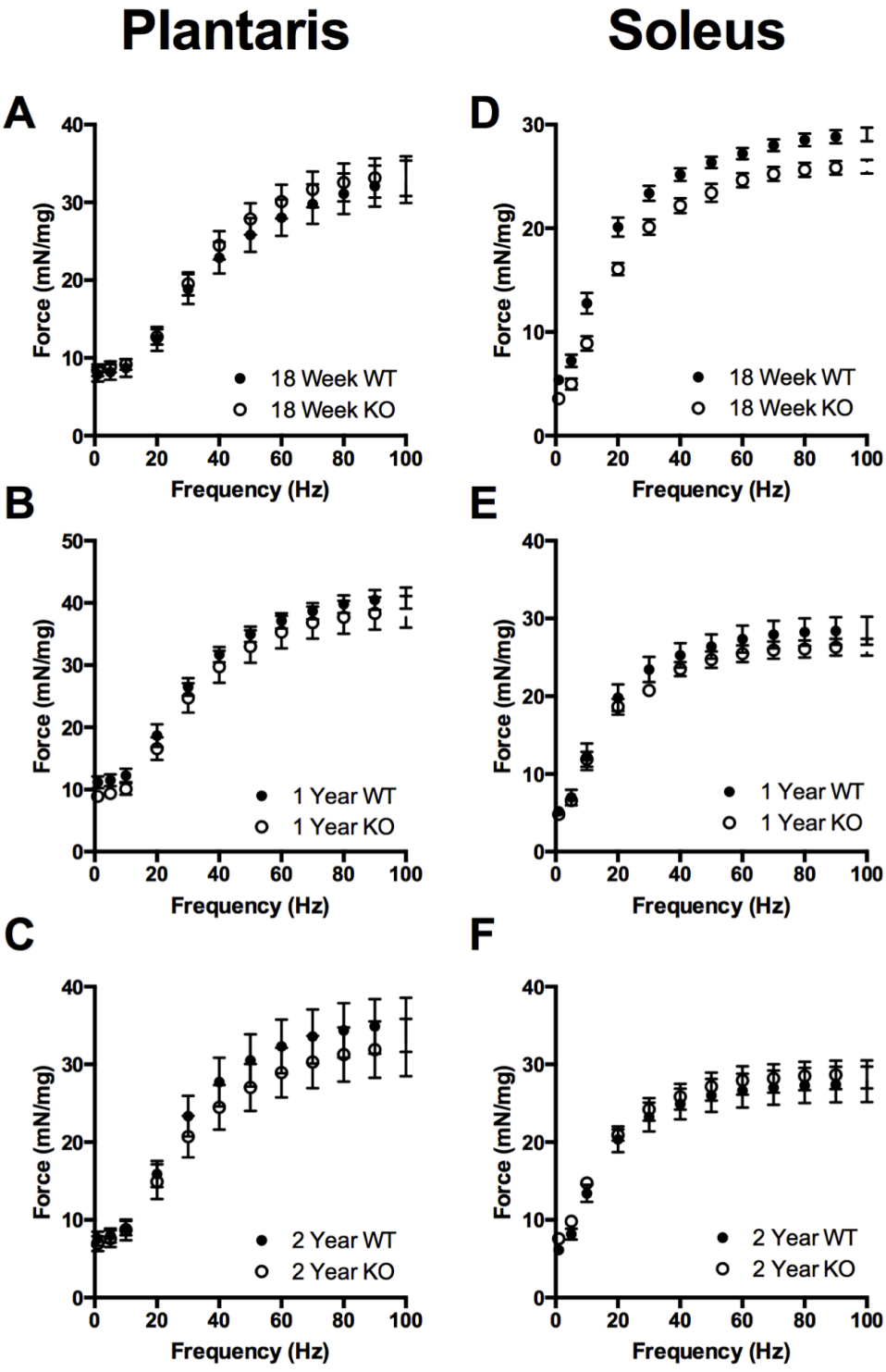

Appendix Figure 2. Analysis of muscle contractility measurements. A-C: Force-frequency curve in the plantaris of wild type (WT) and ARC knockout (KO) animals. D-F: Force-frequency curve in the soleus of WT and ARC KO animals (n=5-8). Data are expressed as means ± SEM.

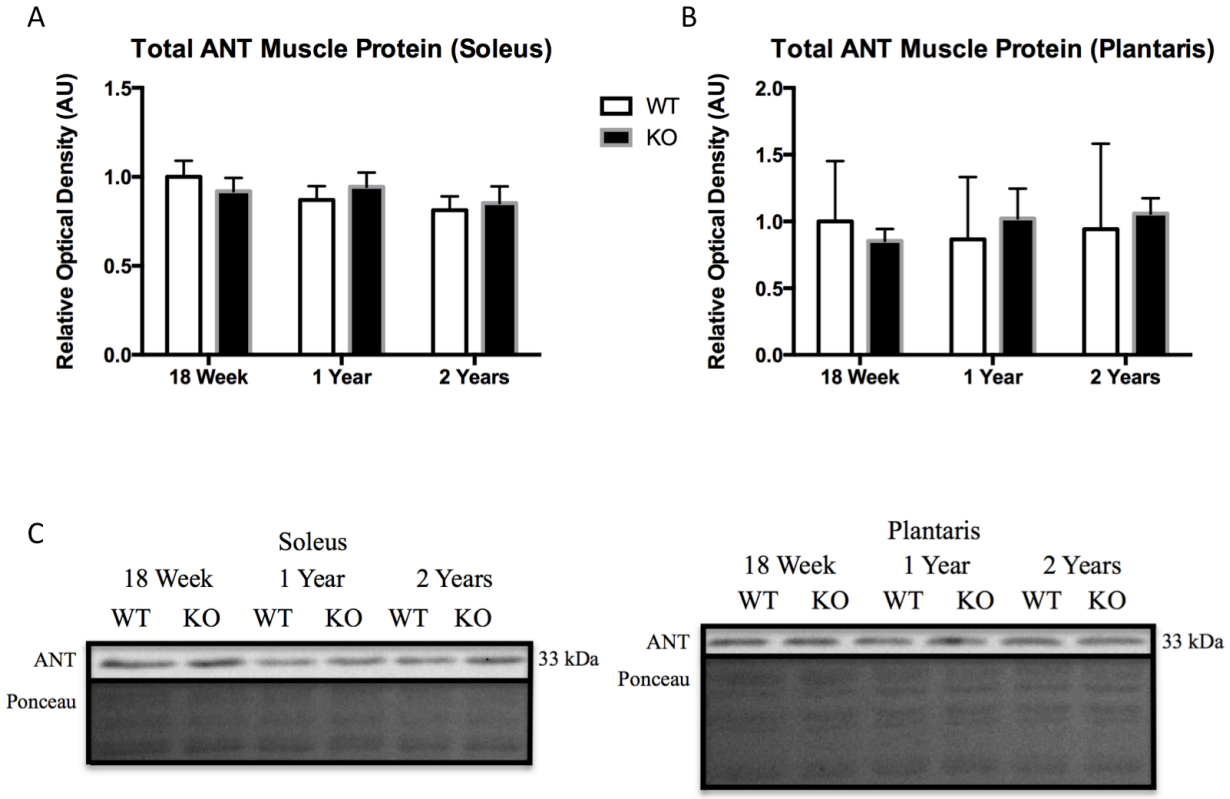

Appendix Figure 3. Expression of whole tissue mitochondrial protein. A-B: Quantification of ANT protein expression in the soleus and plantaris of wild type (WT) and ARC knockout (KO) animals (n=8). C: Representative immunoblots of ANT in soleus and plantaris of WT and ARC KO animals. Ponceau stained membranes are shown as a loading control. Data are expressed as means ± SEM.